The GH-IGF-I axis and breast cancer

Christiana Laban

MD (Res) Thesis

Queen Mary College
University of London

Department of Breast Surgery,
St Bartholomew's Hospital,
West Smithfield,
London ECIA 7BE.

I certify that the work presented in this thesis is entirely my own except where indicated in the text.

Christiana Laban

August 2010

ACKNOWLEDGEMENTS

I would like to thank my supervisor Dr Paul Jenkins for his continued guidance and support throughout this project. I would also like to thank Professor Stephen Bustin and Mr Robert Carpenter for their expert help, advice and also their valuable time.

I would like to thank Mr Carpenter and the other Breast Surgeons at St Bartholomew's Hospital as well as the Pathology Department there for all their help in setting up and maintaining the tumour bank of breast cancer specimens. Without them it would not have been possible to access such a valuable resource of tissue. I am also indebted to all the women who participated in this study and agreed to give specimens of blood and tissue for this research to be carried out.

I am very grateful for all the practical help in the laboratory from Sahira Khalaf and William Ogunkolade without whom I would have struggled to master some of the techniques vital for this project. They were extremely patient and generous in teaching me all the techniques required and without their expertise, it would not have been possible.

Lastly I would like to thank my fellow research students Claire McVittie and Kathryn McCarthy for their enthusiasm and cheerfulness in the lab.

LAY ABSTRACT

Breast cancer remains one of the most common causes of death amongst women today. Worldwide approximately 1.3 million women are diagnosed as having breast cancer every year. Much research has been done in trying to unravel the cause and behaviour of breast cancer and hormonal influences are known to play a role. In particular, two hormones known as growth hormone (GH) and insulin-like growth factor (IGF-1) have been found to play an important role in breast cancer growth and development. It has been found that women with breast cancer have higher levels of IGF-1 in their blood compared with women without breast cancer. Further studies have shown that if IGF-1 is added to breast cancer cells in laboratory conditions they grow rapidly. This evidence points to a strong link between IGF-1 and breast cancer. The majority of circulating IGF-1 is made by the liver in response to growth hormone, but as IGF-1 is also found in most cells in the human body, it is uncertain whether its possible effects on breast cancer may be due to local production of IGF-1 by breast cancer cells or to IGF-1 circulating in the blood. This research aims to study the link between IGF-1, GH and breast cancer. In order to do this, small specimens of breast tissue will be taken from women who are undergoing surgery for treatment of their breast cancer. Most cells removed will be cancer cells, but a rim of normal cells will surround them. I will then look at the different levels of IGF-1, growth hormone and other related hormones produced by the cancer or normal cells. During further research, I will aim to keep these cells alive for a few hours and see how they respond when various hormones are added to them. This research will give us more information about the hormonal control of breast cancer growth and may lead to novel treatments for breast cancer in the future.

TABLE OF CONTENTS

LIST OF FIGURES

LIST OF TABLES

TABLE OF ABBREVIATIONS

GH	Growth hormone
IGF-1	Insulin-like growth factor
GHRH	Growth hormone-releasing hormone
GHS	growth hormone secretagogue
GHSR	Growth hormone secretagogue receptor
IGFBP	Insulin-like growth factor binding proteins
mRNA	messenger Ribonucleic acid
ER	Oestrogen receptor
PgR	Progesterone receptor
VEGF	Vascular endothelial growth factor
RLT	RNeasy Lysis Buffer
RWI	RNeasy wash buffer
RPE	RNeasy wash buffer
RDD	RNase-Free DNase buffer
RT-PCR	Reverse Transcriptase polymerase chain reaction
DEPC	0.1% Diethyl pyrocarbonate treated water
HRP	Horseradish peroxidise
DAB	3.3’ Diaminobenzine liquid
PBS	Phosphate buffered saline
Substrate buffer	Stable peroxidise substrate buffer

1. Introduction

1.1 The GH-IGF-1 axis

The growth hormone /insulin-like growth factor-1 (GH/IGF-1) axis plays an essential role in the development of the breast by regulating cell proliferation, differentiation and apoptosis. GH is a peptide hormone synthesized and secreted mainly by the anterior pituitary gland in response to hypothalamic factors. Three hypothalamic peptides, growth hormone-releasing hormone (GHRH), the endogenous GH secretagogue (GHS) ghrelin and somatostatin, generally control GH release from somatotropes. GHRH and ghrelin, stimulate its release, while somatostatin is inhibitory. Although these hormones are known to be produced in the hypothalamus and stomach, a production in local tissues resulting in an autocrine/paracrine mode of action has been ascertained[1]. Binding sites for GH secretagogues are present in breast tissue and ghrelin exerts GH independent effects [2] although the local expression of ghrelin in breast is undetermined. Octreotide, a somatostatin analogue, appears to have antiproliferative effects in breast cancer by inhibiting GH release and therefore reducing IGF-1 levels[3]. Although several phase 1 and 2 clinical trials have investigated its effects, results have been variable. However a meta-analysis of all trials showed that in patients with metastatic breast cancer, a tumour response of over 40% was achieved with few side-effects[3].

1.1.2 Ghrelin

Ghrelin is a 28 amino-acid peptide with an *n*-octanoylated serine at residue 3, which is essential for its GH-releasing activity. It was originally identified from rodent stomach tissue, based on its ability to bind with high affinity and specificity to the GH secretagogue receptor (GHSR)[2]. Likewise in the human, ghrelin is synthesized and secreted from a distinct endocrine cell type found in the submucosal layer of the stomach[4]. It is similarly synthesized and secreted from other parts of the gastrointestinal tract, such as the duodenum, ileum, caecum and colon[5]. Several post-transcriptional and post-translational variants of ghrelin have been reported. Des-octanoylated ghrelin is a non-modified molecular form of ghrelin and is unable to activate GHSR expressing cells as it lacks the Ser3 octanoic acid[2]. A 27 amino acid splice variant that has lost the glutamine 14, known as Des-Gln14-ghrelin has also been identified and shown to have similar biological actions to full-length ghrelin[6]. Ghrelin acts directly on the anterior pituitary gland to stimulate GH release, and in vivo studies in humans involving intravenous injections of ghrelin demonstrate that the GH response to ghrelin is greater than that to GHRH [7]. However, despite its potent effect on GH release, there is some doubt over the primary role for ghrelin in the regulation of GH secretion, following a report indicating that no specific phenotype was observed in a ghrelin knockout mouse[8]. *In vitro* ghrelin has been reported to cause inhibition of proliferation of breast cancer cell lines, albeit at supraphysiological concentrations[2]. Many recent reports have suggested that ghrelin has a physiological effect not only on GH release, but also on gastric acid secretion and gastric motor activity. Ghrelin is also known to have an appetite-inducing function with experiments demonstrating ghrelin-induced adiposity[9]. It has a major stimulatory

effect on appetite in rat models, and plays a physiological role in meal initiation in humans[10]. Some studies suggest that sequence variations in the ghrelin gene may be part of the aetiology of human obesity[11].

Ghrelin and growth hormone secretagogue receptor (GHSR) have both been found to be expressed in normal breast tissue and breast cancer[12;13]. The GHSR is thought to mediate growth inhibitory effects on breast carcinoma cells in vitro[14].

1.2 IGF-1 and 2

IGF-1 consists of 70 amino acids (7.65 kDa) and IGF-2 of 67 (7.47 kDa). They share 62% homology in amino acids sequence and there is 40% homology between the IGFs and proinsulin[15,16]. As their name suggests they are growth factors with growth promoting properties in numerous tissues and are present in high concentrations in serum. However, unlike insulin, IGF-1 and IGF-2 are expressed mainly from the liver during adult life, and IGF-1 mediates most of the growth effects of growth hormone. Although both IGFs are known to be mitogens, IGF-2 is much more active during prenatal life than IGF-1, whereas IGF-1 is the principle regulator of linear growth. IGF-1and 2 are unique as peptide growth factors. In addition to autocrine/paracrine functions demonstrated in numerous tissues, it serves as an endocrine hormone promoting postnatal somatic growth and maintaining lean tissue mass.

The IGFs circulate in a molar ration of 2:1 (IGF-2:IGF-1)[17]. They bind with high affinity to six related IGF binding proteins[18] (IGFBP1-6) with ninety nine percent of IGF-1 and IGF-2 bound in serum to IGFBPs[19]. Less than 1% of IGF-1 and IGF-2 circulate in an unassociated form.

IGFBP-3 is the most abundant IGFBP in adults and 90% of circulating IGF-1 is carried in a complex with IGFBP-3 and an acid labile protein[20]. The smaller complexes are able to pass the vascular endothelial barrier and therefore may be important modulators of IGF-1 activity at the cellular level[21]. IGFBPs especially IGFBP-3 have independent effects on cell growth, for example IGFBP-3 has pro-apoptotic activities both dependent on and independent of p53[22]. IGFBP-3 may indirectly influence tumourigenesis by binding IGF-1 and thereby inhibiting the mitogenic effects of IGF-1. It may also directly affect tumourigenesis by its own anti-proliferative and pro-apoptotic effects. In this way IGFBP-3 is thought to play a cancer protective role.

The IGFBPs affect cells in both an IGF-dependant and –independent manner. By binding IGF-1 and IGF-2 they serve as circulating reservoirs transporting the IGFs, prolonging their half-lives, and regulating access of the IGF ligands to the IGF receptors. The same binding protein can have both inhibitory and stimulatory effects depending on its concentration, phosphorylation status and proteolytic fragmentation. In experimental systems the addition of IGFBPs generally inhibits the activities of IGFs, presumably by sequestering a high proportion of the free growth factor[23]. In this way IGFBPs act as regulators of IGF action and increase their half-life.

1.2.1 IGF-1 receptor

There are two transmembrane receptors IGF-1 receptor and IGF-2 receptor, the first of which resembles the insulin receptor to some extent. IGF-1 exerts its effects on cellular proliferation and apoptosis via the IGF-1 receptor(IGF-1R), which is a transmembrane tyrosine kinase receptor and is over expressed in breast cancer tissue[24]. The IGF-2 receptor has a higher affinity for IGF-2 and is a mannose 6-

phosphate receptor. The IGF-1R is transcribed from a single gene as a precursor that is then processed into an α-subunit and a β–subunit. The functional receptor is a heterotetrameric consisting of two α-subunits and two β-subunits that are linked by disulfide bonds. The α-subunits are extracellular and form the ligand-binding domain. The β-subunits, which contain short extracellular and transmembrane segments and a larger intracellular segment, transmit the ligand-induced signal. Binding of the IGF-1 to the IGF-1R causes autophosphorylation and transphosphoprylation of the β-subunit of IGF-1R. The action of this receptor usually requires the use of intermediate docking proteins for the propagation of its numerous signal transduction cascades. IGF-1 receptor phosphorylates cytosolic proteins such as the insulin receptor substrate-1 (IRS-1). This protein has no intrinsic enzymatic property but is thought to act as a link between the activated receptor and downstream components of the signaling cascade. IGF1R signal transduction involves the activation of various intracellular signaling pathways, including the Ras/Raf/MAP kinase and the phosphoinositide-3 kinase pathways[25] (Fig 1). There are also hybrid receptors between IGF-1R and insulin receptor (InsR) and it is thought that these hybrids behave more like IGF-1R than InsR. Thus binding of IGF-1 to IGF-1R or the hybrid receptor stimulates a cascade of signaling events leading to cell growth and inhibition of apoptosis. Abundant IGF-1 receptors exist on the surface of breast tumour cells and exposure to the IGFs increases their proliferation rate[26]. Conversely targeted disruption of the IGF-R gene, which suppresses the expression of IGF-1 and thus inhibits its function, can abolish cell transformation[27].

Figure 1 – IGF-1 binding to IGF-1 Receptor and activation of intracellular signalling pathways

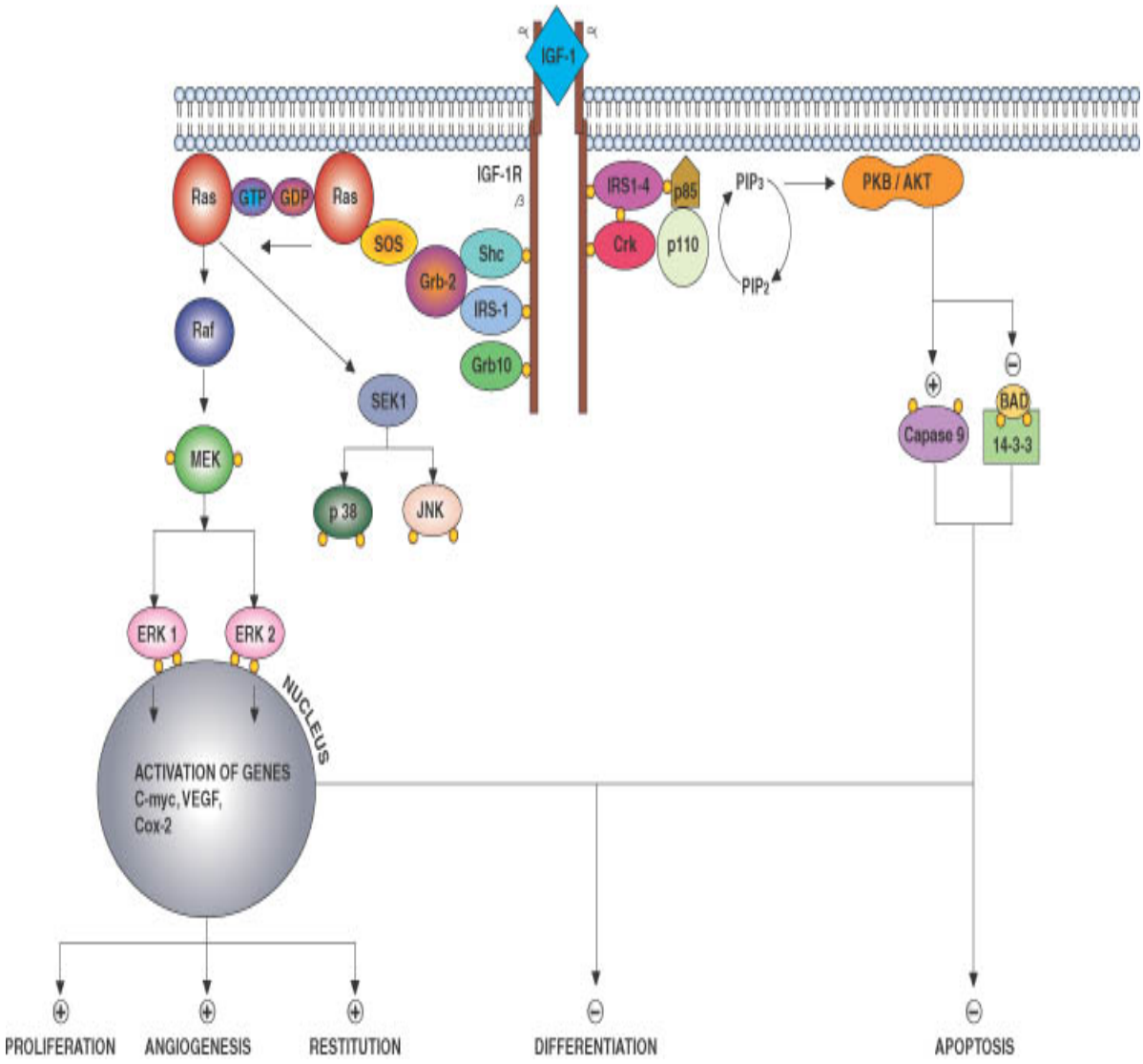

1.2.2 IGFBP protease

Another component of the IGF regulatory system is the IGFBP protease system. This comprises of a group of enzymes that cleave the IGFBPs and therefore alter their ability to bind IGFs[28]. IGFBP-3 protease activity is abundant in normal extracellular tissue[29].

Prostate-specific antigen (PSA) is an example of a well-known IGFBP specific protease. PSA cleaves IGFBP-3 and is thought to play an important role in metastatic prostate cancer[30], perhaps by increasing levels of circulating free IGF-1 and IGF-2 resulting in proliferation of prostate cancer cells[30]. A number of patients with advanced breast cancer also have increased plasma IGFBP-3 protease activity which correlates with clinical stage and alterations in tumour burden due to therapy[31].

1.3 IGF-1 and breast tissue

RNA extracted from breast tissue has easily detectable IGF-1 mRNA. In situ hybridizations show that IGF-1 mRNA is expressed in the stromal cells and not by normal or malignant epithelial cells[32]. Cullen et al also showed that IGF-1 mRNA was commonly expressed in fibroblasts derived from non malignant biopsy specimens[33]. This data shows that IGF-1 is expressed in normal breast tissue and is thought to play an important role in normal breast tissue development.

IGF-1 is synthesised mainly in the liver under the control of pituitary growth hormone, which is itself controlled by growth hormone releasing hormone from the hypothalamus. (Fig 2) For this reason plasma concentrations of IGF-1 largely reflect

Figure 2 – Summary of growth hormone-IGF-1 axis demonstrating the production of IGF-1 and IGFBP-3 from the liver and the formation of the ternary complex

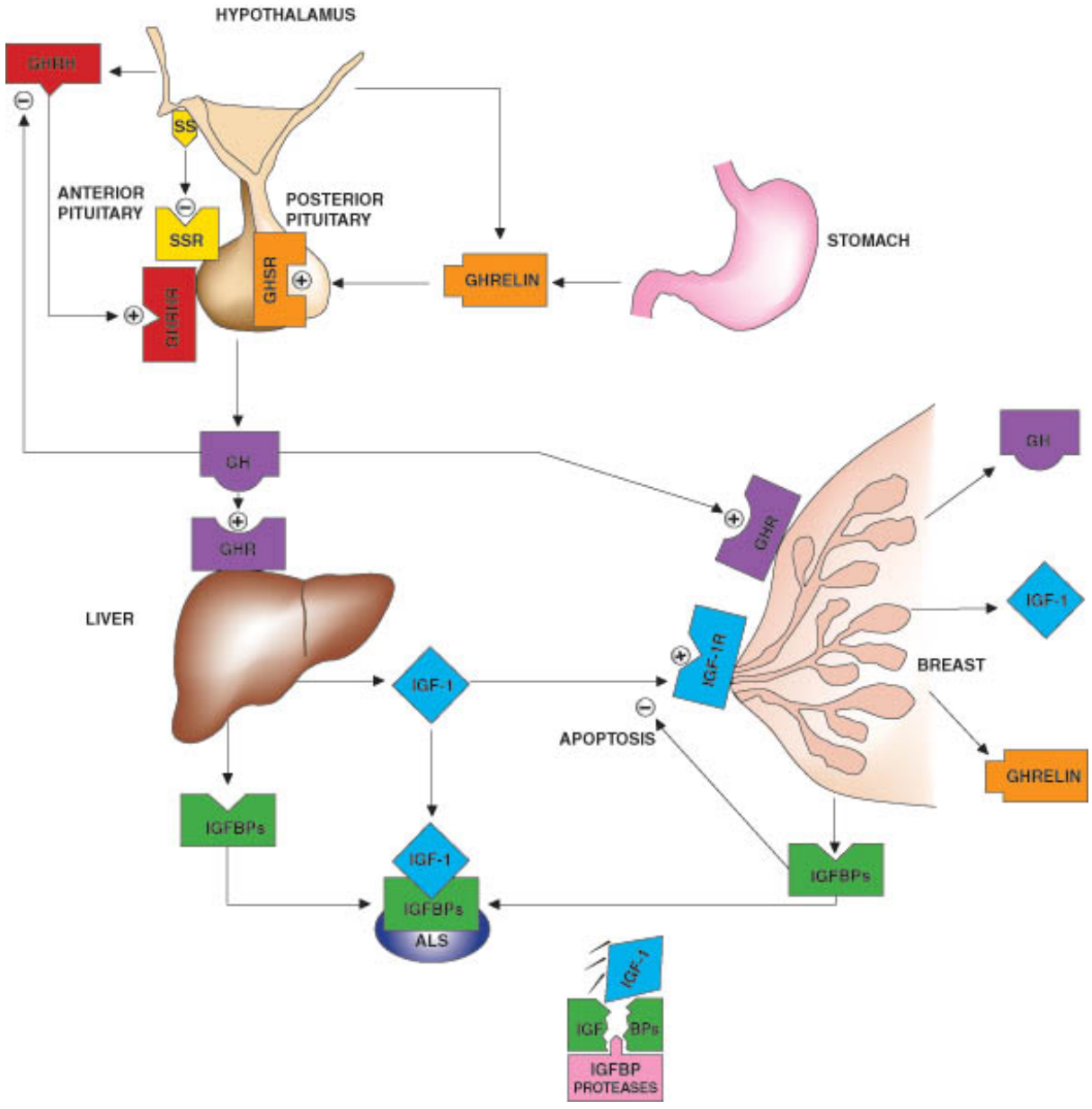

the activity of growth hormone. In fact the correlation of IGF-1 and GH has been found to be so reliable that IGF-1 levels in serum are used to monitor treatment with GH in GH deficient states[20]. In animals and humans, expression of both IGF-1 and IGF-1R are necessary for normal growth. The insulin-like growth factor family of ligands, receptors, and binding proteins is intimately involved in the normal growth and development of the human fetus and adult. The IGF surge during puberty is associated with the normal development of the breast. IGF plasma concentrations are also known to change with nutritional status, sex, age and oestrogen level[34]. Serum IGF-I and IGFBP3 levels increase with age and decline after puberty, suggesting an age-dependant expression[35]. Hence, the IGF-1 concentrations may be particularly relevant to breast cancer risk in premenopausal women, especially as oestrogen has been shown to enhance the action of IGF-1 in the breast. GH that raises the circulating IGF-1 levels also upregulates IGF gene expression within the mammary gland[36]. IGF-1 appears to be a required factor for normal mammary gland development[36]. In primates, infusion of GH alone results in a fourfold increase in mammary glandular size, although whether this results from direct effect of GH or induction of local production of IGF-I is unknown[37]. Regardless, development of the human mammary gland can be divided into several stages all of which are influenced by the GH/IGF-I axis and enhanced by estrogens (Fig 3). In addition IGF-I is required for ductal morphogenesis; in its absence mammary development does not occur even in the presence of estrogens[38].

However tissue IGF bioactivity is influenced not only by circulating IGF-1 and IGF-2 levels but also by autocrine and paracrine secretion of these growth factors, and by IGFBP levels and IGFBP proteases.

An IGF-related ligand can act as an autocrine growth factor for many cancer cell lines

Figure 3 – Diagram of stages of normal breast development

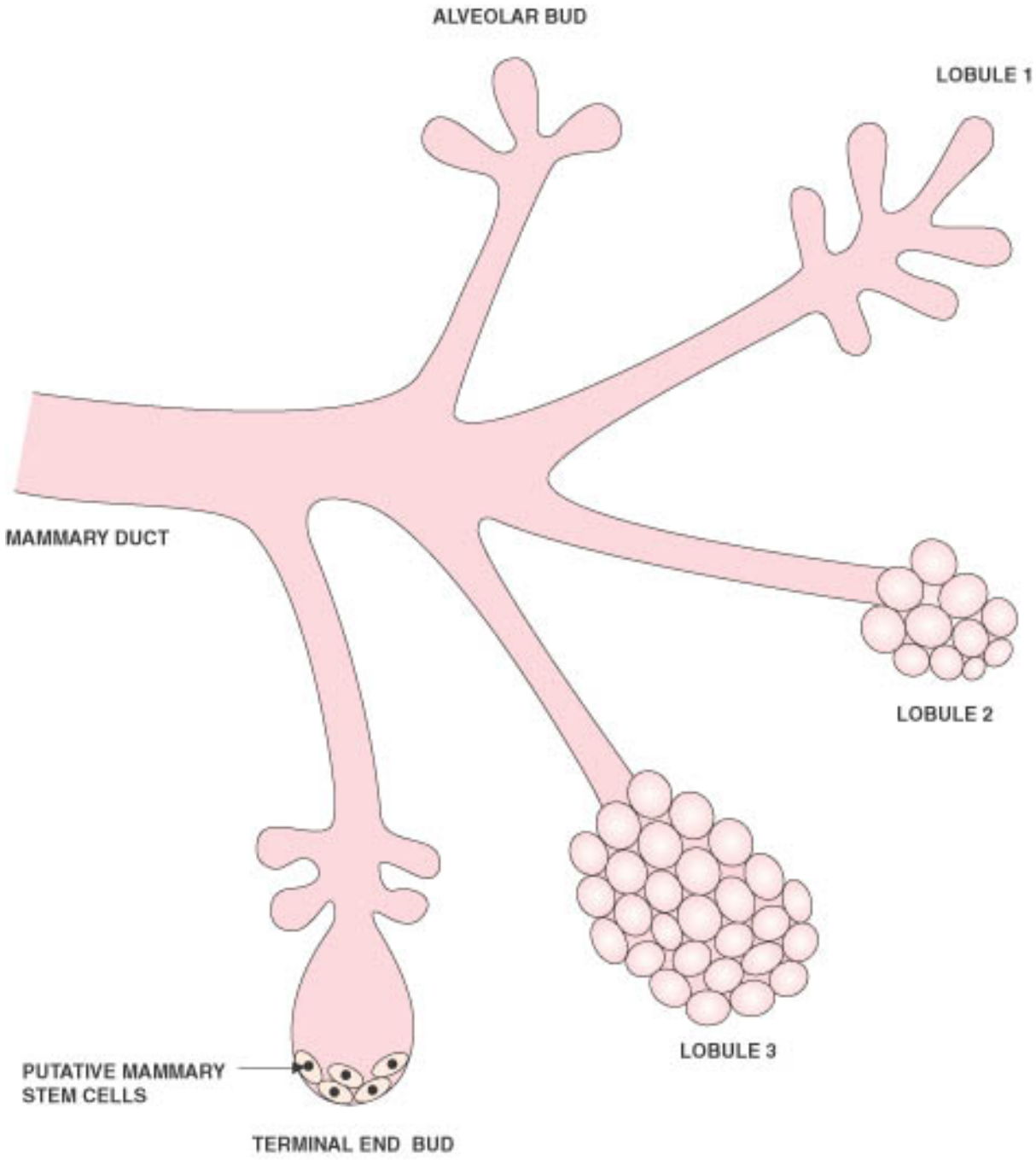

via the type I IGF receptor (IGF-R). The human breast is continuously exposed to the insulin-like growth factors (IGFs). In addition to high endocrine levels, IGF-1 and IGF-2 also originate from distinct cell populations within the breast itself[39;40]. IGFs are mitogenic for malignant breast epithelium. IGF-1 receptors exist on the surface of breast tumour cells, and exposure to the IGFs increases their proliferation rate. Until recently it was thought that hepatic IGF-1, acting in an endocrine manner was responsible for growth and development. However it is now clear that autocrine/paracrine production of IGF-1 is at least as important.

1.3.1 IGF-1 and Oestrogen

Considerable evidence suggests that the GH/IGF-1 axis and ER signaling act through a complex cross-talk mechanism to stimulate the proliferation of normal mammary epithelium to increase the risk of breast cancer[41;42]. The oestrogen antagonist Tamoxifen blocks IGF-1 mediated proliferation of breast cancer cells *in vitro*[43] and has been used successfully in chemoprevention of breast cancer, with several studies showing how it reduces IGF-1 serum concentration *in vivo*[44;45]. This latter effect is due to several actions. Suppression of pituitary GH secretion occurs first, in part, by enhancing somatostatin actions[46] and second by a direct inhibitory influence on IGF-1 expression[47]. Tamoxifen also inhibits IGF-1 gene expression in common secondary sites for breast cancer metastasis[47;48]. Oestradiol markedly increases GH-mediated expression of IGF-1 mRNA in normal mammary tissue, as well as upregulating expression and activation of the IGF-1R in ER-positive breast cancer cells[49]. Indeed a synergy occurs between Oestradiol and IGF-1 in mediating the proliferative response in ER+ cells[50]. The expression of nearly all members of the IGF system is under transcriptional control of the ER. IGF has also been reported to activate ER. IGF-1

causes transcriptional activation of ER in human breast cancer cells, and the inhibition of ER action by IGFBP-1 suggests that IGF-1 signaling maybe necessary for maximal ER activation[51]. While GH is believed to be the pituitary factor responsible for mammary ductal morphogenesis, it has been reported that IGF-1 mimics the action of GH on mammary development in hypophysectomized, gonadectomized rats[25].

1.3.2 The role of the GH-IGF-1 axis in breast cancer

The growth hormone (GH)/ insulin-like growth factor (IGF-1) axis is implicated in the pathogenesis of human breast cancer[52]. Historical data reveals that women with breast cancer who had undergone hypophysectomies had an improved prognosis[53]**.** This effect was still apparent in those who had had prior total hysterectomy and oophrectomy suggesting that gonadotrophin independent pituitary derived factors influence the behavior of breast cancer[53;54]**.** Subsequent epidemiological data have shown a positive association between risk of breast cancer and increased height. As GH and IGF-1 are major determinates of the latter, this indirect evidence suggests that these hormones might influence breast tumourgenisis[55]. Conversely, low birth weight, which is associated with low serum IGF-1 levels, correlates with subsequent low breast cancer risk[56]. Nutritional intake is a major determinate of hepatic IGF-1 secretion[57] and high calorie intake in childhood has been associated with a significant increased risk of breast cancer in later life[58]. Dietary restriction, which decreases the serum concentration of IGF-1 in both humans and rodents, reduces the incidence of cancer in many rodent models. A further association is provided by studies demonstrating serum GH concentrations to be elevated in a significant percentage of

breast cancer patients compared to controls[59] and also to be increased in women at high risk for familial breast cancer[60]. Circulating levels of IGF-1 have been found to be increased in women with breast cancer compared to control subjects[61]. That these elevated levels of IGF-1 are not due to the cancer itself is discounted by a study by Hankinson et al[62] who established a prospective link between serum IGF-1 levels and subsequent risk of breast cancer. An increased risk of 2.3 fold in pre-menopausal women was associated with circulating IGF-1 concentrations in the upper tertile of the normal range. This relative risk increased to 4.6 fold in pre-menopausal women less than 50 years old, and controlling for IGFBP-3 concentrations increases the risk to 7.3 fold. Similarly Byrne et al observed that mammographic breast density in post-menopausal women, which is a strong predictor of the risk of breast cancer, was positively correlated to plasma IGF-1 and inversely correlated to plasma IGFBP-3[63]. A further paper has also shown mammographic density to be positively associated with IGF-1, negatively with IGF-2, but not with IGFBP-3. The study supported the hypothesis that endogenous hormones affect density of mammograms in premenopausal women, in particular showing a positive association with oestrogen levels and mammogram density[64]. High serum concentrations of IGF-1 are associated with an increased risk of breast, prostate, colorectal and lung cancers[65]. In patients with acromegaly, high concentrations of growth hormone stimulate production of high concentrations of IGF-1 and this has been associated with an increased risk of colorectal and breast cancer[66, 67]. Most studies have focused on the risk of cancer in relation to serum or plasma concentrations of IGF-1, IGF-2 and IGFBP-3 and have shown that high IGF-1 and low IGFBP-3 predicts increased cancer risk[68]. In fact a recent paper has shown that circulating IGF-1 is positively associated with breast cancer risk. The association was not substantially modified by IGFBP-3 and did not

differ markedly by menopausal status but seemed to be confined to oestrogen-receptor-positive tumours[69]. IGF-1 accelerates the progression of precancerous changes to invasive lesions. Therefore a decrease in serum IGF may help reduce the risks of breast, prostate and colon cancer, especially for members of high-risk families.

1.3.3 In vitro and animal studies

In vitro, IGF-1 exerts marked proliferative and anti-apoptotic effects on breast cancer cell lines[15,70].Administration of IGF-1 may rescue breast cancer cell lines from chemotherapy induced cell death by induction of proliferation and inhibition of apoptosis[70]. Substantial evidence from animal studies also supports the view that the GH/IGF-1 axis plays an integral role in breast tumorigenesis. Early studies revealed a positive correlation between the activity of the GH-IGF-1 axis and development of breast tumors in mice[71]. Subsequently, transgenic mice that over express growth hormone have been shown to exhibit both mammary gland epithelial cell hyperplasia[72] and have an increased frequency of mammary tumours, as do mice with over expression of IGF-1R agonists[73]. In contrast, ductal hypoplasia is seen in transgenic animals that over express a GH antagonist[74]. Similarly antibodies against the IGF-IR inhibit *in vivo* growth of subcutaneous breast tumours transplanted into nude mice[75]. Liver IGF-1 deficient mice with a 75% reduction in circulating IGF-1 levels demonstrate a reduction in tumour development[76].

Whilst this evidence seems to suggest a role for the GH/IGF-1 axis in breast cancer, the relative importance of endocrine versus paracrine effects of GH/IGF-1 axis in the breast has not been investigated. It is also unknown whether GH may exert IGF-1

independent effects in this tissue, although GH has been shown to stimulate transcription of c-myc, a proto-oncogene. IGF-1 also regulates the expression of several genes associated with breast tumourigenisis; c-myc, VEGF, progesterone receptor (PgR) and cathepsin D[77].

A new antagonist of GH action, Pegvisomant, is a powerful inhibitor of GH secretion and may be an active anti-cancer agent. Preliminary reports suggest that Pegvisomant could have anti-tumour effects in several model systems[78]. Thus lowering serum IGF-1 levels with Pegvisomant could directly test the contribution of endocrine IGF-1 to cancer biology.

The IGF system seems to have important implications in the treatment of breast cancer. The expression of IGF components has been linked to malignant transformation and disease progression, suggesting that this system might be an effective target for breast cancer therapy. There is increasing experimental evidence that interventions which reduce circulating IGF-1 levels reduce proliferation of breast neoplasms. This has increased the interest in developing novel endocrine therapies that target the GH/IGF-1 axis.

2. Hypothesis and Aims

2.1 Hypothesis

Paracrine/autocrine expression of IGF-1 within the breast is important in the growth of breast cancer.

2.2 Aims

1. Determine and quantify mRNA levels of IGF-1 and its receptor in normal and malignant breast tissue.
2. Confirm mRNA expression at a protein level by immunohistochemistry (IHC).
3. Investigate expression of putative IGF-1 responsive genes and correlation with IGF-1 expression.
4. Examine the microarray gene profile to investigate IGF-1 regulated genes.
5. Use an *in vitro* system of breast tissue explant incubation to determine effects of growth hormone on local IGF-1 expression
6. Measure levels of IGF-1 and IGFBP3 in serum of women with breast cancer before and after surgery
7. Association of IGF-1 with clinical phenotype

3. Materials

3.1.1 Major

Tissue Homogeniser Ultraturrax T8 – GMBH & Co, Germany.

Rneasy RNA extraction kit, Qiagen Ltd, Crawley, West Sussex, UK.

RNA 6000 Nano Labchip kit (RNA quantification), Agilent Technologies UK Ltd, Cheshire, UK.

Ribogreen (RNA quantification), Molecular Probes, Amsterdam, The Netherlands.

Wallac Victor^2 1420 Multilabel Counter (plate reader), Perkin Elmer Life Sciences, Cambridge, UK.

Mx4000^{TM} RT-PCR mutiplex quantitative PCR system, Stratagene, The Netherlands.

Brilliant^{TM} plus single step quantitative RT-PCR core reagent kit, Stratagene, The Netherlands.

Primers and probes designed by Primer Express software, ABI Perkin Elmer, Warrington, UK.

ABC kit, Vector Labarotories, USA.

NuaireTM DH Autoflow aotomatic CO2 Incubator, Triple Red Lab Technology Ltd, Oxfordshire, UK.

Balance, Satorius 1800, Sartorius Ltd, Sussex UK.

MTS proliferation assay, Cell Titer 96 Aqueous One Solution Assay Promega,Southampton, UK.

LDH cytotoxicity detection kit, Roche Molecular Biochemicals, NJ,UK.

Immunofluorescence, TSA^{TM}, Perkin Elmer, USA.

Affymetrix U133A Chip protocol

Gene Spring 6.0 expression analysis software

3.1.2 Minor

RNA later, Ambion (Europe) Ltd, Huntingdon, UK.

Cryogenic 2ml vials, Corning Inc, NY, USA.

Scalpels blade no. 10, Fisher Scientific UK, Loughborough, UK.

Pipette tips, Starlab, Helsinki, Finland.

24 well and 96 well microplates, Abgene UK.

Microcentifuge tubes, Starlab, Helsinki, Finland.

Depex mounting medium, Gerr, Canada.

Ethanol (96%), VWR International Ltd, Lutterworth,UK.

Amphotericin (0.25μg/ml), Invitrogen Ltd, Paisley, UK.

Penicillin (10mg/ml), Invitrogen Ltd, Paisley, UK.

Streptomycin (10mg/ml), Invitrogen Ltd, Paisley, UK.

Dulbecco's Modified Eagle Medium, GibcoBRL, Paisley, UK.

Bovine serum albumin, Sigma Poole.

4. Methods

4.1 Ethics

This study was approved by The Local Research Ethics Committee of the East London and City Health Authority. All involved patients signed a consent form designed specifically for this study (Appendix A). Fully informed consent was obtained prior to collection of all samples from theatre, and a copy of the consent form was filed in the patient's notes, given to the research department, given to the patient and also given to the pathology department.

4.2 Tissue collection

Samples of normal and malignant breast tissue were collected from 185 women undergoing mastectomy or segmental mastectomy for breast cancer (see Appendix B – patient tumour characteristics). The patients were aged 20 to 90 years old and were operated on at St Bartholomew Hospital. The tumours were all greater than 1cm in diameter. Smaller tumours were not taken as this may have affected histological results. The breast specimens were taken to the pathology department directly after removal in theatre, where a pathologist orientated the specimen and inked the margins. A section of normal and malignant tissue was identified macroscopically and dissected out. Areas of breast fat were avoided, as were inked areas. Normal tissue was harvested as far away from malignant tissue as possible. Samples were then placed immediately into 'RNA later' (Ambion, UK). The samples were then snap frozen in liquid

nitrogen and stored at -80^{o}C. The tumours histology was noted as either invasive ductal, lobular, tubular, medullary, mucinous, the tumours size, grade and presence or abscence of DCIS. Also the lymph node status was recorded along with the ER and PR status of the tumour.

4.3 RNA extraction

Successful extraction of RNA requires disruption of the tissues, inhibition RNases activity (enzymes that degrade RNA) and removal of any contaminating genomic DNA or proteins.

All tissue samples were stablilised in 'RNA later' prior to archival storage at–80^{o}C. Use of this reagent allows immediate stabilisation of RNA there by preventing any changes in gene-expression pattern that may occur with RNA degradation. All eppendorfs used had been previously autoclaved.

Tissue samples of approximately 20-30mg were subsequently excised after removal from 'RNA later'. Due to poor yield of RNA from adjacent normal breast tissue, sample size of these samples was increased to 50mg. Qiagen 'Rneasy' kit was used to extract RNA. This technique allows isolation of RNA molecules longer than 200 nucleotides. This therefore provides mostly mRNA as most RNAs less than 200 nucleotides in length are excluded. Lysis buffer RLT, containing guanidine thiocyanate and B-mercaptoethanol, was used. This buffer is effective in inactivating RNases to allow isolation of intact RNA. Tissue disruption was achieved using a tissue homogeniser.

4.3.1 Tissue homogenisation

500µl of buffer RLT was added to 30mg of frozen tumour or 700µl RLT to 50mg of frozen adjacent normal tissue.

A rotor 'Ultra-turrax' homogenizer was used to disrupt the tissues for approximately 20 minutes at speed setting 4. Care was taken to avoid over-heating and foaming. The rotor homogenizer disrupts the tissues using turbulence and mechanical shearing. The disrupted sample was then snap frozen using liquid nitrogen.

For subsequent mRNA extraction, all samples were defrosted for 5 minutes in a water bath at 55-65^{o}C. They were then placed into a centrifuge for 5 minutes at 13,000 rpm. The supernatant was carefully transferred into a new eppendorf, discarding any unhomogenized tissue. An equal volume of 70% ethanol was then added to the supernatant. The samples were then mixed by vortexing. 700µl of the mix was pipetted into the Rneasy mini column, which was placed into a collection tube. The column and tube were centrifuged at 9000rpm for 1 minute. The mini column contains a silica-gel-based membrane, which allows binding of total RNA whilst contaminants may be washed away. Although the protocol states that the follow through may be discarded, after several extractions with poor yield of RNA, it was discovered that it was beneficial to pipette the follow through back into the mini column and re-centrifuge for a further minute before discarding.

This process was then repeated for the remaining buffer/ethanol mix.

350µl of buffer RWI (ethanol containing) was then added to the mini column and the column was left to stand for 15 minutes with its lid open. After 15 minutes, the column was placed into the centrifuge at 9000 rpm for 1 minute. At this point a DNase step was performed. This step is optional but used for the purpose of this study as Taqman PCR analysis is sensitive to even small amounts of DNA.

4.3.2 DNase Step

A mixture of 10µl DNase stock solution and 70µl buffer RDD was made up, for each sample. This was then mixed gently by inverting the tube. 80µl was pipetted directly onto the membrane within the mini column and left, with lids open for 15 minutes. After 15 minutes, a further 500µl of buffer RWI was pipetted into the mini column and the column centrifuged at 8000 rpm for 1 minute. At this point the follow through was discarded and the mini column placed into a new collection tube. 500 µl of RPE was then added to the mini column and centrifuged at 9000 for 1 minute. The follow through was then discarded and a further 500 µl RPE added, centrifuged at 9000 rpm for 3 minutes and discarded. The mini column was then centrifuged at 10,000 rpm for 3 minutes in order to dry out the membrane and then transferred into a new collection tube.

80µl of RNase free water was then added directly onto the membrane and left to stand for 2 minutes. The mini column was then centrifuged at 10.000 rpm for 3 minutes. A further 65µl of RNase free water was then added and the mixture left to stand for 5 minutes. The column was then centrifuged at 13000 rpm for 4 minutes. 145µl of follow through was then collected into two new eppendorfs; 10µl in one eppendorf for RNA

quantification and the remaining 135µl into another for archival storage at –80^{o}C.

4.4 RNA analysis

There are many different methods of analysing and quantifying RNA. Usually, the quality is checked by gel electrophoresis whereby two distinct bands form; 28s and 18s. The ratio of 28S:18S should be at least 2:1 thereby confirming that the RNA has not undergone significant digestion by RNases. If the RNA has degraded, the ratio will be reversed. With this method of quality control it is the ribosomal (rRNA) and not the messenger RNA that is checked as it is the rRNA which produces the strong bands. Messenger RNA only produces a faint smear on a gel.

Initially the 'Ribogreen RNA quantification' kit was used to quantify the RNA. It is a fluorescent nucleic acid stain that is able to accurately quantify or detect as little as 5ng/ml RNA. Those samples mostly included normal breast tissue, which due to its high fat content tended to produce lower yields of mRNA. Breast tumour tissue, however produced much higher quantities of mRNA and so for these samples, the Agilent bioanalyzer was used.

4.4.1 Ribogreen RNA Quantification Kit

The Ribogreen method of RNA quantification is a sensitive fluorescent nucleic acid stain that may be used in conjunction with a fluorescence microplate reader. The Ribogreen reagent is an unsymmetrical cyanine dye which demonstrates a >1000 fold increase in fluorescence when bound to RNA. Free nucleotides and contaminating proteins do not interfere with the measurement. It is essential that all samples have had DNA removed as it also binds to the Ribogreen reagent.

Samples to be quantified were removed from –80^{o}C storage and kept on ice. Clean disposable gloves were used throughout to minimise contamination from RNases. TE assay buffer was provided at 20x strength required. It comprised 10mM Tris-HCL and 4mM EDTA at pH 7.5 and was diluted to 1/20 using nuclease-free water (2ml TE was added to 38ml water). Nuclease-free water was prepared by treatment of distilled de-ionised water with 0.1% diethyl pyrocarbonate (DEPC) followed by incubation for 2-3 hours at 37^{o}C and then autoclaved for 15 minutes. This sterilizes the water and eliminates the DEPC.

4.4.1.1 Tumours and normal tissue

400µl of TE was pipetted into each autoclaved eppendorf meant for tumour. 2µl of tumour RNA was then pipetted into the TE buffer. 300µl of TE was used for each sample of normal breast tissue. 5µl of normal RNA was then pipetted into the TE buffer.

The Ribogreen reagent was then made into a 1 in 200 solution by taking 50µl of Ribogreen and 9.95ml of TE buffer and protecting from light. 200µl of the Ribogreen solution was then added to each of the above tumour or normal tissue samples. 100µl of this mix was then pipetted into three consecutive wells within a 96 well plate and incubated for 2-5 minutes.

4.4.1.2 Standard Curve

A standard curve was then prepared to display the linear correlation between RNA concentration and fluorescence. Ribosomal RNA was provided at 100µg/ml and diluted to 2µg/ml using 10µl of standard RNA in 490µl of TE buffer

The following solutions were then prepared:

Vol of 2µg/ml RNA (µl)	Vol of TE (µl)	1:200 Ribogreen agent	Concentration of RNA (ng/ml)
160	40	200	800
120	80	200	600
100	100	200	500
80	120	200	400
60	140	200	300
40	160	200	200
20	180	200	100
10	190	200	50
0	200	200	0

At each concentration, 100µl of solution was pipetted into 3 consecutive wells within the above mentioned 96 well plate and incubated for 2-5 minutes.
The 96 well plate containing the sample RNA and the standard curve was then placed in a fluorescence microplate reader and measured at 450-520 nm. The instruments gain was set so that the sample containing the highest RNA concentration yielded fluorescence intensity near to the maximum. This ensured that all sample readings remained in the detection range.

The average of all three fluorescence values was calculated for each sample. The fluorescence value of the blank reagent was subtracted from each of these values. For the standard curve graph, this resulting value was then plotted as a scatter graph against the RNA concentrations (Figure 4). From the plots on the graph a trend line was then added and from this the y-intercept value was calculated.

Figure 4. Representative standard curve of different sample RNA concentrations (each value is the mean of three fluorescence values) quantified using the Ribogreen assay fluorescence.

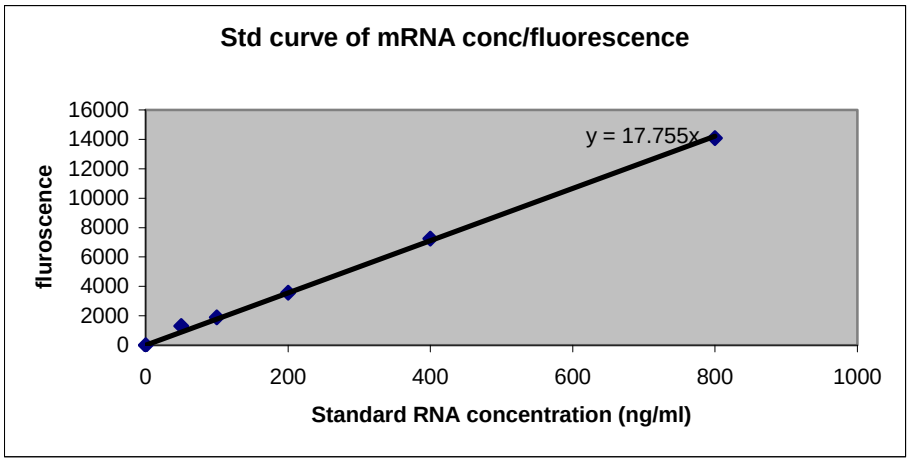

4.4.1.3 Calculation of RNA from standard curve

The mean of three fluorescence values was calculated per sample. The fluorescence value of the blank reagent was then subtracted from this value. This value was then used to calculate the concentration of RNA according to the dilution factor used in making up the RNA/TE and ribogreen solutions.

4.4.1.3.1 Tumour

[Fluorescence/y-intercept] x [400/2] x [400/200] = concentration of RNA ng/ml.

4.4.1.3.2 Normal tissue

[Fluorescence/y-intercept] x [300/5] x [400/200] = concentration of RNA ng/ml.

4.4.2 Agilent Bioanalyzer

The RNA 6000 Nano Labchip Kit simultaneously measures quantity and quality of messenger or total RNA (Figure 5). It comprises a lab chip and a bioanalyzer attached to a PC. Each sample is injected into a well and then moves sequentially from its well to a central separation microchannel, where it is separated electrophoretically. As the fragments move down the central separation channel, they separate by size and are detected by fluorescence and recorded by the bioanalyzer machine.

Samples were removed from –80^{o}C storage and placed on ice. The protocol recommends that all RNA samples should be heat denatured at 70^{o}C for 2 minutes. However due to the poor yield of RNA this practice was not continued.

The Bioanalyzer electrodes were cleaned prior to each chip. This was performed by adding 350µl RNase ZAP to one of the wells of an electrode cleaner. This cleaner was then placed into the Agilent 2100 bioanalyzer and left for 1 minute. It was then removed and a second electrode cleaner was filled with 350µl RNAse free water. This was placed into the Agilent 2100 bioanalyzer for 10 seconds and then removed. Another 10 seconds was then waited to allow the water on the electrodes to evaporate.

The gel was prepared by pipetting 400µl of RNA 6000 Nano gel matrix into the top receptacle of a spin filter. The spin filter was then placed in a microcentifuge and spun at 4000 rpm for 10 minutes. 130µl of filtered RNA gel matrix was added to an RNase free 1.5 ml microfuge tube and 2µl of 6000 Nano dye concentrate was then added. The tube was then

closed and vortexed thoroughly. The eppendorf was then centrifuged for 10 minutes at 14 000 rpm.

The chip priming station base plate was placed in position ‘C’. An RNA Nanochip was removed from a sealed bag and placed on the chip priming station. 9µl of the gel dye mix was pipetted into the bottom of the well marked ‘G’. Care was taken to avoid bubbles. The plunger was then advanced to the 1ml level, the chip priming station was closed and the plunger pushed into place by the syringe clip. This remained in position for 30 seconds. After 30 seconds the plunger was pulled back to the 1ml position. The chip primary station was then opened and the back of the chip was checked for airbubbles. Commonly small bubbles will be seen in the wells after pipetting but the vortex procedure will commonly remove these bubbles. If bubbles were present in the channels of the chip the plunger was again pressed down and bubbles were checked for. This is a fairly rare occurrence but can occur if a good seal is not formed when the chip is pressurized the first time. The priming station was then opened and 9µl of gel dye mix pipetted into the two wells above the one marked ‘G’.

Figure 5. RNA Nano Labchip in chip priming station. Each chip analyses 12 samples simultaneously. G represents the well containing the gel-dye mix and # represents the well containing the ladder.

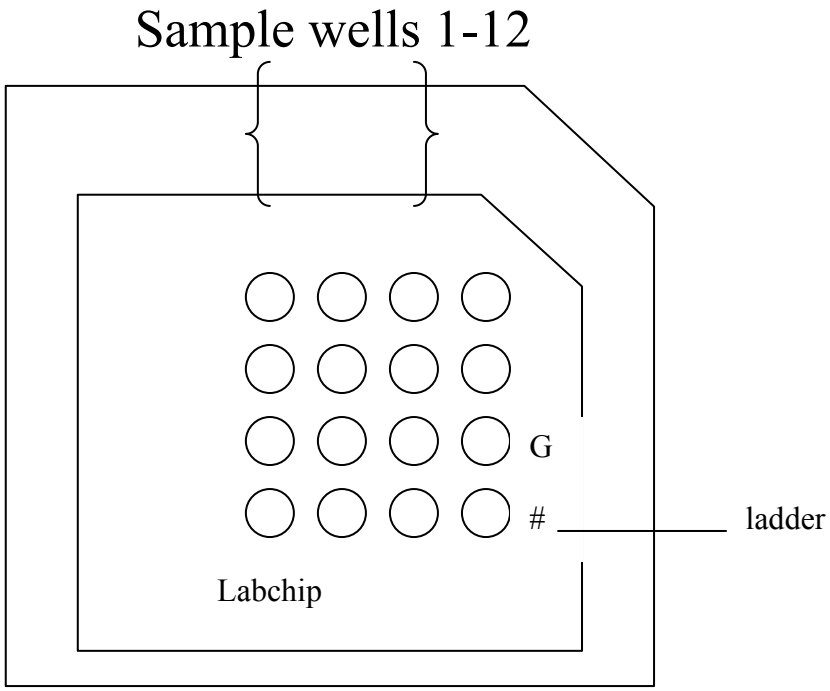

5µl of RNA 6000 Nano marker was pipetted into the well marked 'ladder' and then into each of the 12 wells consecutively. All 12 wells should be filled with sample buffer, even when running less than 12 samples. None of the wells should be left empty or the chip would not run properly. An additional 1µl of RNA 6000 Nano marker should be added to the 5µl of sample buffer in the unused sample wells.

4.4.2.1 Loading the ladder and samples

3µl of RNA 6000 ladder was pipetted into an autoclaved eppendorf and denatured at 70^{o}C for 2 minutes. 1µl was then pipetted into the bottom of the well marked with a ladder sign (#).
1µl of each sample to be analysed was pipetted into each of the 12 sample wells. The chip was then placed into the adapter of the vortex mixer and vortexed for 1 minute at set point 2400 rpm.

After vortexing, the chip should be placed in the Agilent 2100 bioanalyzer and the run should be started within 5 minutes. The chip fits into the receptacle one way, and should not be forced into position. The lid should be closed. The software instructions on the accompanying PC were then followed; the correct assay selected, the sample wells labelled and the 'start' button clicked to commence the assay. All RNA concentrations were then collected from the PC at the end of the assay.

4.5 Real time reverse transcriptase polymerase chain reaction (RT-PCR)

RT-PCR is a sensitive, *in vitro* method used to detect messenger RNA (mRNA). It is used to measure the abundance of specific RNA or DNA sequences in clinical samples and may also be used to screen for mutations and single nucleotide polymorphisms. The Taqman assay has been used to quantify transcription from individual cells[79] and paraffin embedded tissue[80]. It has wide ranging clinical applications and has been used to screen serum for genetic diseases[81] and has been useful in the detection of erb-B2 transcription in breast cancer[82].

The technique relies on having unique, known sequences of DNA either side of the segment to be amplified. Short DNA oligonucleotides complementary to the flanking sequences are required and are known as primers. DNA may be heated in order to denature the double helix and become single strands. Upon cooling, double stranded DNA reforms. If an excess of oligonucleotide primers complementary to the sequences flanking the segment of interest are added, they will preferentially anneal to the segment and with the addition of a DNA polymerase enzyme, a second strand complementary to this segment will be produced. The DNA polymerase of the thermophile algae Thermus aquaticus (Taq.) is stable at the temperatures required to cause dissociation of double stranded DNA[83]. Use of Taq polymerase allows a rapidly repeating cycle of denaturation, primer annealing and sequence extension to occur and is known as a polymerase chain reaction (PCR). It is a process that was first reported in 1985[84] and has since been modified to incorporate Taq polymerase and an automated thermocycler[85]. The PCR reaction amplifies DNA. mRNA may be reverse transcribed in order to form complementary DNA (cDNA) using a reverse transcriptase (RT) enzyme. RT enzymes were originally derived from retroviruses and are now manufactured from cloned viral genes. Using this technique, it is possible to rapidly detect very small amounts of mRNA.

The first step in the assay is the enzymatic conversion of RNA to a single-stranded cDNA template. This is followed by exponential amplification in a PCR reaction (Figure 6). Dedicated RNA and DNA dependant DNA polymerises may be used in single or separate reactions. This allows for the customisation of individual RT-PCR assays. Separation of the RT and PCR steps allows a stable library of cDNA to be

generated which may be stored for long periods, alternatively a single polymerase which acts as both an RNA and DNA-dependant DNA polymerase may be used in a single reaction thereby minimising error and risk of contamination.

4.5.1 Reverse transcription

Two commonly used reverse transcriptases (RTs) are avian myeloblastosis virus revere transcriptase (AMV-RT) and Moloney murine leukaemia virus reverse transcriptase (MMLV-RT). RNA transcripts may have significant secondary structure that affect the ability of the RNA-dependant DNA polymerase (RT) to generate transcripts[86] and may also affect RT-PCR quantification. AMV-RT is the most robust RT, retains significant polymerisation up to 55^{o}C and may also eliminate any problems associated with RNA secondary structure. MMLV-RT however has significantly less RNAse H activity, which can interfere with the synthesis of long amplicons[87;88].

The RT step may be primed by specific primers, random hexamers or oligo-dT primers. Use of random hexamers and oligo-dT primers can maximise the number of mRNA molecules that may be analysed from a very small sample of RNA. mRNA specific primers were used for the purposes of this research however since they decrease background priming and use of random hexamers can overestimate mRNA copy numbers up to 19-fold[89].

Figure 6. PCR reaction. The graph demonstrates product accumulation during the exponential and plateau phases of the reaction (log scale).

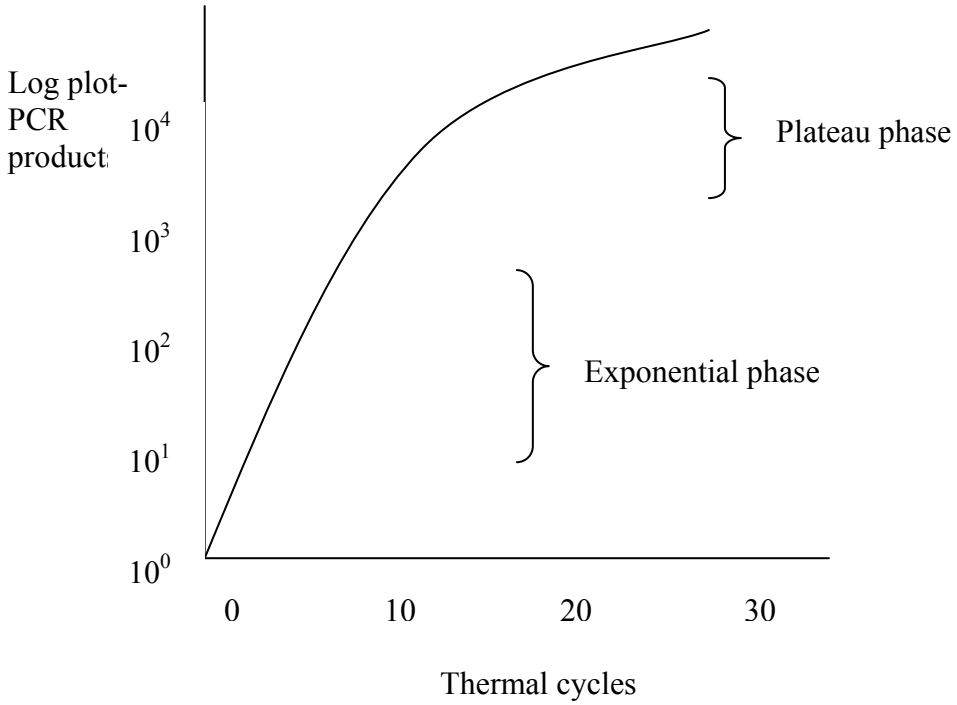

4.5.2 The Polymerase Chain Reaction

A variety of thermostable DNA-dependant polymerases are available and differ in their processivity, thermal stability, fidelity and ability to read modified triphosphates such as deoxyuridine and deoxyinosine in the template strand[90;91].

The most commonly used enzyme, Tag DNA polymerase was used for the purpose of this research. It has an oligonucleotide which is labelled at one end (5') with a fluorescent group and has a quencher at its 3' end (Figure 7). It has a 5'-3' nuclease activity but lacks a 3'-5' proofreading exonuclease activity.

The labelled oligonucleotide and primers were added to the PCR assay. When the fluorescent and quenching groups are close together, the emissions from the reporter dye are absorbed by the quencher dye and so the fluorescent emission is low. As the DNA is amplified, an increasing amount of oligonucleotide probe hybridises to the denatured DNA. During the extention phase of the PCR cycle, the 5'-3' exonuclease activity of the polymerase cleaves the fluorophore from the probe. As the fluorophore moves away from the quencher, there is an increase in fluorescence. This is measured in proportion to the amount of DNA synthesized during the PCR. The Stratagenee Mx4000 as used in this study, contains photomultiplier tubes in order to detect the fluorescence.

4.5.3 One-enzyme RT-PCR

The one enzyme system is useful where target RNA contains extensive secondary structure. It utilises *Thermus thermophilus* (Tth) polymerase which is a DNA polymerase with intrinsic RT but no Rnase H activity[92]. This technique is particularly useful in reducing the amount of hands-on time in the experimental set up and therefore minimises the potential contamination of reaction mixtures. A study has also shown the RT-PCR reactions using Tth polymerase may be more robust and resistant to inhibitors[93]. The drawbacks of this technique are that it is not as sensitive as the two-enzyme technique[94;95], the presence of Mn^{2+} ions reduces the fidelity of nucleotide incorporation[96], Tth polymerase lacks a 3'-5' exonuclease proofreading activity and first strand synthesis must be initiated from specific rather than random primers.

Figure 7. Polymerase chain reaction using Taqman technology. I: oligo labelled with fluorescent group, II: polymerase cleaves the fluorophore from probe, III: probe fluoresces as DNA polymerase seperates fluorophore from quencher.

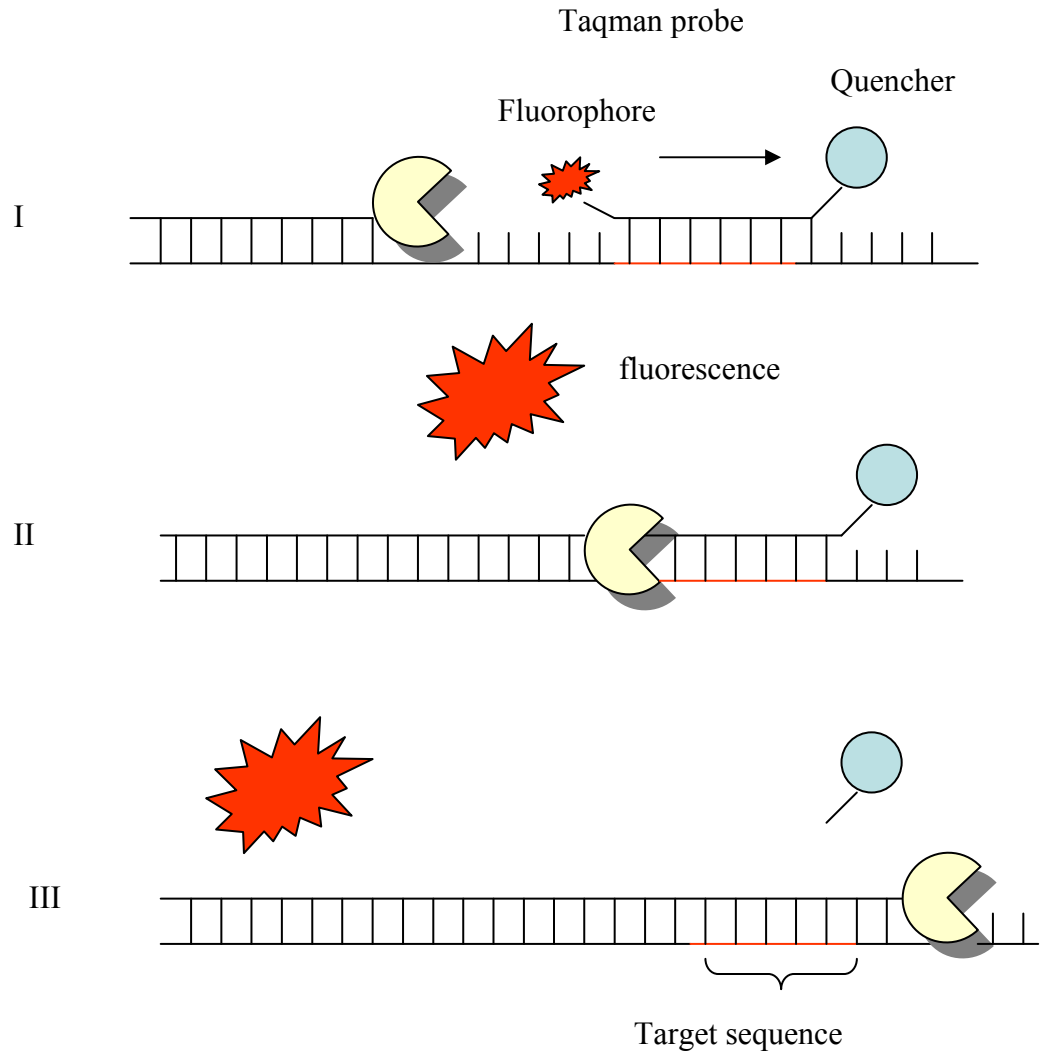

4.5.4 Instrument

The Mx4000 real-time multiplex quantitative PCR system was used to accurately quantify mRNA. It is a fluorescence based kinetic technique that uses a halogen lamp in order to excite fluorescence. It also contains an integrated personal computer that operates independently from the instruments embedded microprocessor, which is useful in protecting against loss of data.

All PCR was performed using the Mx4000 Mutiplex OPCR System. Samples were prepared in a 96 well microplate, which consisted of 12 strips of 8 wells. The strips were then placed in the thermal cycler. Amplification and detection occur in the same tube thereby minimising handling of samples ('one step' technique). The wells are cone shaped to improve temperature conductivity. The light source of the Mx4000 is a quartz tungsten halogen lamp. It excites a wide variety of fluorophores. Light from the halogen lamp is directed into the 4 fibre optic illumination paths.

Target sequences were amplified and detected in the same instrument and the rate of accumulation of amplified DNA was measured by the machine over the course of the PCR assay. The greater the concentration of target sequences, the fewer the number of cycles required to achieve a yield of amplified product. The concentration of target sequences may be expressed as the fractional cycle number (Ct) required to achieve a threshold of amplification. Ct may then be plotted against the log of the copy number to give a standard curve. This graph may then be used to quantify target sequences of unknown samples.

With every PCR assay, fluorescence values are recorded during each cycle and represent the amount of product amplified to that point in the amplification reaction. The greater the RNA template at the start of the reaction, the fewer the number of cycles taken to reach the point in which the fluoresecent signal is statistically higher than the background value. This point is referred to as the Ct and always occurs during the exponential phase of amplification.

The reporter signal is normalised to the fluorescence of an internal reference dye to allow for corrections in fluorescent fluctuations caused by changes in concentration or volume, and a Ct value is reported for each sample. The value may then be translated into a quantitative result by constructing a standard curve.

4.5.5 Optimisation

4.5.5.1 One step RT-PCR

The Brilliant^{TM} plus single-step quantitative RT-PCR core reagent kit was used for all RT-PCR assays. The single-step technique is useful for performing cDNA synthesis and PCR amplification in one tube and using one buffer. This permits the RT reaction to be carried out at increased temperatures using primers and significantly higher melting temperatures, while reducing both hands on time and the likelihood of introducing contaminants into reaction mixtures.
The kit also includes Stratascript^{TM} reverse transcriptase which is a novel Moloney murine leukaemia virus reverse transcriptase (MMLV-RT)

without any Rnase H activity. This mutant of MMLV-RT is able to produce larger yields of full length cDNA transcripts than wild type MMLV-RT which has substantial Rnase H activity. Rnase H has a highly undesirable degradative activity which can affect the reverse transcriptase function.

Surestart™ Taq DNA polymerase is used as part of the single-step technique. It is a modification of Taq2000™ DNA polymerase with hot start capability. Surestart™ Taq is able to reduce background and increase amplification of desired PCR products. The main drawback of this technique is that is may not be as sensitive as two-enzyme technique[94;95].

4.5.5.2 Primers and probes

The primers and probes used in this study included IGF-1, IGF-1R, IGFBP-3, GH, GHR, ghrelin, ghrelin 1B receptor, somatostatin, somatostatin receptor 5, c-myc, cycloxygenase-2 (COX-2), PCNA, vascular endothelial growth factor (VEGF 165 and 189), 1 alpha hydroxylase, Vitamin D receptor and HTERT. They were newly designed using Primer Express software and are shown in Table 1.

Table 1. Table of primer and probe sequences. Forward and reverse primers and Taqman probes (sequence 5'-3') used in RT-PCR.

Genes	Forward Primer	Reverse Primer	Taqman probe
IGF-1	CTTCAGTTCGTGTGTGGAG ACAG	CGCCCTCCGAC TGCTG	TTTTATTTCAACAAGC CCACAGGGTATGGC
IGF-1R	CTCCTGTTTCTCTCCGCCG	ATAGTCGTTGC GGATGTC GAT	TGGCCCGCAGATTTC TCCACTCGT
IGF-BP3	AGCACAGATACCCAGAACT TCTCC	TCCATTTCTCT ACGGCAGGG	CATATTCTGTCTCCCG CTTGGACTCGG
GH	CCC TCCAACAGG GAGGAAA	CGACTGGATGAG CAGCAG G	AGAAATCCAACC TAG AGCTGCTCCGCATCT
GHR	TTTGGAATATTTGG GCTAACAGTG	TCACCTCCTCTAA TTTTC CTTCCTT	AAGGATTAAAATGCT GATTCTGCCCCCAGT
Ghrelin	GGGCAGAGGATGAACTGGAA	CCTGGCTGTGCTG CTGGTA	TCCGGTTCAACGCCCCCT TTG
Ghreli 1B rec	TCGTGGGTGCCTCGCT	GCTGAGACCCACC CAGCA	AGGGACCAGAACCACAA GCAAACCG
Somatostatin	TCGCTGCTGCCTGAGGACCT	GCCAAGAAGTAC TTGGCCAGTTC	AACTGATTTCATCGGAAG CACCGG
SomatRec5	GCCGGCCTCTACTTCTTCGTG	CCGTGGCGTCAGC GTCCTTGG	CCGTCCTCTCAGGCTTCCT CTCGGA
cMyc	TGAGGAGACACCGCCCAC	CAACATCGATTTC TTCCTCATCTTC	CCAGCAGCGACTCTGAGG AGGAACA
Cox-2	GAATCATTCACCAGGCAAATTG	TTTCTGTACTGCG G GTGG AAC	TTCCTA CCACCAGCA ACCCTGCCA
PCNA	TTAAATTGTCACAGA CAAGTAATGTCG	TGGCTTTTGTAAA GAAGT TCAGGTAC	TGGTTCATTCATCTCTAT GGTAACAGCTTCCTC CT
VEGF-165	TGTGAATGCAGACAAAGAAAGA	GCTTTCTCCGCTC TGAGCAA	AGAGCAAGACAAGAAAA TCCCTGTGGGC
VEGF-189	TGTGAATGCAGACCAAAGAAAG A	CGTTTTTGCCCCT TTCCC	AGAGCAAGACAAGAAAA TCCCTGTGGGC

1α hydrox	GCTATTGGCGGGAGTGGAC	GCCGGGAGAGCTCATACAGA	CCCAAGAGAGCGTGTTGGACACCG
Vit D recep	ATCTGCATCGTCTCCCCAGAT	AGCGGATGTACGTCTGCAGTG	TGATTGAGGCCATCCAGGACCGC
htert	AGTTGCAAAGCATTGGA	ACCTCTGCTTCCGACAGC	AGCTGCACCCTCTTCAAGTGCTGTCTGA

Taqman probes are linear with the fluorophore at the 5' end and the quencher either at the 3' end or internal. If the probe is intact, no fluorescence is emitted from the fluorophore. During the annealing phase, the primer and probe hybridise with the target. The DNA polymerase then displaces the probe and the 5' nuclease activity of the DNA polymerase separates the fluorophore from the quencher. During each PCR cycle, fluorescence may then be detected as it accumulates. The probes should have a melting temperature of 7-10^{o}C higher than that of the primers. The ideal concentration should be determined empirically, ideally being the lowest concentration, which results in the lowest Ct with an adequate fluorescence.

Probe concentration is usually in the 100nM range and they must compete for binding to their target with the amplification primers, which are present in greater concentrations. As amplification primers are extended as soon as they bind to their targets, the hybridisation target sequence is rapidly masked with newly synthesised DNA. Therefore the melting temperature (Tm) of the probe must be significantly greater (approximately 10^{o} C) than that of primers, to ensure that they hybridise before the primers. Most probes used here were approximately 30 bases in length with a G/C content of approximately 50%. This ensures good specificity and a Tm high enough to be useful under PCR conditions.

Primers should bind to separate exons to avoid false positive results arising from amplification of contaminating genomic DNA. RNAse-free DNase was used in the purification of RNA preparations, as the intron/extron boundaries were unknown. Primer selection is based on estimated melting temperatures (Tm), the desire for small amplicon size and location of the probe. They must be designed to exact specifications

and the Taqman technology provides its own primer and probe design programme known as Primer Express.

The optimal concentration of upstream and downstream primers is also the lowest concentration which results in the lowest Ct with an adequate fluorescence. When used with Taqman probe, the primer concentration may be varied between 50 to 300 nM and should be determined empirically. Too great a primer concentration may result in mispriming and accumulation of non-specific product. Too low a primer concentration is less problematic for real-time assays as target copy numbers will have been calculated well before the primer supply is used up.

The optimal length for single stranded primers is approximately 15-20 bases, the G/C content should be between 20-70% and their Tm should not differ by more than 1-2^{0}C. The minimum Tm should be 58^{0}C and the maximum should be 60^{0}C. PCR primers were designed with similar annealing temperatures for all targets to be amplified.

4.5.5.3 Magnesium chloride

Magnesium chloride concentration requires strict control as it can affect the specificity of the PCR primers and probe hybridisation. The ideal concentration is that which results in the lowest Ct and the highest fluorescence at a given target concentration. The $MgCl_2$ concentration may be titrated from 2-6mM with increments of 0.5mM; in these experiments, $MgCl_2$ concentration of 3mM was found to be optimal.

In addition, $MgCl_2$ can increase the melting temperature (Tm) of double stranded DNA and forms soluble complexes with dNTPs which can produce the actual substrate that the polymerase recognises. High concentrations of dNTPs therefore interfere with polymerase activity and affect primer annealing by reducing free $MgCl_2$.

4.5.5.4 Internal reference dye

A passive reference dye was used to provide a stable baseline to which the samples were normalised. The dye provided was diluted to 1:200 and a fresh solution was made up for each assay.

4.5.6 PCR Reaction and conditions

The Brillant^{TM} plus single-step quantitative RT-PCR core reagent kit was taken from storage at -80^{0}C and defrosted on ice. The reference dye was diluted to a solution of 1:200 with DEPC water. Each experimental reaction was made up to a volume of 25µl per sample. Each reaction was performed in duplicate, therefore the final volume per sample was 50µl.

The following reagents were then pipetted, in order, into an autoclaved eppendorf. A master mix for all samples was made up at the beginning of an experiment to reduce pipetting error.
2.5µl of 10x core RT-PCR buffer
1.5µl of 50nM magnesium chloride
2µl of dNTP mix
1.25µl of primer mix (forward and reverse)
0.25µl of StrataScript RT poymerase
0.25µl of SureStart Taq DNA polymerase
0.38µl of diluted reference dye
0.5µl of probe
2µl of RNA template
14.37µl of nuclease-free DEPC water to make solution up to a final volume of 25µl

This solution was then placed in the centrifuge at 13,000 rpm for 2 minutes. 46µl of the mix was then pipetted into each individual microcentrifuge tube and 4µl of experimental RNA was added. For each assay 2 positive controls (liver RNA), 2 negative controls (water) and approximately 6 amplicons (serially diluted) were run in parallel.

Pipetting up and down then mixed each one and the pipette tip was discarded each time. The microcentrifuge tubes were then placed in the centrifuge for 3 minutes at 300 rpm. 25µl of each experimental reaction was then aliquotted into duplicate microcentrifuge tubes. The optics caps were then carefully and firmly positioned onto the microcentrifuge tubes. The tubes were then placed into the centrifuge for a further 3 minutes at 300 rpm.

Taking care not to disturb the samples, the microfuge tubes were then transferred into the thermal plate. The reaction and thermal profile were then set up using the software package on the connecting PC. The thermal profile used for each PCR reaction in shown below (Figure 8).

The data was collected at each 'END' point. Using the software, it was possible to determine the Ct values for each sample performed in duplicate.

Figure 8. Thermal reaction conditions for each PCR reaction. Stages 1 and 2 =RT, stage 3=PCR (45 cycles).

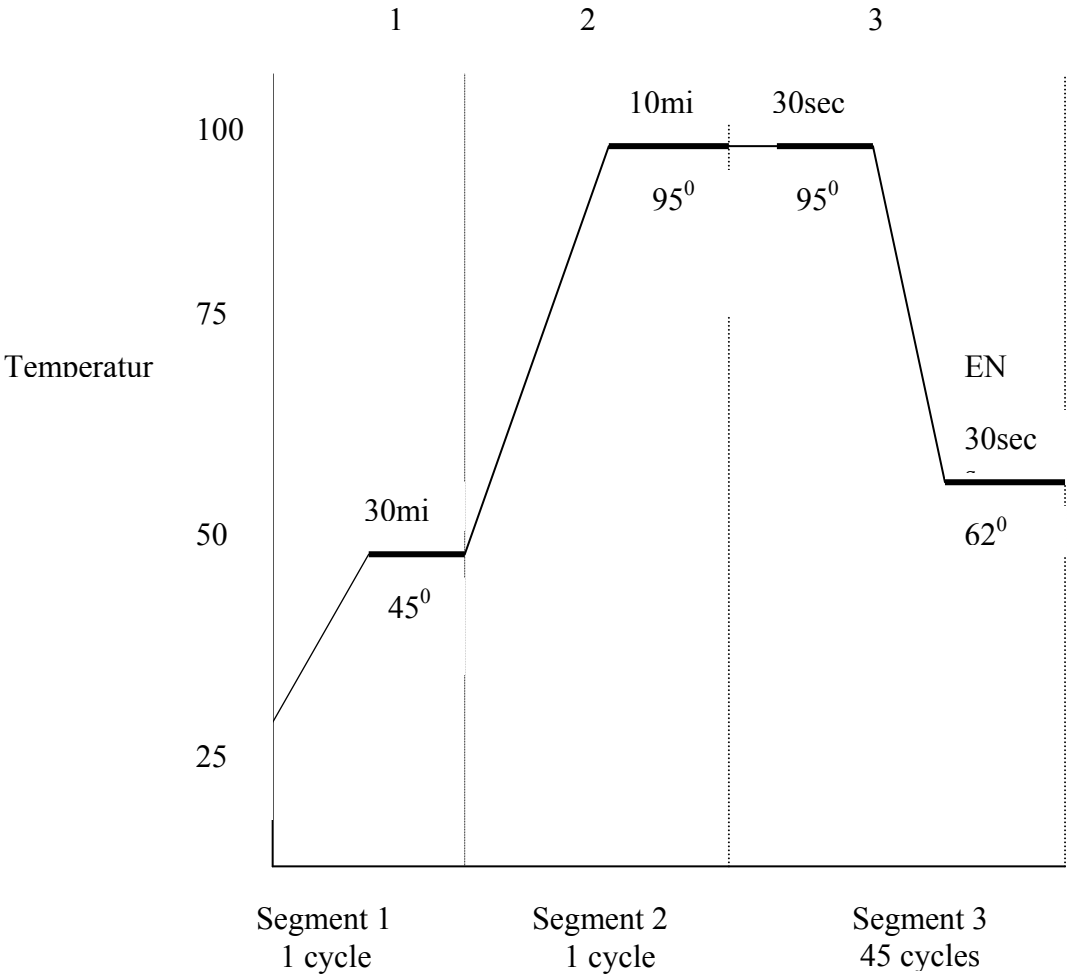

4.5.7 Quantification

Quantification of mRNA may be performed by quantitative or semi-quantitative methods[97]. Commonly, semi-quantitative methods are employed by sampling the RT-PCR reaction mixture and dot-blot analysis[98] which are not precise and laborious. Quantitative techniques may be competitive or non-competitive[99;100].

Non-competitive RT-PCR involves the co-amplification of the target with a second RNA molecule under reagent concentrations and conditions so that there is no competition between target and standard[101]. In these circumstances, quantification may be unreliable as the efficiencies of the RT and PCR steps may vary. Competitive quantification involves spiking into the RNA samples before RT of known amounts of RT-PCR amplifiable competitors that should be synthetic RNA molecules. The internal standard shares the same primer recognition and internal sequences as the primary target and so competes for reagents. Both should be amplified with the same efficiency as they are virtually identical and their amplicons may be distinguished by the addition of a restriction enzyme site to the standard[102] or by varying its size[103]. A series of PCR tubes containing the target are spiked with serial dilutions of known copy numbers (10^7, 10^6, 10^5 etc) of the internal standard. The higher the concentration of the internal standard, the more likely the primers will bind and amplify it rather than the target. Gel electrophoresis may therefore be performed and a comparison can be made of ethidium bromide stained standard and target amplicons to allow target quantification[104]. There is still however, approximately 10% error and this method may still not result in absolute quantification as differences in amplification efficiency between target and competitor will remain

undetected.

4.5.7.1 Normalisation

It is well established that an appropriate standard needs to be used within each PCR experimental assay. The accepted method is to amplify a cellular RNA at the same time as the target, which serves as an internal reference against which other RNA may be normalised[105]. The ideal standard should be expressed at a constant level among different tissues, at all stages of development and should be unaffected by experimental treatment[106]. The problem with this method is that errors easily occur in the amount of starting material between samples. There may also be differences in the amount of RNA obtained from different tissue types e.g normal and malignant tissue, and differences also exist when samples have been taken from different patients. Therefore, obtaining an ideal standard that accommodates these differences is an important part of the assay.

Three commonly used RNAs to normalise gene expression include the mRNAs specifying the housekeeping genes glycerldehyde-3-phosphate-dehydrogenase (GAPDH), β-actin and ribosomal RNAs (rRNA). GAPDH is ubiquitously expressed by most tissues and its expression has been shown to be constant at different times throughout experimental manipulation[107;108]. Evidence does suggest however that GAPDH concentrations vary greatly amongst individuals[109], during pregnancy[110], with developmental stage[111;112] and during cell cycle[113]. It has also been shown to be up regulated in tumours and this variation therefore suggests that its use as a normal control may be inappropriate.

β-actin is also moderately expressed in most cell types. It is traditionally used as an internal standard in PCR assays. Several studies however have shown that transcription levels may vary widely in breast epithelium cell culture studies[114]. rRNA constitutes 85-90% of total cellular RNA are generated by a distinct polymerase[115] and their levels are less likely to vary under conditions that affect the expression of mRNAs[116]. rRNA transcription can however be affected by biological factors, drugs and may vary amongst individuals[114]. It is also expressed at much higher levels than target mRNAs and cannot be used for normalisation when targets have been enriched for mRNA as it is lost during mRNA purification.

There are obviously inherent problems associated with normalising to an internal standard and with comparing copy numbers between samples obtained from different individuals or tissues. In this study we normalised copy numbers relative to total RNA concentration. Little is known however about the total RNA content per cell of different tissues *in vivo* or how this may vary between individuals and between normal and malignant tissue. Bustin *et al* addressed some of these issues by obtaining blood from healthy patients and counting and purifying nucleated blood cells. RNA content was quantitated and little variation was observed in amount of total RNA per cell thereby confirming the validity of this technique in comparing results between individuals[117].

RNA concentration was determined accurately using the Agilent Bioanalyzer and also confirmed using Ribogreen quantification as described earlier. Copy numbers of target genes were then recorded as copy numbers per μg total RNA. The drawbacks of this approach include the fact that total RNA may be increased in highly proliferating cells and

so this may affect the accuracy of comparing absolute copy numbers between normal and malignant tissue[106]. In order to compare our normalisation technique with the standard housekeeping gene method, GAPDH mRNA expression was measured on all samples according to the PCR protocol.

4.5.7.2 Generation of standard curves

Standard curves were constructed with each experimental reaction in order to determine the absolute quantification of mRNA transcription. This method allows the copy number per cell to be determined. A standard curve was constructed for each amplicon thereby ensuring accurate reverse transcription and PCR amplification profiles (99). The amplicons were diluted serially as follows; 10^{-10}, 10^{-9}, 10^{-8}, 10^{-7}, 10^{6}, 10^{5}, 10^{4}, 10^{3}, 10^{2} and 10^{1} using TE buffer. These samples were then run alongside each RT-PCR assay and the Ct values obtained were used to construct an absolute standard curve. A linear graph was obtained from three independent serial dilutions of amplicon and assaying each dilution in duplicate, together with positive and negative controls. This allows the copy number per cell to be determined from absorbance. The dilutions were made over the range of copy numbers expected from the target mRNA expected in the experimental samples in order to maximise accuracy.

4.6 Immunohistochemistry

4.6.1 Introduction to immunohistochemistry

Immunohistochemistry allows the identification and localisation of proteins on tissue sections using antibodies linked to enzymes that produce colour changes in indicator dyes. This involves the binding of a primary antibody to the antigen and secondly, the detection and visualistion of the bound antibody by one of a variety of enzyme based chromogenic systems. The type of chromogenic substrate depends in the type of enzyme used e.g aminoethyl carbazole (AEC) and diaminobenzidine (DAB) may be used with horseradish peroxidise. DAB substrate has a high sensitivity and produces an insoluble, permanent brown precipitate which has a high contrast in photographs. Amplification of the staining may be achieved by using antibodies and enzymes which combine through binding proteins such as the avidin biotin system. This system essentially involves three steps; primary antibody, biotin-labelled secondary antibody and avidin-biotin-peroxidise complex. A lattice-like complex is therefore produced which is attracted to the site of biotin-labelled antibody to give sensitive staining[118].

4.6.2 Tissue and its preparation

4.6.2.1 Sample preparation

Immunohistochemistry against IGF-1 was performed on 3□l sections of paraffin embedded blocks of 24 randomly selected paired samples of breast tumour and adjacent normal tissue, which had previously undergone RNA analysis. The avidin biotin complex (ABC) immunohistochemistry method was used[119].

4.6.3 Protocol for DAB staining

Tissues were prepared using standard fixation and paraffin embedding techniques courtesy of the Pathology Department, St Bartholomew's Hospital. Paraffin sections were then dewaxed and rehydrated according to the following standard procedures. Novozymes GroPep's IGF-1 Antiserum (PABCa) was used for IGF-1 detection in paraffin sections. For each specimen, one slide was stained as per protocol and one was used as a negative control and so was treated with just horse serum and no antibody. Sections of paraffin embedded human liver were used as a positive control.

4.6.3.1 Standard dewaxing procedure

The slides were placed into a metal rack and then placed into a glass jar containing xylene for 5 minutes. The rack was then placed into a second container of xylene for another 5 minutes to dewax. The samples were then rinsed in 100% absolute alcohol (BDS) for 3 minutes, then in separate containers of 100% alcohol for 3 minutes, 90% alcohol for 3

minutes and 70% alcohol for 3 minutes. The slides were not allowed to dry between any of the steps.

100ml of 10x citrate buffer was added to 900ml of distilled water. This citrate buffer was then added to a microwave dish and its pH was made sure to be 6.0. HCL or NaOH was added if needed to make the pH=6.0.

4.6.3.2 Antigen retrieval

After the dewaxing procedure, slides were placed into a glass jar containing 3% H_2O_2 in methanol (30 mls of 3% H_2O_2 in 270ml of methanol) for 10 minutes. The 100ml citrate buffer was placed in the microwave for 12 minutes to heat up. Slides were then moved into a plastic rack, as the metal rack cannot go into the microwave. The plastic rack was rinsed in water and then placed into the hot citrate buffer. The microwavable container was then closed and heated in the microwave for 4 minutes.

Once finished the container was removed and the plastic rack of slides was placed under running water. Water was poured into a metal tray. Each slide was taken from the rack, excess water was drained off by blotting with paper taking care not to disturb the tissue section. The margins of the tissue section were then marked using an Immedge pen to aid viewing of the small section. Horse serum was defrosted under running water. The slide was then placed on the tray and the tissue section covered in horse serum, taking care to use enough volume to completely cover the section. The tray was then left for 5 minutes at room temperature.

4.6.3.3 Primary antibody incubation

Novozymes GroPeo's IGF-1 Antiserum, affinity purified for Immunohistochemistry (Product code PABca) was made up in solution of 1 in 50 using phosphate buffer saline (PBS): 12µl antibody plus 600µl PBS. This antibody was added only to positive slides and left out for the control slides. 200µl of antibody was used for big tissue sections like breast samples and 100µl for smaller sections such as the liver samples. The horse serum was then removed from the positive samples and a good covering of primary antibody was added. The lid was placed on the metal try to provide a humidified atmosphere. The tray was then placed in the incubator at 42^0C for 1.5 hours.

4.6.3.4 Secondary antibody incubation

The secondary antibody solution was made up of 2.35ml of PBS, 150ml of horse serum (3 drops) and 50ml of secondary antibody, biotinylated anti-rabbit IgG antibody (1 drop), all using Vectastain kit (ABC kit). This mixture was vortexed and then placed in the fridge.

The tray was then removed from the fridge. The slides were placed back into the rack and then into a glass jar containing PBS for 2 x 5 minutes to wash off excess antibody. Excess PBS was blotted off the slide using tissue paper, taking care to avoid tissue section. The slides were then placed back onto the metal tray, the edges dried and each tissue section was covered fully with the secondary antibody solution. The lid was then placed onto the tray and incubated at room temperature for 30 minutes.

4.6.3.5 Tertiary antibody incubation

The tertiary complex consisted of HRP-avidin and biotin complex which binds to the secondary antibody. The solution was prepared at least 30 minutes before use.

To prepare the tertiary antibody 2.5ml of PBS, 1 drop of A (avidin) and 1 drop of B (biotin) was added. They were then vortexed quickly and placed in the fridge.

DAB was made using 2.25ml water, 250ml of substrate buffer, 2 drops of liquid DAB and 1 drop of H_20_2. This mixture was then labelled, placed in the fridge and protected from light. The slides were then taken out of the tray and washed twice in PBS for 5 minutes. The slides were then taken out of the wash and dried around the tissue sections. Tertiary antibody was then added and the slides were left at room temperature for 20 minutes in the tray.

After incubation with the tertiary antibody the slides were washed twice with PBS. The slides were then taken out of PBS and covered with DAB to the sections. The DAB was left for 5 minutes, and as soon as the brown colour was seen developing the slides were washed in water.

Each DAB slide was then counterstained by rinsing with Gills haematoxylin for 30 seconds, followed by 1% acid-alcohol for 1 second. Slides were then rinsed under running water for 2 minutes, 70% alcohol for 2 minutes, 90% alcohol for 2 minutes, absolute 100% alcohol for 2

minutes, in another absolute alcohol 100% for 2 minutes, in xylene for 2 minutes and then another xylene for 2 minutes.

The cover-ups were set up by adding Depex mounting medium (Gerr) –to DAB slides. The cover slides were then placed onto the slides and left to dry overnight, and viewed under the microscope the next day.

Sections of liver were used as a positive control in each run. The sections of normal breast and cancer were randomly mixed prior to staining.

4.6.4 Quantification of Immunohistochemical Staining

Sections of normal and malignant breast tissue were randomly mixed prior to staining. Assessment was performed in a blinded manner on two separate occasions by a single investigator. In order to quantify IGF-1 protein expression, a scoring system based on the proportion of positive cells and intensity of staining was employed. This was scored as follows and a separate score determined for stromal and epithelial staining:

Proportion of positive staining cells:

Number of cells	Score
<5%	1
5-50%	2
>50%	3

Intensity of staining of positive cells:

Intensity	Score
0 (none)	1
+ (weak)	2
++(moderate)	3
+++(strong)	4

The two scores were added together to give a score out of 7. Separate scores were calculated for epithelial and stromal staining. A score of 1-3 was classified as negative and a score of 4-7 was positive. These two scores were combined together to give a total score out of 14: 1-6=negative and 7-14=positive with a subgroup of 10-14= strongly positive. The procedure was repeated again without viewing the first set of results, with the mean of both readings used as a final score.

4.7 Serum IGF-1 and IGFBP-3

4.7.1 Sample collection

5ml of blood was venesected from each patient undergoing breast cancer surgery involved in the study. Blood was taken from 36 patients on the day prior to breast surgery (pre-operative) and from 35 patients up to 6 months after surgery (post-operative). These samples were not paired. Of the post-operative group patients were classified into those taking Tamoxifen (T) and those not taking Tamoxifen (NT).

The blood was collected aseptically into glass tubes containing no additives and care was taken to avoid needlestick injury. All samples were centrifuged at 10,000rpm for 15 minutes at room temperature. Serum was separated from red cells by pipetting and collecting in a fresh round bottom eppendorf. These samples were frozen at -80^0C.

4.7.2 Serum IGF-1

This was measured on all samples by an in-house radioimmunoassay after formic acid-acetone extraction, courtesy of the Growth Factor Lab, St Bartholomew's Hospital[120]. Total IGF-1 was measured after the samples were separated from their binding proteins by acetone extraction. The mean intra- and inter- assay coefficient of variation were 2.7% and 10.4%, respectively. The assay sensitivity was 45ng/ml.

4.7.3 Serum IGFBP-3

Serum IGFBP-3 was measured using active IGFBP-3 enzyme-labeled immunosorbent assay (ELISA Kit; Diagnostic Systems Laboratories, Inc. Webster, Tx, USA). The mean intra- and inter- assay coefficients of variation were 7.2% and 10.2% respectively. The assay sensitivity was 0.04 ng/ml. All samples and reagents were brought to room temperature before the assay. Serum samples were thoroughly mixed prior to use and diluted to 1:100 in the standard dilutent containing 0ng/ml IGFBP-3 (in a protein based buffer). Wells to be used were then marked on the microtitration strips, all samples were performed in duplicate. 25µl of each standard (2,5,20,50 and 100 ng/ml IGFBP-3), control (samples of

high and low concentration IGFBP-3) and the unknown diluted samples were pipetted into each well. 50µl of assay buffer was then added to each well. The wells were then placed in a microplate shaker at approximately 700 rpm for 2 hours (room temperature). Each well was then aspirated and washed five times with wash solution. The microplate was then inverted and blotted dry on absorbant material.

The conjugate solution was then prepared by diluting the antibody-enzyme conjugate concentrate at a ratio of 1:50 using the assay buffer. 100µl of this solution was then added to each well. The microplate was then shaken again at 700 rpm for 1 hour at room temperature. Each well was then washed and aspirated a further five times followed by inverting the plate and blotting dry.

100µl of tetramethylbenzidine (TMB) solution was then added to each well and the plate then re-shaken at 700 rpm for 10 minutes at room temperature. 100µl of stopping solution (0.2M sulphuric acid) was then added to each well. The micropate was then placed in a microplate reader and absorbance measured at 450nm (background absorbance was set to 600nm).

4.8 *In vitro* tissue explant culture

4.8.1 Tissue collection

Fresh breast tissue samples were obtained from breast cancer patients undergoing surgery. As before, fully informed consent was obtained (Appendix A). All cancers were clinically palpable (>1-2cm in size).

4.8.2 Tissue processing

Each breast specimen was transported from surgery to the Department of Pathology immediately after removal from the body. The specimen was orientated, inked and a sample of tumour (T) and adjacent normal tissue (AN) was excised by the pathologist. AN was macroscopically normal tissue taken as far away from the tumour as possible. Care was taken when dissecting normal tissue to obtain glandular tissue and avoid fat. Each sample was then placed into separate sterile cryogenic vials containing serum-free Dulbecco's Modified Eagle's Medium (DMEM) and transported quickly to the laboratory.

4.8.2.1 Preparation of the medium

The stock solution used for all experiments contained 500ml DMEM, 1g of bovine serum albumin, 5ml of penicillin/streptomycin mix (10mg/ml) and 0.5ml of amphotericin (0.25µg/ml). All were added to the medium via a sterile filter and stored at $+4^0$C. In order to carry out this culture technique, large tumours were necessary to provide enough tissue. The size of the specimen therefore was a limiting factor. The samples of

normal and malignant breast tissue were then cut into 6 small pieces (~5-10 mg) under sterile conditions. One sample was retained as 0hrs sample. The remaining 5 pieces were placed in the wells of a 24 well plate. 100µl of stock solution was added to each well. They were then incubated at 37^0C in an incubator with 5% carbon dioxide. A sample was removed after 6hrs, 18hrs, 24hrs, 48hrs and 72hrs and immediately frozen for subsequent analysis at a later date using the LDH and MTS assays.

4.8.2 2 MTS Cell proliferation assay

The MTS Cell Proliferation Assay was used to assess viability of the tissue explant technique. The assay uses mitochondrial respiration as an indicator of cell viability. It is based on the reduction of the MTS reagent (a tetrazolium salt) to form an insoluble dark blue formazen product with the emission of light at 490nm, by active mitochondria with NADPH/NADH. This bioreduction results in a coloured product soluble in tissue culture medium.

A solution of 5mg/ml MTS dissolved in PBS was made up and filter sterilised. 100µl of MTS dye was added to the tissue after incubation in 500µl media. All experiments were carried out in duplicate in a 24 well plate. The plate was then incubated in a CO_2 incubator at 37^0C for 4 hours. After 4 hours, 100µl of the media/dye mix was taken from the sample and control wells and an absorbance reading at 490nM wavelength was performed.

For each time frame there was a corresponding well with medium only + explant and dye. This positive control was subject to the same conditions as the other experimental wells and was assayed with MTS in the same

way. Triton-X results in maximum disruption of plasma membranes and was used as a negative control. To make up a solution of 2% Triton, 200µl of triton 100 was added to 9.8ml medium and mixed thoroughly. 500µl of this solution was then added to a well containing an explant and incubated as protocol.

In order to assess the effect of the different tissue weights on the MTS absorbance, normal and malignant breast tissue was dissected into approximately 20 explants of visibly different sizes. These explants were placed into a 24 well plate. MTS dye and medium were added to each sample well including 2 control wells. After 4 hours of incubation at 37^0C 5% CO2, the plate was removed from incubation. The tissue samples were removed, blotted dry using absorbant paper and weighed. The absorbances were read and MTS values adjusted according to their weights. Results were obtained as absorbance minus that of negative control (media only).

4.8.2.3 LDH Cytoxicity detection

The lactate dehydrogenase (LDH) assay is another colorimetric method, which is used to evaluate cell death. It is based on the measurement of cytoplasmic enzyme activity that is released by damaged cells into cell culture medium upon damage to cellular plasma membranes. In contrast to the MTS assay, which measures metabolic activity, this assay quantitates cell death and lysis. The amount of enzyme activity detected in the culture medium correlates to the proportion of lysed or dead cells[121].

A two-step enzymatic reaction occurs when LDH containing tissue free media is incubated with the reaction mixture provided in the kit. The first reaction involves reduction of NAD+ to NADH/H+ by LDH catalysed conversion of lactate to pyruvate. In the second step, a catalyst from the reaction mixture transfers H/H+ from NADH/H+ to tetrazolium salt INT. This transfer results in the reduction of INT (yellow) to formazoan (red). The amount of red colour produced therefore correlates with the amount of formazoan formed and hence the amount of dead/ membrane damaged cells in the medium. Absorbance may then be read spectrophotometrically.

100µl of assay medium was added into duplicate wells of a 96 well plate. The reaction mixture was prepared immediately prior to the assay: by mixing 250µl of bottle 1 (catalyst) with 11.25ml of bottle 2 (INT dye solution). After mixing thoroughly, 100µl of reaction mixture was added to each well and incubated for 30 minutes at 20-25^{0}C. The plate was protected from light during this time. The 96 well plate was then placed into a microplate reader and the absorbance read at 490nm.

A negative control of medium only was used for each time point. A positive control of 2% Triton added to an explants was also used for each time frame. Triton was used to ensure maximum LDH release for the purposes of a positive control.

In order to assess the inter-assay variability of the LDH assay, duplicate sets of samples were used, where tissue availability allowed. Also intra-assay variability was assessed by assaying each well 12 times.

4.9 Affymetrix Chips Protocol

We have demonstrated that IGF-1 is expressed in both normal and malignant breast tissue, but that approximately 10% of primary breast cancers reveal no IGF-1 mRNA expression. However the molecular difference between IGF-1 positive and IGF-1 negative tumours is unknown. To investigate the molecular differences between IGF-1 positive and IGF-1 negative breast cancers cRNA microarray analysis was used. The IGF-1 expression status of 76 primary breast cancers was identified using real-time RT-PCR ('Taqman'). Two IGF-1 positive and two IGF-1 negative breast tumours were subsequently randomly selected and cRNA microarray analysis was performed using the Affymetrix U133A Chip protocol. The resultant data was analysed using Gene Spring 6.0 expression analysis software.

A flow diagram of the steps involved is:

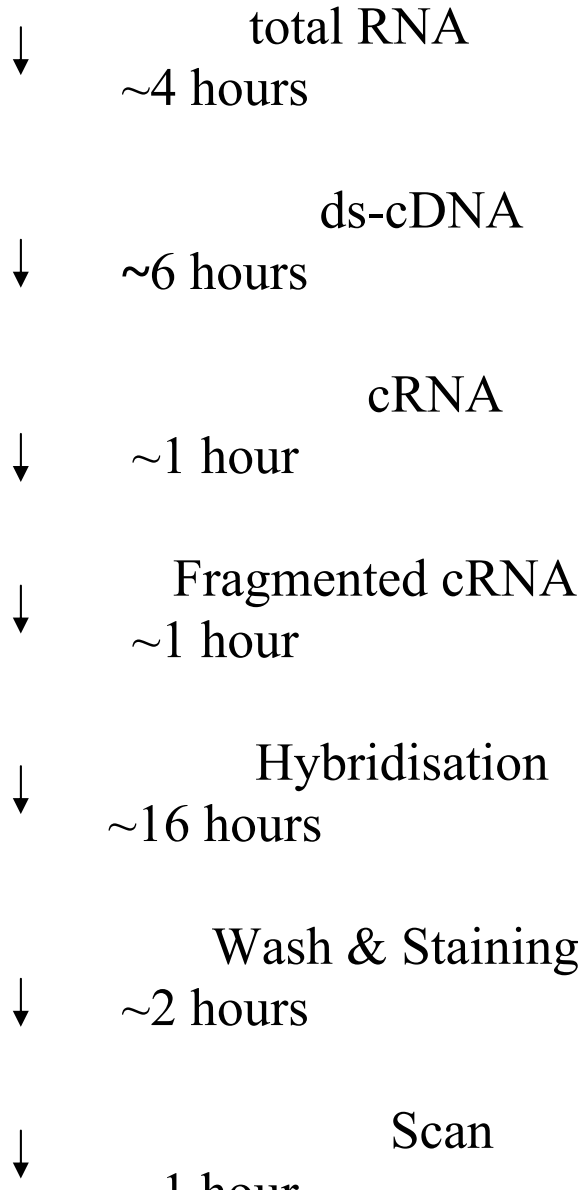

~ 4 working days

4.9.1 First strand cDNA synthesis

RNase free microtube tubes and pipette tips were used throughout this experiment. We started with 5-10µg total RNA per sample.
The following were placed in a microfuge tube on ice:

5-10 µg total RNA	5-10µl
T7-(T)24 primer (100pmol/µl) HPLC purified	1µl
DEPC dH2O	0-5µl
Final volume	11µl

This mixture was pipetted and spun briefly as necessary. It was then incubated at 65-70^{0}C for 10 minutes. The tubes were then placed on ice, and a master mix was made up on ice:

(5x) First Strand Buffer (thraw at 37^{0}C, put on ice)	4µl
DTT (0.1M)	2µl
DNTPs (10mM each)	1µl
Final volume	7µl

This was mixed by pipetting and spun briefly as necessary. 7µl of master mix was added to each reaction tube, and then incubated at 42^{0}C for 2 minutes. Superscript II reverse transcriptase (200U/µl) was added (1µl for 5µg of total RNA or 2µl for 10µg) making a final volume of 20µl. The

tube was tapped to mix and spun briefly as necessary. It was then incubated at 42^0C for 1 hour in a waterbath then placed on ice before proceeding to "Second strand cDNA sythesis".

4.9.2 Second strand cDNA sythesis

All the reagents and first strand reaction tubes were placed on ice. The master mix was assembled in a new microfuge tube on ice:

DEPC treated dH2O	91µl
(5x) Second Strand Buffer	30µl
dNTPs (10mM each)	3µl
E. Coli DNA Ligase (10U/µl)	1µl
E. Coli DNA Pol I (10U/µl)	4µl
E. Coli Rnase |H (2U/µl)	1µl
Final volume	**130µl**

The mixture was mixed by vortexing and then spun as briefly as necessary. 130µl of this master mix was added to each of the first strand reaction tubes (150µl final volume). This was mixed with pipetting and spun briefly. It was then incubated at 16^0C for 2 hours in a water bath in a cold room. This reduces condensation. 2µl (10U) T4 DNA Polymerase was added. It was then incubated for 5 minutes at 16^0C. 10µl 0.5M EDTA pH 8.0 was then added, causing the final volume to be 162µl. The tube was placed on ice and proceeded to "Clean-up of double stranded cDNA".

4.9.3 Clean-up of double stranded cDNA

This method used Phase-Lock tubes, which contained a gel that acts to separate the aqueous and organic layers in the phenol extraction permitting more complete recovery of the aqueous phase. The Phase-Lock tube was spun in a microfuge at maximum for 30 seconds to allow the gel to settle to the bottom of the tube. To the sDNA reaction, an equal volume (approximately 162µl) of at room temperature buffer saturated phenol was added. This was made by adding 65µl of Alkaline Buffer (10mM Tris HCL pH 8.0, 1mM EDTA) to 1ml of phenol-chloroform-isoamyl alcohol 25:24;1 (AMBION 9732). It was then vortexed for 2 minutes and spun. The mixture was placed into a Phase-Lock tube and not vortexed again. It was spun at maximum in a microfuge for 2 minutes. The upper (aqueous) phase was transfered to a new tube, and to this was added:

0.5 x volume NH40Ac (7.5M)	75µl
Glycogen (5mg/ml)	4µl
2.5 x volumes Ethanol (100%)	375µl

The solution was mixed by tapping the tube. It was then spun at maximum at room temperature in a microfuge for 20 minutes. The supernatant was decanted being careful not to displace the pellet. The pellet was washed twice with 500µl (80%) cold ethanol, then spun at

maximum for 5 minutes. All the ethanol was removed with a pipette (it was spun again briefly to collect any residual ethanol on the sides of the tube and ethanol was removed a second time using a pipette). The pellet was allowed to air dry for 5-10 minutes, then resuspended in 12µl of DEPC treated H2O, before proceeding to the *in vitro* transcription reaction.

4.9.4 Synthesis of cRNA (IVT reaction & labelling)

All the reagents and double stranded cDNA were thawed at room temperature. The following reaction was assembled at room temperature:

Ds-cDNA	12µl
DEPC treated dH2O	10µl
(10x) HY Reaction Buffer	4µl
Biotin-labelled ribonucleotide	4µl
DTT	4µl
RNase Inhibitor Mix	4µl
T7 RNA Polymerase	2µl
Final volume	**40µl**

The above reagents were mixed by pipetting and spun as briefly as necessary. These were incubated at 37^0C for 5 hours. The reaction was gently mixed every half hour by tapping the tube and spun as briefly as necessary, before proceeding to the "Clean-up of cRNA" step.

4.9.5 Clean-up of cRNA and quantification

This required the Qiagen Rneasy Mini Kit. The following was added to the *in vitro* transcription tubes (40µl final volume):

DEPC treated H2O	60µl
RLT buffer	350µl

The solutions were mixed thoroughly by pipetting. 250µl (100%) ethanol was added. The solution was mixed by pipetting but not spun. The sample (700µl) was applied to an RNeasy spin column sitting in a 2ml collection tube. It was then spun at 8000 xg for 15 seconds.
The RNeasy spin column was transferred into a new 2ml collection tube. 500µl RPE buffer was added and spun at 8000 xg for 15 seconds. The RNeasy spin column was transferred into a new 2 ml collection tube. 500µl RPE buffer was added, and spun at maximum speed for 2 minutes. The spin column was transferred to a fresh 2ml tube to prevent any carry-over of the RPE buffer. It was then spun at maximum speed for 1 minute to dry the RNeasy membrane from ethanol. The spin column was transfered into a new 1.5ml collection tube. The cRNA was eluted by placing 50µl DEPC dH2O on the middle of the membrane of the column. It was left at room temperature for a couple of minutes, then spun at 8000 xg for 1 minute to elute.

The Ribogreen RNA Quantification Kit (see previously in Methods) was

used to discover the concentration of cRNA. The minimum required cRNA concentration for the Affymetrix chip is 0.6µg/ul.
A sample of the cRNA (500ng-1µg)(denature cRNA at 65-70^{0}C for 10 minutes in denaturing loading buffer) was run on a 1% agarose gel along with a marker spanning 200bp to 3 kb (a DNA marker gives a rough idea of the size). The product should look like smear from about 100 bp to 2 kb with a brighter region from 500bp to 1 kb. Denaturing loading buffer contained:

(10x) MOPS	0.5µl
Deionized Formamide	5µl
Formaldehyde 37%	1.75µl
(10x) loading buffer (50% glycerol, 0.1 mg/ml BB)	1µl
DEPC treated dH2O	1.7µl
EtBr (10mg/ml)	0.05µl
Final volume	10µl

10µl was added to 1-1.5µg of cRNA
It was then frozen by placing tube on dry ice and storing at –80^{0}C.

The following was added to the eluate:

0.5 x volume NH40Ac (7.5M)
2.5 x volumes Ethanol (100%) ice cold

It was precipitated at –20^{0}C for 1 hour to overnight. It was then spun at maximum for 30 minutes at 4 ^{0}C. The pellet was washed twice with 500µl (80%) cold ethanol, and spun at maximum for 5 minutes. All the ethanol was removed with a pipette (spun again to collect any residual ethanol on the sides of the tube and ethanol was removed a second time

using a pipette). The pellet was allowed to air dry for 5-10 minutes. It was then resuspended to a final concentration of 1 or 2 µg/µl. The tube was placed on dry ice to freeze and then stored at -80^0C or proceed directly to cRNA fragmentation.

4.9.6 cRNA Fragmentation

Example for 0.75µg/µl final concentration:

30µg cRNA	1 to 32µl
5x Fragmentation Buffer	8µl
DEPC treated dH2O	to 40µl

5x Fragmentation Buffer (200mM Tris-acetate, pH 8.1, 500mM KOAc,150mM MgOAc)
The fragmentation buffer is made with Rnase free reagents. Tris-containing solutions should not be treated with DEPC; however once H_2O has been DEPC-treated it can be used for making the Tris solution.
The following components were combined to a total volume of 20mL.

4.0mL 1M Tris acetate pH8.1 (Triza base adjusted with glacial acid)
0.64g MgOAc
0.98g KOAc
DEPC-treated H_2O to 20 mL

They should be mixed thoroughly and filtered through a 0.2um vacuum filter unit. They were then aliqoted and stored at room temperature.

They were then incubated at 94^0C for 35 minutes in a PCR block, and then placed on ice after incubation. A sample of the fragmented cRNA (~1µg) was run on a 1% agarose gel along with a marker spanning 200bp to 3 kb (a DNA marker gives a rough idea of the size). The fragmentation should produce a distribution of RNA fragment sizes from approximately 35 to 200 bases. The fragmented cRNA was stored undiluted at -80^0C until ready to perform the hybridisation.

4.9.7 Hybridisation Cocktail for human HGU133A arrays

Before adding to the cocktail, one vial of the 20x Eukaryotic Hybridisation Controls and one vial of the Oligo B2 were heated at 65^0C for 5 minutes. The two vials were completely thawed before heating. They were vortexed for complete mixing then spun briefly. The following were mixed for each target:

Fragment cRNA	15µg
Control Oligonucleotide B2	5µl
20x Eukaroyatic Hybridisation Controls	15µl
Herring sperm DNA (10mg/ml)	3µl
Acetylated BSA (50mg/ml)	3µl
2x Hybridisation buffer	150µl
DEPC dH2O to final volume	**300µl**

2x Hybridisation buffer (Final 1X concentration is 100mM MES, 1M [NaCl], 20mM EDTA, 0.01% Tween 20)

For 50 mL:

8.3 mL of 12X MES Stock

17.7mL of 5M NaCl

4.0mL of 0.5 M EDTA

0.1mL of 10% Tween 20

19.9mL of water

store at 2-8^{0}C, and shield from light

The tissue samples were sent to the Affymetrix operator for washing, staining and scanning of U133A chips. U133A chips were equilibrated to room temperature for use. The probe cocktail was heated to 95^{o}C for 5 minutes, cooled to 48^{o}C then centrifuged at top speed for 5 minutes. The probe cocktail was hybridised to the chip overnight at 45^{o}C in a rotating hybridization oven set at 60rpm. Next day the cocktail was removed and replaced with low stringency wash buffer. The chips were washed and stained with Streptavidin Phycoeurythrin (SAPE) in a GeneChip 400 Fluidics wash station using protocol EukGE_WS2v4. Chips were scanned using an Agilent GeneArray 2500 Scanner. Data supplied was an average of 2 scans.

5. Statistical Evaluations

All statistical calculations were carried out using Stats Direct (Ashwell, Herts, UK). P values<0.05 were considered significant.

5.1. RT-PCR data

All RT-PCR data was expressed as a copy number per µg total RNA. The median value was calculated for normal and malignant tissue for each marker. The differences in median copy number between tissue types for each marker were then calculated using non-parametric tests (Mann Whitney U).

In order to determine any correlation between markers, Spearman Rank correlation was used. In order to assess any correlation between IGF-1 mRNA expression and clinico-pathological variables, samples were divided according to each variable i.e. ER positive, ER negative, lymph node positive and lymph node negative. The difference in median copy numbers for each variable was then calculated using a non-parametric test, Mann Whitney U.

5.2 IGF-1 protein expression

The differences in staining between the normal breast tissue versus tumour and stromal versus epithelial staining were evaluated using a two sided Fisher exact test or a chi-square test as appropriate. Correlation with clinicopathological parameters used Spearmen rank correlation.

5.3 Serum IGF-1 and IGFBP-3 levels

In order to calculate differences in serum IGF-1 and IGFBP-3 levels in pre and post-operative breast cancer patients, Mann Whitney U non-parametric tests were used. For determining the IGF-1 ratio for each patient, each value was first corrected for age and then ratios were obtained and compared again using the Mann Whitney U test.

5.4 Tissue explant culture

For MTS and LDH assays absorbance readings were recorded and mean values and standard errors of the mean were calculated. The differences were then compared using the Mann Whitney U test.

6.0 Results

6.1 Results of the RNA quantification

6.1.1 Ribogreen standard curve results

Table 2 demonstrates the RNA concentration of normal and malignant breast samples using the Ribogreen Method. Each value is a mean of 3 values of fluorescence. The Ribogreen method is particularly useful for detecting smaller concentrations of RNA. For example, it can be seen that normal breast tissue produces approximately 3-4 fold less RNA than breast tumours. This technique was therefore used to detect the smaller quantities of RNA extracted from normal breast tissue. Unfortunately, unlike the Agilent Bioanalyzer, this technique only provides information on quantity and not quality of RNA.

Table 2 RNA concentration (ng/ul) quantified using Ribogreen

Normal	RNA conc ng/ul	Tumour	RNA conc ng/ul
100N	62.31	101T	32.3
106N	150.66	104T	14.27
108N	125.83	107T	31.26
109N	3.48	108T	325.8
110N	29.91	109T	158.36
111N	68.83	110T	394.26
112N	15.23	111T	28.59
113N	34.94	116T	273.51
114N	10.1	118T	60.22
116N	6.14	119T	128.99
117N	8.55	120T	142.64
118N	22.26	121T	99.36
121N	7.02	122T	184.65
122N	13.11	123T	146.39
123N	23.75	124T	143.45
124N	103.93	126T	126.99
125N	26.29	127T	240.68
126N	76.83	128T	521.35
127N	20.36	129T	150.08
129N	28.35	130T	3.04
130N	6.91	131T	15.82
131N	6.08	132T	67.15
132N	3.14	133T	11.89
133N	18.59	134T	71.35
134N	5.44	136T	97.5
135N	4.58	135T	99.81
137N	5.47	137T	28.52
139N	6.17	140T	595.3
140N	55.49	141T	127.75
147N	12.96	147T	201.9
150N	35.32	150T	197.84
153N	14.26	153T	28.25
155N	5.31	155T	61.17
156N	42.83	156T	331.07
157N	44.31	157T	353.93
160N	17.35	160T	95.69

6.1.2 Results of Agilent Bioanalyzer

For each lab chip analysed, the well marker ladder should produce 7 clear peaks in order to confirm that the gel has worked (Fig 9). Figure 10 shows a typical electropherogram and an autoradiograph of extracted RNA from a breast sample using the Agilent Bioanalyzer. The graph shows three peaks, the first is a marker and indicates if the gel is working well. The next two peaks represent the two ribosomal peaks, with a ratio that should be 2:1 (28S:18S). This ratio in conjunction with a smooth baseline indicates good quality RNA. RNA degradation is seen with a decreasing ratio of ribosomal bands, additional peaks and a decrease in the RNA signal or shorter fragments. The height of the peaks should also compare well with the marker peak thereby indicating a good concentration of RNA. The Agilent software is then able to calculate the ratio of the sample peaks to the marker peak thereby providing the RNA concentration for each sample.

Figure 9 Representative electropherogram (A) and autoradiograph (B) of a single RNA sample. The ladder demonstrates 6 RNA peaks and 1 marker peak. The marker allows comparison with other chips.

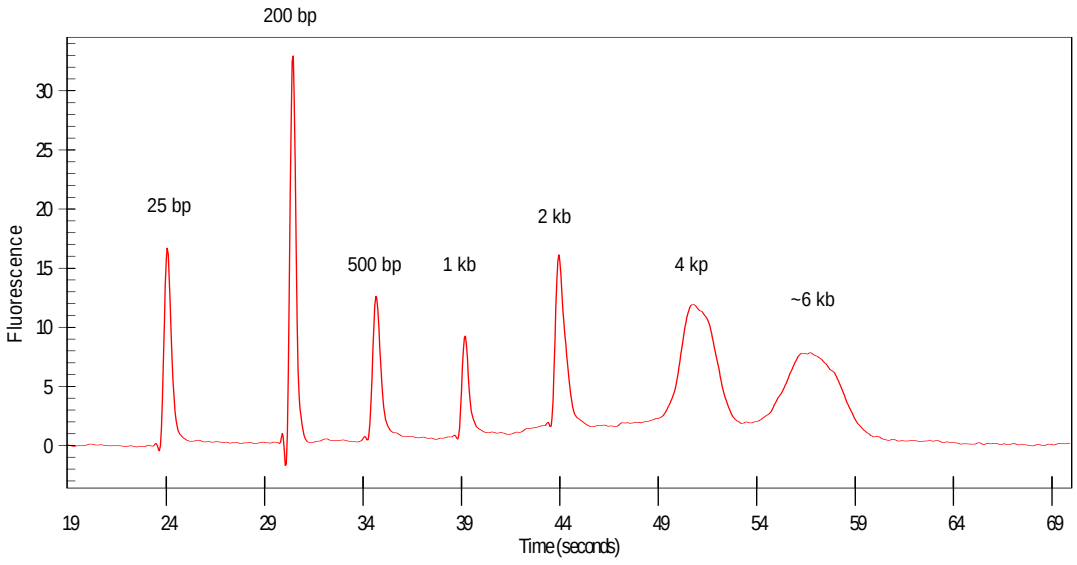

A B

Figure 10. Electropherogram of extracted RNA from a breast sample demonstrating high quality and quantity of total RNA. Two ribosomal peaks are seen with a ration of 2:1.

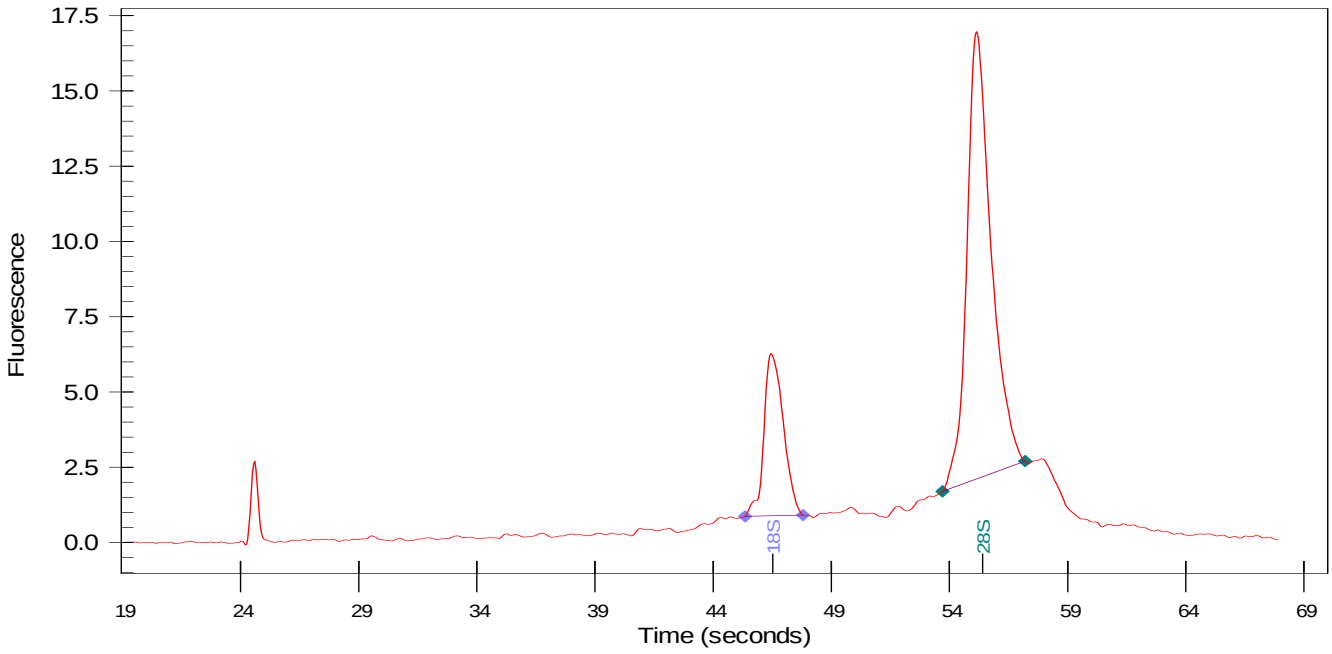

6.2 Results from RT-PCR

6.2.1 Results from generation of standard curve from amplicons

A linear graph was constructed for each amplicon, the high and low Ct values were discarded to correct for pipetting errors and the average of the remaining values was calculated. The Ct value is inversely proportional to the log of the initial copy number[122]. Standard curves were constructed by plotting the Ct values with 95% confidence intervals against the logarithm of the initial copy numbers. The copy numbers for each of the experimental samples were than calculated after real-time amplification from the linear regression of that standard curve.

Figure 11 demonstrates the amplification plot of IGF-1 amplicon. Serial dilutions of the IGF-1 amplicon were diluted as previously described. The run was repeated if successful amplification did not occur.

Figure 11. Amplification plot of IGF-1 amplicons. Serial dilutions result in different fluorescence values. The smaller the Ct value, the higher the concentration of DNA.

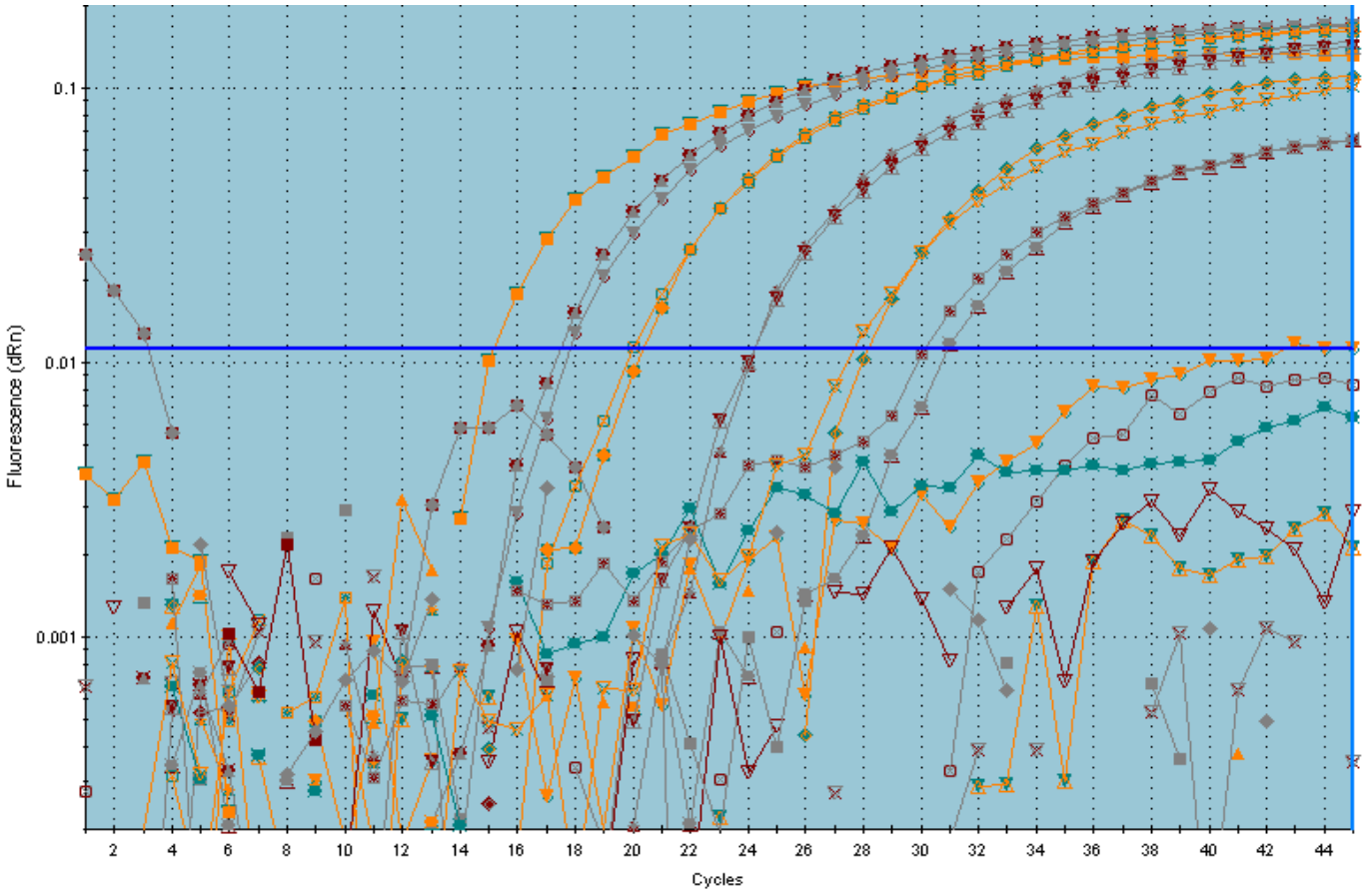

Table 3. IGF-1 expression in normal and malignant breast tissue

Normal	IGF-1	Tumours	IGF-1
108N	4.82E+06	108T	1.35E+06
109N	3.06E+06	109T	9.83E+05
111N	7.64E+06	111T	6.45E+06
116N	4.87E+06	116T	4.02E+07
118N	3.24E+07	118T	1.17E+07
121N	2.48E+07	121T	4.80E+06
122N	2.74E+07	122T	2.22E+07
123N	2.04E+07	123T	1.16E+07
124N	7.80E+07	124T	6.80E+06
126N	2.98E+07	126T	4.53E+07
127N	8.68E+06	127T	1.24E+06
129N	1.21E+07	129T	1.34E+07
130N	4.28E+07	130T	0.00E+00
131N	3.93E+06	131T	5.07E+05
132N	1.43E+07	132T	2.95E+06
133N	1.03E+07	133T	3.61E+07
134N	2.45E+07	134T	0.00E+00
135N	0.00E+00	135T	3.36E+06
136N	7.83E+07	136T	5.29E+06
137N	4.91E+07	137T	1.50E+07
140N	7.88E+06	140T	1.61E+06
147N	3.65E+07	147T	1.62E+07
150N	1.18E+07	150T	2.65E+06
153N	2.40E+07	153T	1.48E+07
155N	1.03E+06	155T	1.67E+05
156N	3.39E+06	156T	1.49E+05
157N	4.54E+06	157T	1.10E+07
160N	3.24E+06	160T	1.15E+07
162N	2.74E+04	162T	2.74E+04
164N	3.19E+07	164T	9.18E+06
166N	1.67E+07	166T	2.36E+07
167N	5.48E+06	167T	0.00E+00
172N	7.96E+06	172T	0.00E+00
173N	2.54E+06	173T	4.57E+05
174N	2.14E+06	174T	2.23E+06
175N	3.60E+07	175T	4.08E+06
176N	8.54E+06	176T	1.24E+07
178N	3.36E+07	178T	7.16E+06
181N	9.30E+06	181T	6.33E+06
183N	1.23E+07	183T	5.18E+06
184N	4.11E+07	184T	2.63E+07
185N	3.65E+07	185T	2.51E+06
186N	2.80E+07	186T	2.78E+06
187N	0.00E+00	187T	0.00E+00

194N	0.00E+00	194T	2.15E+06
196N	1.26E+07	196T	1.04E+07
200N	4.65E+06	200L	6.81E+06
202N	1.43E+07	202T	0.00E+00
203N	1.76E+07	203T	1.02E+07
204N	1.48E+07	204T	0.00E+00
205N	1.17E+07	205T	9.55E+06
206N	5.52E+06	206T	2.19E+06
209N	2.59E+06	209T	2.07E+07
210N	4.21E+06	210T	3.63E+05
212N	6.60E+06	212T	7.52E+05
215N	3.08E+05	215L	3.30E+06
216N	1.04E+06	216L	2.60E+06
217N	9.22E+06	217T	0.00E+00
218N	2.60E+06	218T	1.41E+06
220N	4.98E+06	220T	4.72E+05
225N	8.53E+05	225T	2.29E+06
227L	1.37E+05	227T	2.23E+05
232N	5.39E+06	232T	1.97E+06
234N	2.68E+06	234T	9.45E+06
241N1	1.01E+06	241T	4.22E+04
242N2	3.66E+06	242T	6.05E+05
243N2	3.15E+05	243T	0.00E+00
245N2	2.24E+05	245T	1.23E+05
248N2	3.98E+05	248T	2.25E+06
249N2	8.21E+05	249T	3.29E+04
258N	1.37E+06	258T	3.74E+06
259N	7.24E+04	259T	0.00E+00
269N	1.87E+06	269T	2.38E+06
273N	1.12E+06	273T	3.97E+05
278N	7.01E+06	278T	8.12E+05

Normal	IGF-1	Tumours	IGF-1
100NB	3.45E+06	101T	6.69E+06
106N	2.45E+06	104T	2.67E+06
110N	1.82E+07	107T	1.24E+06
112N1	4.44E+06	115T	3.03E+06
113N	1.44E+07	119T	5.97E+06
117N	2.27E+06	128T	1.39E+05
139N	2.42E+06	141T	1.10E+05
149N	7.84E+05	157T1	1.80E+03
154N	1.25E+06	161T	1.52E+06
159N1	3.37E+06	189T	6.14E+06
165N	5.79E+07	192T	2.87E+06
168N	8.37E+05	193T	1.48E+07
169N	7.20E+06	195T	5.70E+05
170N	1.93E+06	197T	2.93E+05
171N	1.03E+07	199L	1.33E+06
177N2	1.71E+06	214L	4.14E+05
182N	9.37E+05	222T	1.78E+05

191N	1.12E+07	223T	1.85E+05
198N	4.84E+06	224L	1.43E+08
199N	5.32E+03	233L	1.12E+07
201N	8.04E+06	266T	1.85E+06
207N	0.00E+00	267T	9.49E+05
208N	4.91E+07	279T	5.57E+05
221N	9.92E+05		

6.2.2 Results from individual markers

6.2.2.1 IGF-1 mRNA

IGF-1 mRNA was significantly down regulated in breast tumours compared to normal breast tissue, $2.3x10^6$ copy no/μg total RNA in tumours vs $6.6x10^6$ in normal breast tissue, $p<0.0001$. The range for IGF-1 mRNA expression in breast tumours is $1.80x10^3 – 1.43x10^8$. The range within normal breast tissue expression is $5.32x10^3$- $7.83x10^7$. In addition 10 tumours (4%) and 4 normal tissues (2%) did not express IGF-1 at all indicating an IGF-1 negative sub-group of breast tumours.

Looking at IGF-1 expression and correlating with clinical characteristics there was a significant increase in IGF-1 expression in lymph node positive tumours compared to lymph node negative tumours, $6.9x10^6$ copy number/μg total RNA in lymph node positive vs $1.5x10^6$ in lymph node negative tumours ($p=0.03$).

There was also an increase in IGF-1 expression in grade 2 and 3 tumours compared to grade 1 tumours, $7.9x10^6$ copy number/μg total RNA in grade 2 and 3 tumours vs $2.6x10^6$ in grade 1 tumours ($p=0.05$).

There was no significant difference in IGF-1 expression in presence of DCIS, vascular invasion, ER and PR status.

6.2.2.2 IGF-1 Receptor

This was expressed in all normal and malignant samples, with significant increase in expression in malignant tissue compared to normal tissue, $2.25x10^7$ copy number/μg total RNA in malignant tissue vs $1.17x10^7$ in normal tissue, $p=0.003$.

6.2.2.3 IGFBP-3

All the breast samples expressed IGFBP-3. There was a high level of expression of IGFBP-3 in all samples but no difference between the expression in normal and tumour tissue, $1.86x10^8$ copy no/μg total RNA in normal tissue vs $1.71x10^8$ in malignant tissue, non significant, p=not significant.

6.2.2.4 Growth hormone

In all the samples both normal and malignant expressed low levels of growth hormone with no significant difference between the two groups. Normal tissue vs malignant tissue was $8.4x10^4$ copy no/μg total RNA vs $3.18x10^5$, p=0.08.

6.2.2.5 Growth Hormone Receptor

Growth Hormone Receptor (GHR) was expressed in both normal and malignant tissue, but was significantly over expressed in normal tissue. $4.78x10^8$ copy number/μg total RNA in normal tissue vs $1.66x10^7$ in the malignant samples, p=0.0001.

6.2.2.6 Ghrelin

Ghrelin was found to be expressed in normal and malignant tissue with no statistical significant difference between the two. $3.2x10^5$ copy number/μg total RNA in normal tissue vs $5.24x10^5$ in the malignant tissue, p=not significant

6.2.2.7 Ghrelin 1B Receptor

Ghrelin 1B receptor (Ghr-1B-Rec) was expressed in normal and malignant tissue with no significant difference between the two groups. $5.5x10^5$ copy number/µg total RNA in normal tissue vs $2.8x10^5$ in malignant tissue, p=not significant.

6.2.2.8 Somatostatin

This was expressed in normal and malignant tissue with no significant difference in the expression, $3.46x10^5$ copy number/µg total RNA in normal tissue vs $2.07x10^5$ in malignant tissue, p=not significant. However when IGF-1 positive and IGF-1 negative samples were compared there was significantly increased expression of somatostatin in the IGF-1 negative samples, $9.8x10^8$ copy number/µg total RNA in the IGF-1 negative samples vs $1.07x10^5$ in the IGF-1 positive samples, p=0.002.

6.2.2.9 Somatostatin Receptor 5

This was expressed in normal and malignant tissue with no significant difference between the two tissues, $9.8x10^5$ copy number/µg total RNA in normal tissue vs $5.2x10^5$ in malignant tissue, p=not significant. In addition there was no difference between the IGF-1 positive and negative samples, $7.35x10^5$ vs $2.5x10^5$, p=not significant.

6.2.2.10 C-myc

C-myc was found to be expressed in both normal and malignant tissue at similar levels. $8.06x10^7$ copy number/µg total RNA in normal tissue vs $9.09x10^7$ in malignant tissue, p=not significant.

6.2.2.11 COX-2

All samples expressed Cox-2 mRNA. There was no significant difference between normal or malignant tissues, $2.55x10^7$ copy number/µg total RNA in normal tissue vs $1.5x10^7$ in malignant tissue, p=not significant.

6.2.2.12 PCNA

PCNA was expressed in normal and malignant tissue, and significantly was over expressed in tumours compared to normal tissue. $5.4x10^6$ copy number/µg total RNA in malignant tissue vs $2.8x10^6$ in normal tissue, p=0.014.

6.2.2.13 VEGF-165

Normal and malignant samples expressed VEGF with significant overexpression in malignant tissue compared to normal tissue. $5.88x10^8$ copy number/µg total RNA in malignant tissue vs $1.13x10^8$ in normal tissue, p=0.01.

6.2.2.14 VEGF-189

VEGF was expressed in both normal and malignant tissue with no significant difference in the amount of expression between the two groups. $6.79x10^6$ copy number/µg total RNA in normal tissue vs $1.41x10^7$ in malignant tissue, p=not significant.

6.2.2.15 1 alpha hydroxylase

The normal and tumour breast sample tissue expressed similar levels of 1 alpha hydroxylase, with no significant difference between the groups, normal vs tumour was $2.12x10^7$ copy number/µg total RNA vs $3.19x10^7$, p=not significant.

6.2.2.16 Vitamin D Receptor

Median VDR mRNA levels were significantly higher in tumours than normal tissue, $3.06x10^6$ copy number/µg total RNA in malignant tissue vs $1.7x10^6$ in normal tissue, p=0.002.

6.2.2.17 HTERT

HTERT was expressed in both normal and malignant tissue, but statistically was over expressed in malignant tissue. $1.3x10^5$ copy number/µg total RNA in malignant tissue vs $1.45x10^2$ in normal tissue, p=0.0000007.

Table 4. RT-PCR expression of markers in malignant and normal breast tissue. A positive correlation is seen with IGF-1, IGFR, GHR, PCNA, VEGF 165, Vitamin D receptor and HTERT.

Marker	Tumour	Normal	P value
IGF-1	$2.3x10^6$	$6.6x10^6$	P<0.0001
IGFR	$2.25x10^7$	$1.17x10^7$	P=0.003
IGFBP-3	$1.71x10^8$	$1.86x10^8$	P=n.s.
GH	$3.18x10^5$	$8.4x10^4$	P=n.s.
GHR	$1.66x10^7$	$4.78x10^8$	P=0.0001
Ghrelin	$5.24x10^5$	$3.2x10^5$	P=n.s.
Ghrelin 1B receptor	$2.8x10^5$	$5.5x10^5$	P=n.s.
Somatostatin	$2.07x10^5$	$3.46x10^5$	P=n.s.
Somatostatin receptor 5	$5.2x10^5$	$9.8x10^5$	P=n.s.
cmyc	$9.09x10^7$	$8.06x10^7$	P=n.s.
Cox-2	$1.5x10^7$	$2.55x10^7$	P=n.s.
PCNA	$5.4x10^6$	$2.8x10^6$	P=0.014
VEGF 165	$5.88x10^8$	$1.13x10^8$	P=0.01
VEGF 189	$1.41x10^7$	$6.79x10^6$	P=n.s.
1 alpha hydroxylase	$3.19x10^7$	$2.12x10^7$	P=n.s.
Vitamin D receptor	$3.06x10^6$	$1.7x10^6$	P=0.0017
HTERT	$1.3x10^5$	$1.45x10^2$	P=0.0000007

Table 4 Statistics: RT-PCR expression of markers in malignant and normal breast tissue

1. IGF-1 Mann-Whitney U test
Observations (x) in N-IGF-1 =75 median=6641960.35879 Normal
Observations (y) in T-IGF-1 =75 median=2332396.79075 Tumour
Normalised statistic=4.045925 (adjusted for ties)
Lower side p>0.9999 (H_1: x tends to be less than y)
Upper side p<0.0001 (H_1: x tends to be greater than y)
Two sided p<0.0001(H_1: x tends to be distributed differently to y)

95% confidence interval for difference between medians or means:
K=3430 median difference =3819731.4
CI=1800401.3 to 7007661.3

2. IGFR Mann-Whitney U test
Observations (x) in N-IGFR=75 median=11734367.45493 Normal
Observations (y) in T-IGFR=75 median=22521443.790011 Tumour
Normalised statistic=0.508682
Lower side p=0.9981 (H_1: x tends to be less than y)
Upper side p=0.0019 (H_1: x tends to be greater than y)
Two sided p=0.0038 (H_1: x tends to be distributed differently to y)

95% confidence interval for difference between medians or means:
K=1163 median difference=4652398.6
CI=1377619.7 to 9169386.1

3. IGFBP-3 Mann-Whitney U test
Observations (x) in N-IGFBP3=32 median=186400000 Normal
Observations (y) in T-IGFBP3=32 median=171256350 Tumour
Normalised statistic=0.993621 (adjusted for ties)
Lower side p=0.8397962 (H_1: x tends to be less than y)
Upper side p=0.1602038 (H_1: x tends to be greater than y)
Two sided p=0.3204075 (H_1: x tends to be distributed differently to y)

95% confidence interval for difference between medians or means:
K=367 median difference=2795000
CI=-2500000 to 9850000

4. GH Mann-Whitney U test
Observations (x) in N-GH=32 median=84046.993943
Observations (y) in T-GH=32 median=318296.59651
Normalised statistic=-1.718676
Lower side p=0.0428367 (H_1: x tends to be less than y)
Upper side p=0.9571633 (H_1: x tends to be greater than y)
Two sided p=0.0856734 (H_1: x tends to be distributed differently to y)

95% confidence interval for difference between medians or means:
K=367 median difference=-100649.45
CI=-764170.2 to 6086.8

5. GHR Mann-Whitney U test
Observations (x) in N-GH-R=32 median=478500000
Observations (y) in T-GH-R=32 median=16650000
Normalised statistic=4.994958 (adjusted for ties)
Lower side p=0.9999997 (H_1: x tends to be less than y)
Upper side p=0.0003 (H_1: x tends to be greater than y)
Two sided p=0.0001 (H_1: x tends to be distributed differently to y)

95% confidence interval for difference between medians or means:
K=428 median difference=-88348.249
CI=-196236.464 to -21046.492

6.Ghrelin Mann-Whitney U test
Observations (x) in N-Ghrelin=32 median=323500
Observations (y) in T-Ghrelin=32 median=524000
Normalised statistic=-1.45688 (adjusted for ties)
Lower side p=0.0725748 (H_1: x tends to be less than y)
Upper side p=0.9274252 (H_1: x tends to be greater than y)
Two sided p=0.1451496 (H_1: x tends to be distributed differently to y)

95% confidence interval for difference between medians or means:
K=367 median difference=-198800
CI=-2031000 to 43100

7. Ghrelin 1B receptor Mann-Whitney U test
Observations (x) in N-Ghr-1B-Rec=32 median=551345
Observations (y) in T-Ghr-1B-Res=32 median=283255
Normalised statistic=-1.000518 (adjusted for ties)
Lower side p=0.84147 (H_1: x tends to be less than y)
Upper side p=0.15853 (H_1: x tends to be greater than y)
Two sided p=0.31706 (H_1: x tends to be distributed differently to y)

95% confidence interval for difference between medians or means:
K=367 median difference=-1470.5
CI=-858000 to 10

8. c-Myc Mann-Whitney U test
Observations (x) in N-c-Myc=32 median=80600000
Observations (y) in T-c-Myc=32 median=90950000
Normalised statistic=-0.657938 (adjusted for ties)
Lower side p=0.255289 (H_1: x tends to be less than y)
Upper side p=0.744711 (H_1: x tends to be greater than y)
Two sided p=0.5105779 (H_1: x tends to be distributed differently to y)

95% confidence interval for difference between medians or means:
K=367 median difference=-14150000
CI=-51200000 to 27410000

9. PCNA Mann-Whitney U test
Observations (x) in N-PCNA =31 median=2870721.219345
Observations (y) in T-PCNA=31 median=5400355.815812
Normalised statistic=-2.447174
Lower side p=0.0071991 (H_1: x tends to be less than y)
Upper side p=0.9928009 (H_1: x tends to be greater than y)
Two sided p=0.0143981 (H_1: x tends to be distributed differently to y)

95% confidence interval for difference between medians or means:
K=355 median difference=-2277556.7
CI=-5153821.9 to -442362.6

10. VEGF-165 Mann-Whitney U test
Observations (x) in N-VEGF-165=35 median=113000000
Observations (y) in T-VEGF-165=35 median=588000000
Exact probability:
Lower side p=0.005628 (H_1: x tends to be less than y)
Upper side p=0.994372 (H_1: x tends to be greater than y)
Two sided p=0.011256 (H_1: x tends to be distributed differently to y)

95.5% confidence interval for difference between medians or means:
K=65 median difference=-452333
CI=-234553 to 4352227

11. VEGF-189 Mann-Whitney U test
Observations (x) in N-VEGF-189=35 median=6790000
Observations (y) in T-VEGF-189=35 median=14100000
Exact probability:
Lower side p=0.1834376 (H_1: x tends to be less than y)
Upper side p=0.8165624 (H_1: x tends to be greater than y)
Two sided p= 0.3668752 (H_1: x tends to be distributed differently to y)

95.5% confidence interval for difference between medians or means:
K=65 median difference=-4710000
CI=-26800000 to 5380000

12. HTERT Mann-Whitney U test
Observations (x) in N-HTERT=35 median=145
Observations (Y) in T-HTERT=35 median=130000
Exact probability (adjusted for ties)
Lower side p=0.0000003 (H: x tends to be less than y)
Upper side p=0.9999997 (H: x tends to be greater than y)
Two sided p=0.0000007 (H: x tends to be distributed differently to y)

95.1% confidence interval for differences between medians or means:
K=341 median difference=-117872.5
CI=-176831 to -20560

6.3 Results from Immunohistochemistry

6.3.1 Results of IGF-1 staining

6.3.1.1 DAB staining

Immunohistochemical DAB staining of the liver showed staining of IGF-1, with the negative samples not staining up, unlike the positive samples (Figure 12). In addition staining of IGF-1 in normal and malignant breast samples showed that all tissue samples expressed IGF-1 apart from the IGF-1 negative samples which showed no DAB staining (Figure 13).

6.3.1.2 Fluorescent staining

When the breast tumours were then stained with fluoresceine dye, positive staining was noted in the stroma of the tissue (Figure 14). In accordance with the DAB immunohistochemistry there was absence of staining in the IGF-1 negative samples.

Figure 12- IGF-1 staining of liver

A – Liver negative control

B-Liver staining positive for IGF-1

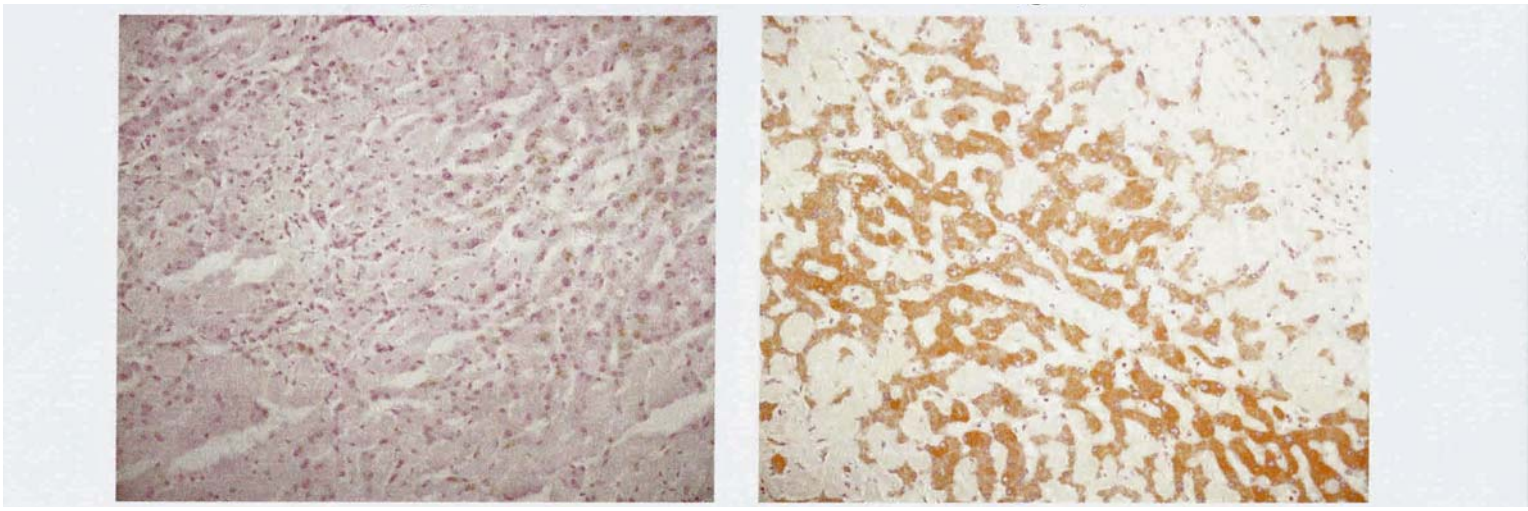

Figure 13- IGF-1 staining of malignant breast tissue

A **Negative control breast tumour staining** **B** **Breast tumour staining positive for IGF-1**

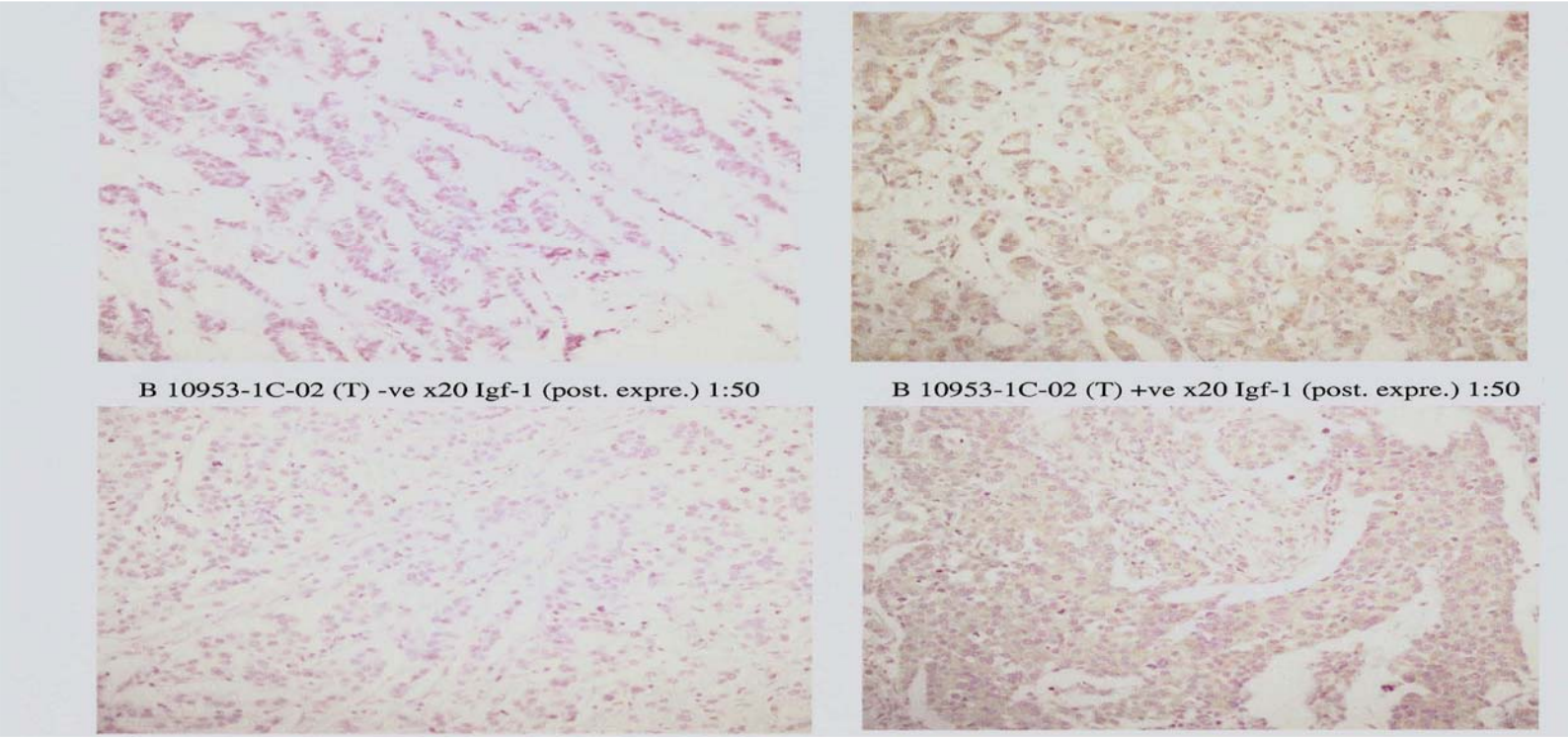

C **No staining in IGF-1 negative tumour** **D** **Staining in IGF-1 positive tumour**

Figure 14 – Fluorescent IGF-1 staining of malignant breast tissue

A – Negative control

B – IGF-1staining breast tissue

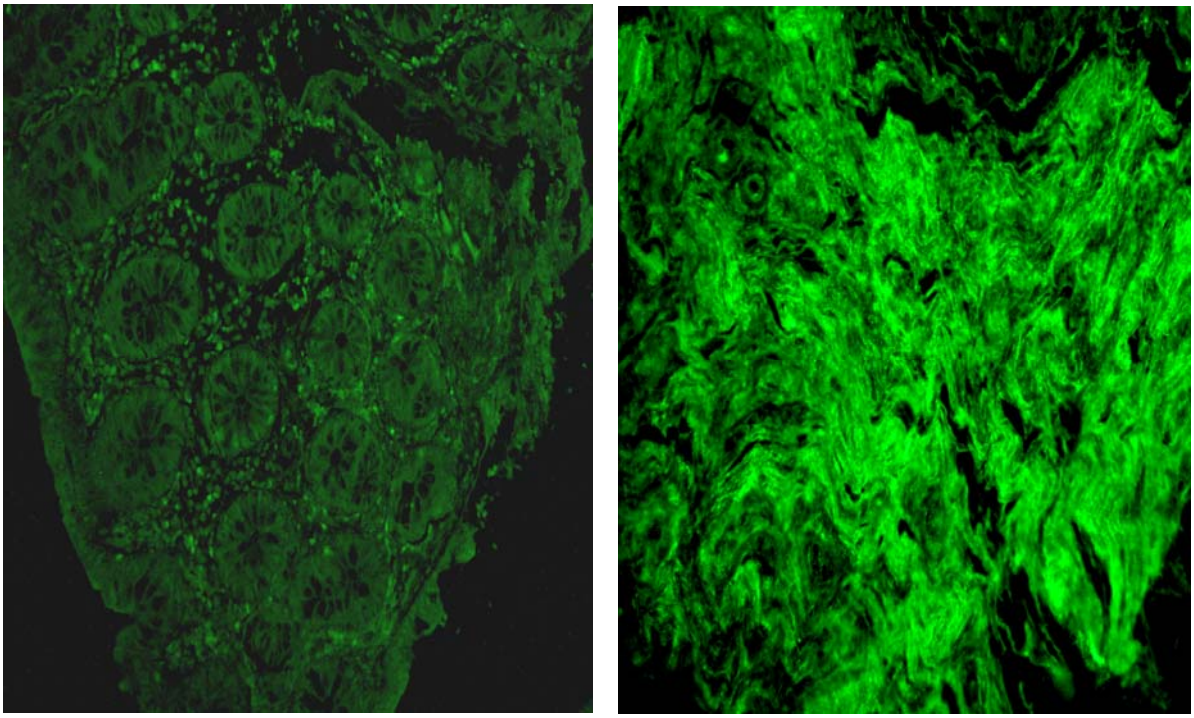

6.3.2 Results of GH staining

The normal and malignant breast tissue samples were then fluorescently stained for Growth Hormone (GH). All 10 samples were positive for staining with Growth hormone with a wide area of staining visible, in both the stroma and epithelial cells of the tissue. 13 negative samples were produced without the stain and these were totally negative results with little staining visible, therefore they were dark in nature.

6.3.3 Results of Ghrelin staining

Immunohistochemical staining of ghrelin in normal and malignant breast tissue was done using fluorescent staining. The samples showed extent widespread staining of fluorescence throughout the tissue (see figure 15).

Figure 15- Ghrelin staining of breast

Negative control

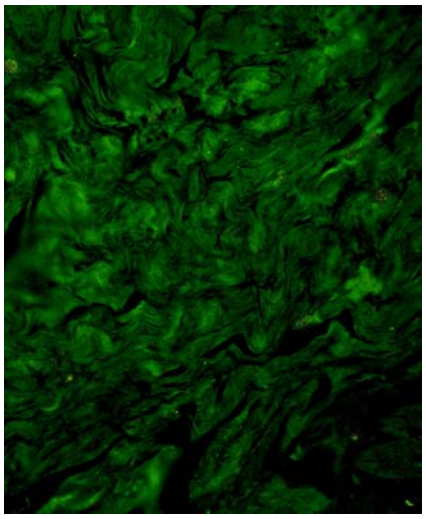

Normal breast tissue

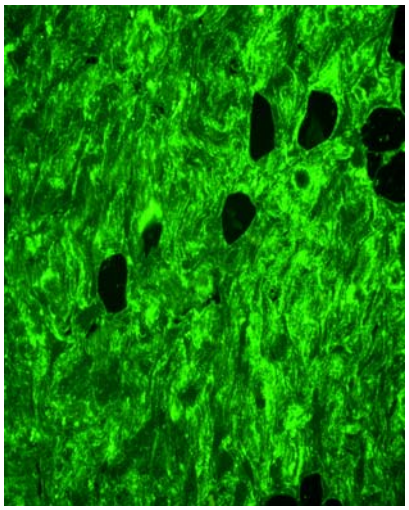

6.4 Results of serum IGF-1 and IGFBP-3

6.4.1 Serum IGF-1

There were two groups of women, those who had IGF-1 and IGFBP-3 blood tests prior to surgery, pre-operative group involving 36 women, and those who had blood tests some time after their breast surgery, post-operative group involving 35 women. These women were not paired. In the pre-operative women, the mean age was 61 years and the mean IGF-1 was 162ng/ml (range 100-425ng/ml). In one woman her IGF-1 level was actually elevated above the normal range (a 36 year old lady with IGF-1 of 425). In the post-operative women the mean age was 58 years and the average IGF-1 was 145ng/ml (range 56-257ng/ml). No women had IGF-1 levels elevated above the normal range. Within the post-operative group 32 (82%) women were taking Tamoxifen (T) and 7 (18%) women were not (NT). The mean age of patients in NT was 55 years and the average IGF-1 was 155ng/ml (range 130-197ng/ml). In the T group the mean age was 57 years, the average IGF-1 was 145mg/ml (range 62-257ng/ml).

As IGF-1 levels are age-dependant, the IGF-1 levels of all of the subjects were corrected for age, according to the normal ranges for each age range (table 3) and expressed as a ratio of upper limit of age related normal range (table 4). Using this correction, serum IGF-1 levels were significantly decreased in the post-operative patients taking tamoxifen when compared to pre-operative patients and post-operative patients not taking tamoxifen (Mann Whitney, $p<0.05$)

Table 5. Normal serum values of IGF-1

Age (years)	Normal (min-max) serum IGF-1 concentration (ng/ml)
19-29	125-329
30-39	120-330
40-49	126-369
50-59	108-263
60-83	108-229

Table 6. Serum IGF-1 levels expressed as a ratio of the upper limit of the age related normal range.

	Median ratio +/- standard deviation
Pre-operative	0.6 +/- 0.18*
Post-operative NT	0.62+/- 0.14*
Post-operative T	0.52+- 0.14

*= $p<0.05$ (Mann Whitney U), when compared to post-operative T.

6.4.2 IGFBP-3

Serum IGFBP-3 levels increase from late childhood to puberty and then fall gradually during adult life. The levels are also higher in females than males (normal range 2.6-5.5mg/l in women versus 1.5-4.6mg/l in men).

In the pre-operative group, the mean patient age was 61 years and the mean serum IGFBP-3 level was 3mg/l (range 1.6-5.5mg/l). In the post-operative group, the mean patient age was 64 years and the average

IGFBP-3 was 3.1mg/l (range 1.3-5.3mg/l). Within this post-operative group, 28 (80%) patients were taking tamoxifen (T) and 7 (20%) were not (NT). The average age of the NT group was 62 years and the average IGFBP-3 level was 2.8mg/l (range 1.4-5.2mg/l). The average age of the T group was 55 years with a mean IGFBP3 level of 3.0mg/l (range 1.3-5.3mg/l). Tamoxifen clearly has no effect on serum IGFBP-3 levels.

6.4.3 IGF-1: IGFBP-3 ratio levels

IGFBP3 is the predominant binding protein for IGF-1 and determines its activity. The IGF-1:BP-3 ratio was determined for the three groups of patients; pre-operative, post-operative NT and post-operative T. To account for the age related decline of both peptides, values were calculated as a ratio of the upper limit of the age-related normal range (Table 5).

The results show that the IGF-1:BP-3 ratio is significantly higher in the pre-operative group than the post-operative T group (Mann Whitney, p=0.05). There is no significant difference however between the pre-operative group and the post-operative group not taking Tamoxifen

Table 7. Serum IGF-1:BP-3 ratio expressed as a ratio of the upper limit of the normal range

	Median ratio +/- standard deviation
Pre-operative	0.051 +/- 0.027*
Post-operative NT	0.054 +/- 0.03**
Post-operative T	0.04 +/- 0.013

*p=0.05, when compared to post-operative T
**p=0.09 when compared to post-operative

6.5 Results of viability of cultured breast explants

6.5.1 Primary breast biopsy culture

The breast cancer samples were collected from theatre and taken straight to the pathology department. The pathology department gave us normal and malignant tissue, which we took back to the lab in a cryogenic tube on ice. The samples were then prepared as explained in the methods.

6.5.2 Results of MTS assay

Figure 16 demonstrates the mean absorbance in a representative normal and malignant tissue breast tissue explant after 0, 12, 18 and 24 hours incubation. The increase in absorbance at 24 hours for both samples indicates their viability after 24 hours of culture and a recover of metabolic activity after excision.

Figure 16:

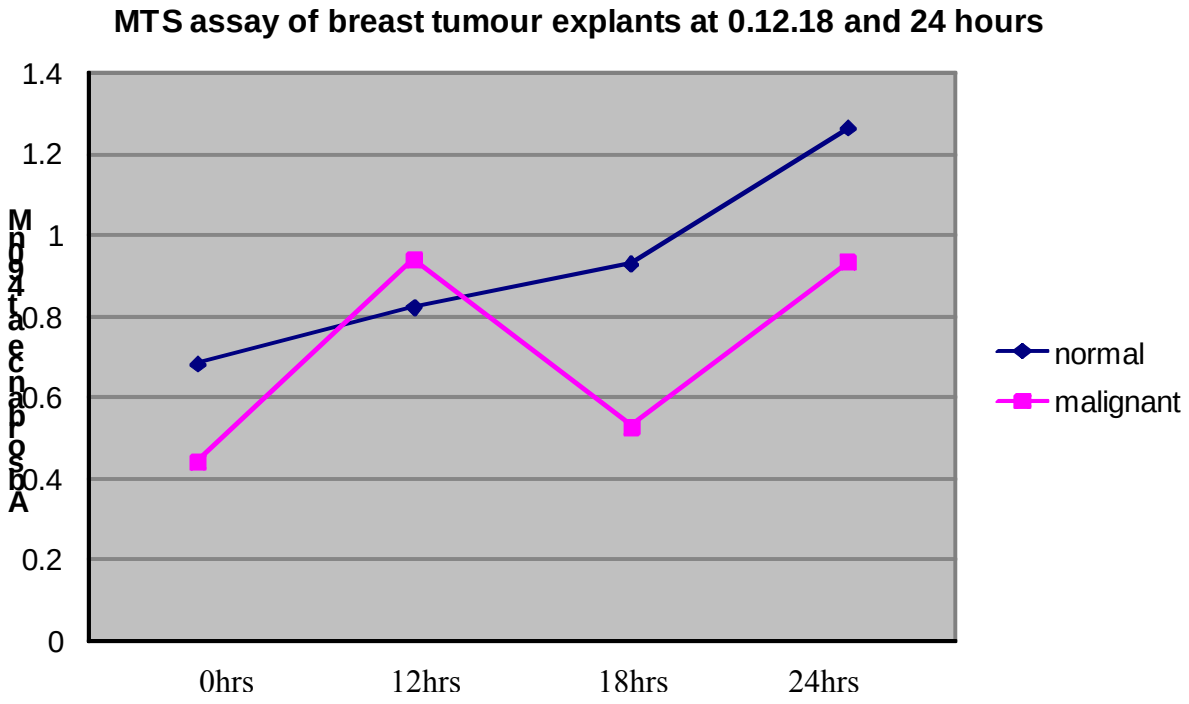

Figure 17 and 18 indicates MTS results from a normal and malignant tissue explant incubated for 96 hours.

Figure 17:

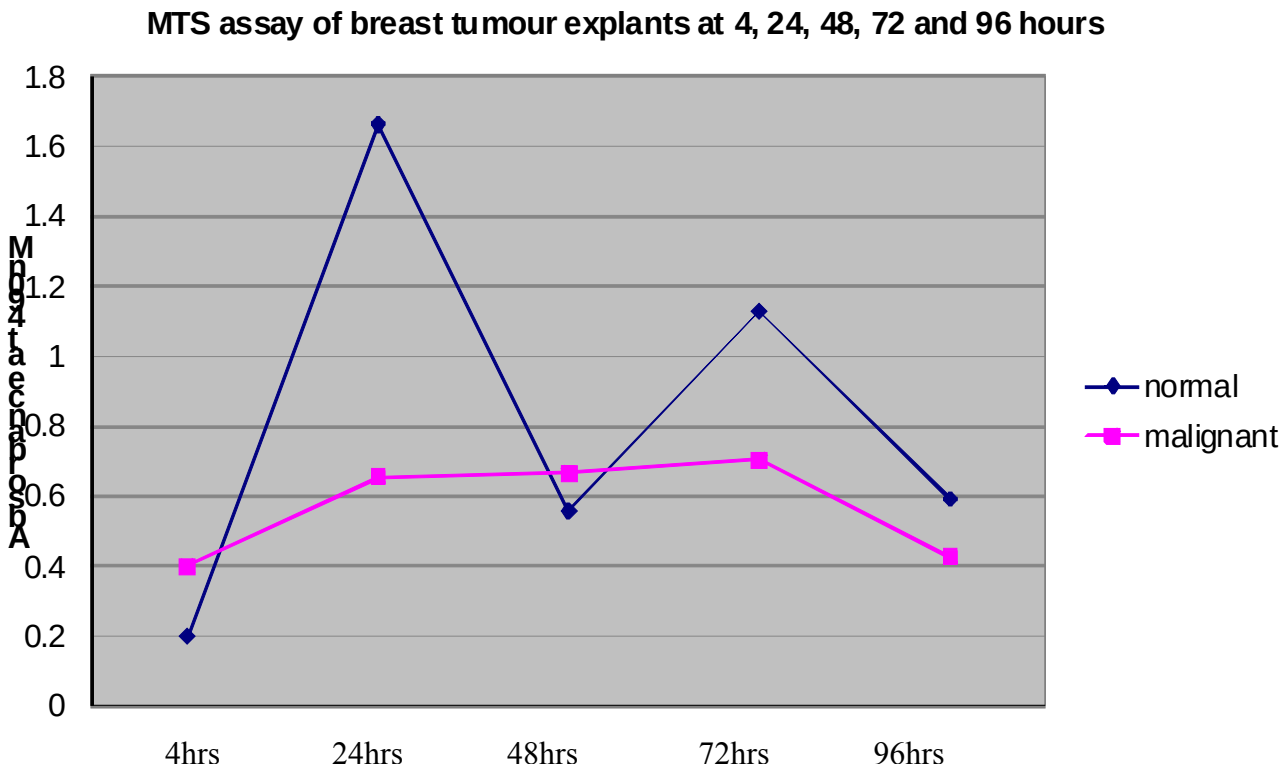

Although there is some variation, the absorbance suggests viability at 72 hours, with a slight decline after 96 hours. It could be seen that normal tissue was alive at 96 hours, see figure 18.

Figure 18:

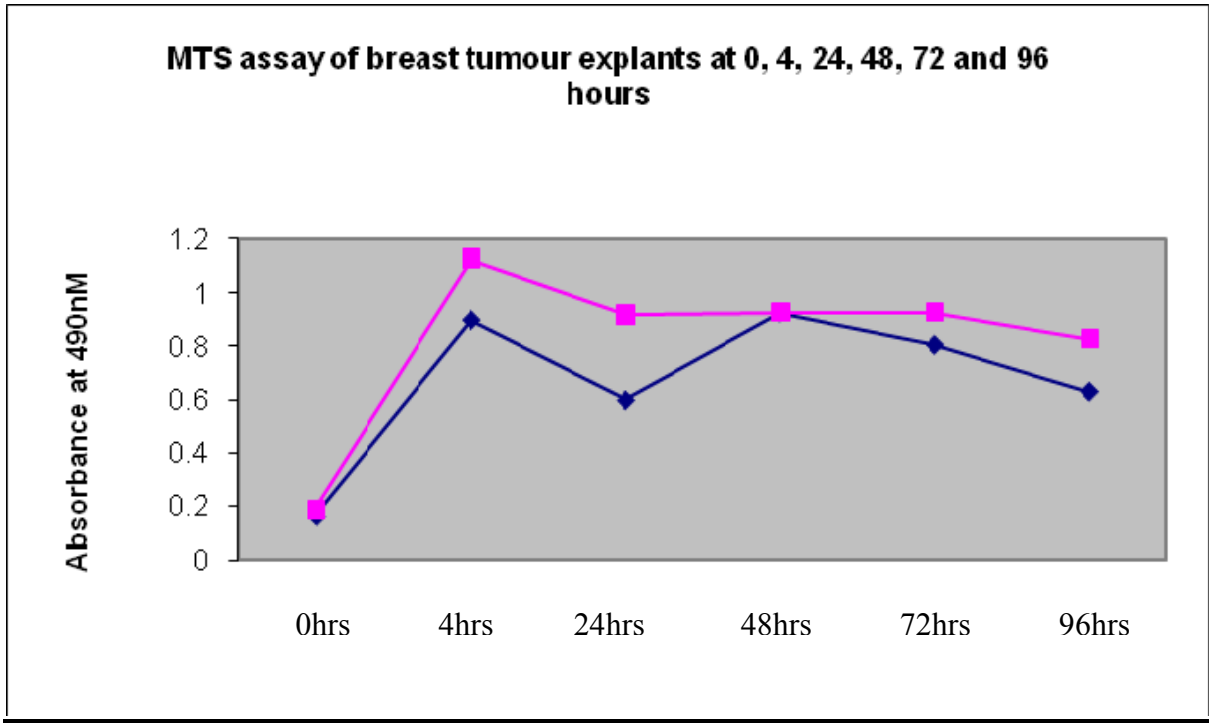
MTS assay of breast tumour explants at 0, 4, 24, 48, 72 and 96 hours
Absorbance at 490nM
1.2
1
0.8
0.6
0.4
0.2
0
0hrs
4hrs
24hrs
48hrs
72hrs
96hrs

6.5.3 Results of LDH assay

Figure 19 and 20 demonstrates the absorbance of 2 samples of normal and malignant tissue up to 96 hours in the LDH assay. There was a slow increase in absorbance over 96 hours. 2% Triton was added to a sample of malignant tissue, used as a positive control and shown to have more absorbance than the normal and malignant tissue. In figure 19 there is a marked increase in LDH release between 24 and 48 hours in the 2% Triton sample indicating cell death, which is to be expected. However in Figure 20 initially there is a decrease in LDH between 24 and 48 hours in the 2% Triton sample which is unexpected. After 48 hours the LDH increases, again indicating cell death.

LDH levels in normal and malignant tissue were steady up to 72 hours, but increased at 96 hours in normal sample, again indicating cell death.

Figure 19:

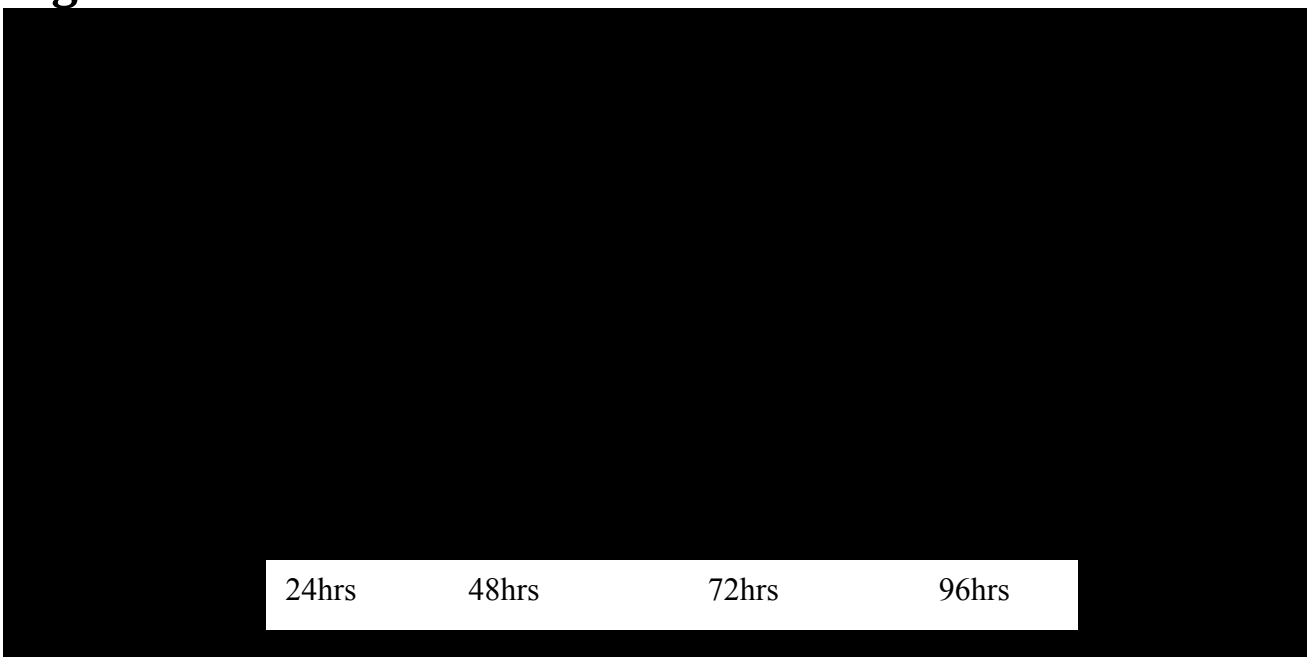

Figure 20:

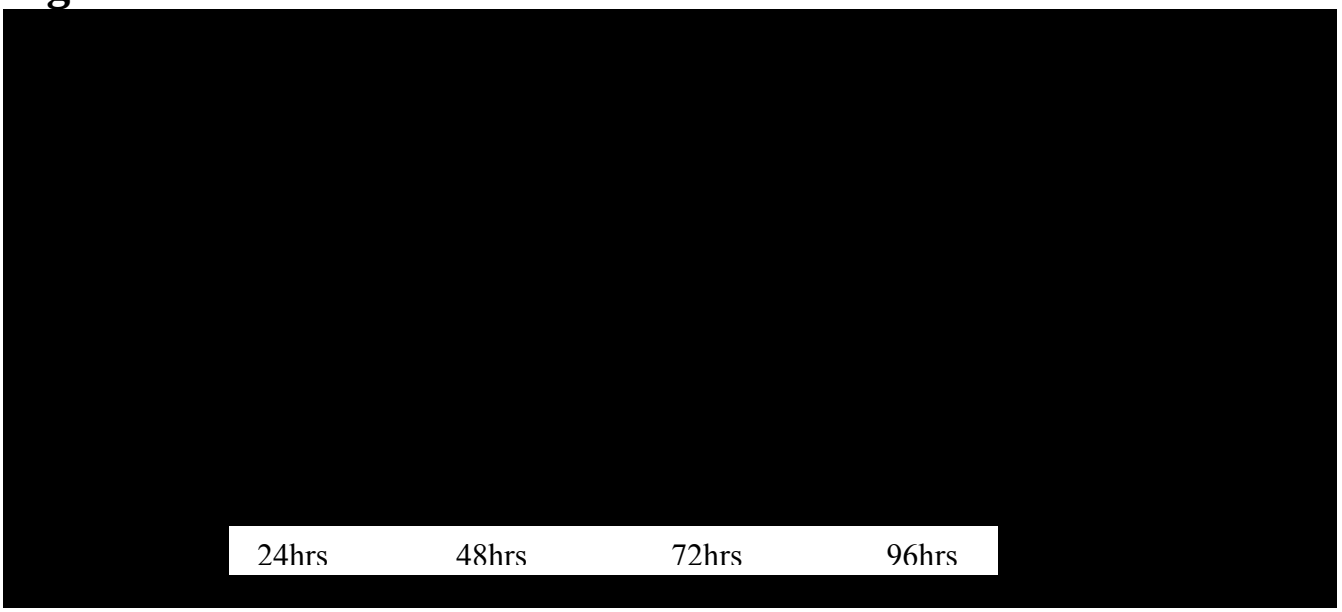

6.5.4 Effects of ghrelin on the expression of IGF-1 in Breast tissue explants

Figures 21- 24 shows IGF-1 mRNA levels in normal and malignant breast tissue samples that were grown in media only or with ghrelin concentration 1ml 10^{-9}M for up to 48 hours. It can be seen that the expression of IGF-1 was significantly reduced in the presence of ghrelin when cultured for 24 or 48 hours.

Figure 21:

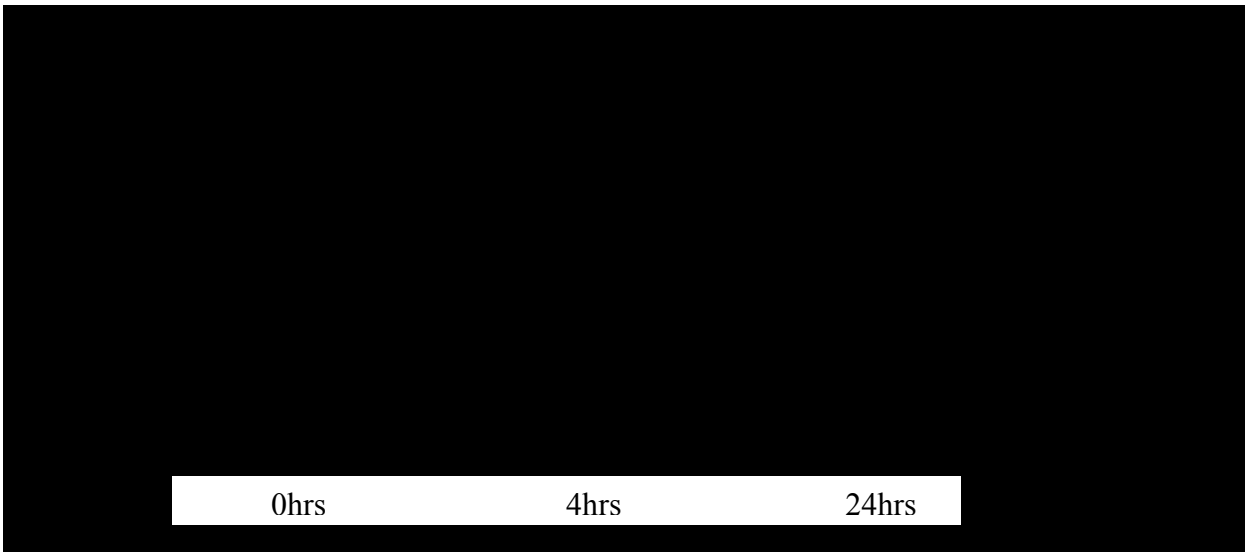

Figure 22:

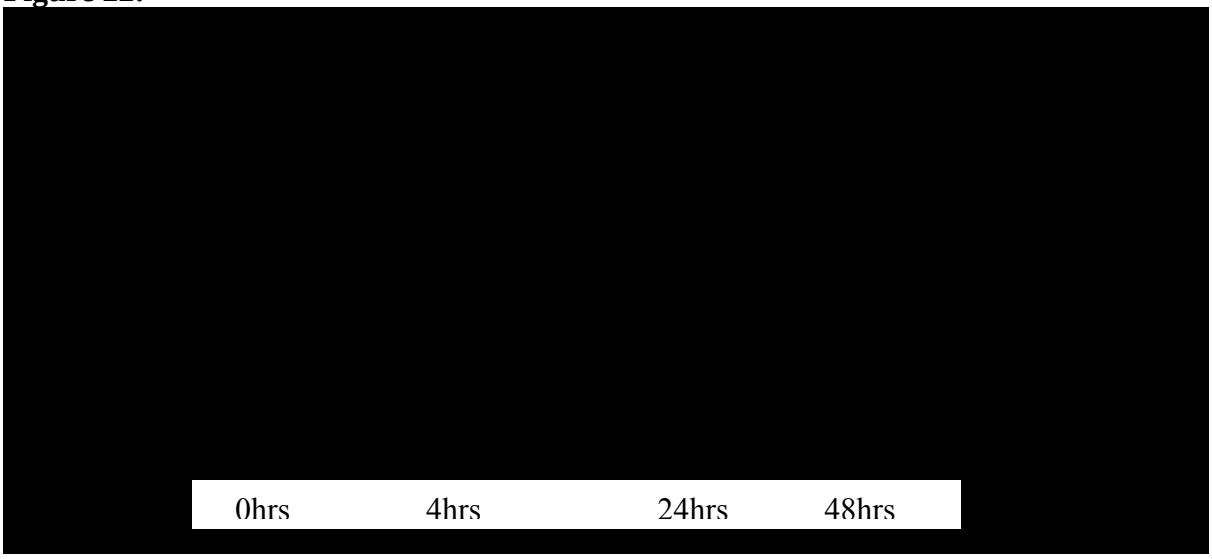

Figure 23:

0hrs 4hrs 24hrs

Figure 24:

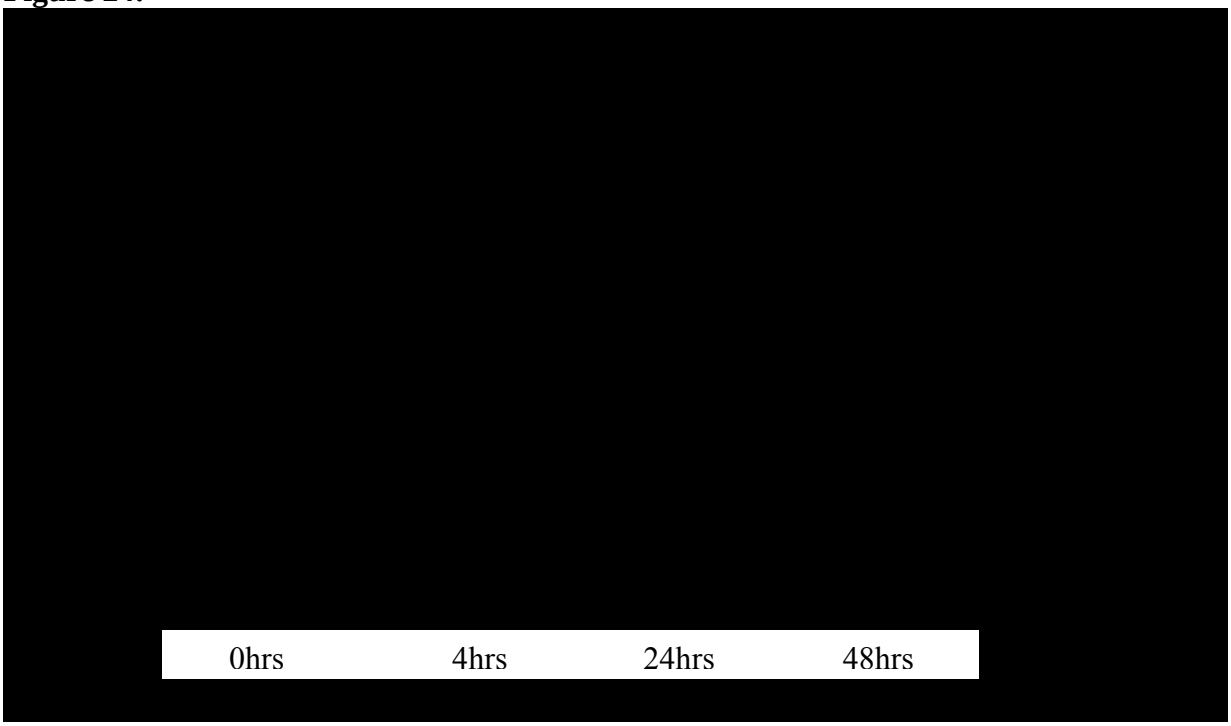

6.6 Microarray analysis of IGF-1mRNA positive and negative breast tumours

39 genes were upregulated (>2 fold) in the IGF-1 positive tumours, compared to the IGF-1 negative tumours. 27 genes were found to be downregulated (<2 fold) in the IGF-1 positive tumours, including suppression of tumourigenicity 13. This is an abundant highly conserved protein that binds heat shock proteins and has previously been shown to be down regulated in breast, colorectal and ovarian carcinoma. Expression of local IGF-1 by breast cancers is accompanied by differential expression of numerous cancer-associated genes. Clarification of these genes will further elucidate the mechanisms by which IGF-1 influences the pathogenesis of breast cancer.

Table 8 – List of genes downregulated in IGF-1 positive breast cancer

Pos/neg	Neg/pos	T test	Unigene title
0.26	3.92	0.04	Chromosome 10 open reading frame 2
0.37	2.69	0.03	Hypothetical protein MGC5306
0.47	2.14	0.04	Trichorhinophalangeal syndrome 1
0.48	2.07	0.01	Hypothetical protein /m/gC3731
0.49	2.06	0.03	Mitochondrial ribosomal protein 63
0.49	2.03	0.02	HSPC003 protein
0.50	1.99	0.02	Tumourgenicity 13; ST 13
0.50	1.99	0.05	Homo sapiens, clone IMAGE:3506202
0.51	1.96	0.01	CGI-115 protein
0.51	1.94	0.04	Hypothetical protein FLJ10359
0.52	1.93	0.05	Cysteine and histidine-rich domain
0.53	1.90	0.04	Endoplasmic reticulum chaperone SIL1
0.54	1.84	0.02	Hypothetical protein FLJ10539
0.55	1.82	0.05	Hypothetical protein MGC10764
0.56	1.78	0.05	Hypothetical protein FLJ20257
0.56	1.78	0.05	Hypothetical ptotein FLJ10514
0.57	1.76	0.04	Hypothetical protein MGC3262
0.57	1.74	0.04	Hypothetical protein FLJ10734
0.58	1.73	0.04	KIAA 1698 protein
0.59	1,71	0.02	Adenylosuccinate synthase
0.61	1.63	0.03	Single Ig IL-1-1R-related molecule
0.63	1.60	0.05	Exosome component Rrp41
0.63	1.59	0.03	Ring finger protein 7
0.63	1.59	0.03	Pan-hematopoietic expression
0.64	1.57	0.01	ATPase inhibitor percursor
0.64	1.56	0.01	Hypothetical protein FLJ23182
0.66	1.53	0.04	KIAA0632 protein

Talble 9 – List of genes upregulated in IGF-1 positive breast cancer

Pos/neg	Neg/pos	T test	Unigene Title
4.01	0.25	0.02	tubulin, alpha 3
3.61	0.28	0.02	complement component 1, q subcomponent, alpha polypeptide
3.61	0.28	0.03	major histocompatibility complex, class II, DR beta 5
3.52	0.28	0.00	duodenal cytochrome b
3.35	0.30	0.02	carcinoembryonic antigen-related cell adhesion molecule 1 (biliary glycoprotein)
3.33	0.30	0.01	EphB3
3.03	0.33	0.05	phosphatidic acid phosphatase type 2A
3.02	0.33	0.03	ADAM-like, decysin 1
2.81	0.36	0.04	myristoylated alanine-rich protein kinase C substrate (MARCKS, 80K-L)
2.81	0.36	0.01	KIAA0603 gene product
2.78	0.36	0.04	RecQ protein-like (DNA helicase Q1-like)
2.77	0.36	0.02	SRB7 (suppressor of RNA polymerase B, yeast) homolog
2.70	0.37	0.02	C-terminal binding protein 1
2.68	0.37	0.02	myotubularin related protein 1
2.64	0.38	0.00	stromal cell-derived factor 1
2.61	0.38	0.03	ephrin-B2
2.49	0.40	0.02	immunoglobulin heavy constant gamma 3 (G3m marker)
2.46	0.41	0.03	CGI-26 protein
2.43	0.41	0.04	cAMP responsive element binding protein-like 2
2.42	0.41	0.03	translocation protein 1
2.40	0.42	0.04	Rho GDP dissociation inhibitor (GDI) alpha
2.37	0.42	0.02	C-type (calcium dependent, carbohydrate-recognition domain) lectin, superfamily member 2 (activation-induced)
2.34	0.43	0.03	Homo sapiens cDNA FLJ32313 fis, clone PROST2003232, weakly similar to BETA-GLUCURONIDASE PRECURSOR (EC 3.2.1.31)
2.26	0.44	0.03	src family associated phosphoprotein 2
2.24	0.45	0.04	S100 calcium-binding protein A4 (calcium protein, calvasculin, metastasin, murine placental homolog)
2.22	0.45	0.01	C-terminal binding protein 1
2.17	0.46	0.01	KIAA0515 protein
2.16	0.46	0.03	lysosomal apyrase-like 1
2.15	0.47	0.04	transforming growth factor, beta 1
2.11	0.47	0.03	ESTs, Weakly similar to AF208855 1 BM-013 [H.sapiens]
2.08	0.48	0.01	iduronate 2-sulfatase (Hunter syndrome)
2.06	0.49	0.02	CD53 antigen
2.05	0.49	0.02	hypothetical protein FLJ20311
2.05	0.49	0.03	SWI/SNF related, matrix associated, actin dependent regulator of chromatin, subfamily a, member 5
2.04	0.49	0.01	Putative prostate cancer tumor suppressor
2.03	0.49	0.03	CD58 antigen, (lymphocyte function-associated antigen 3)
2.02	0.50	0.05	DEAD/H (Asp-Glu-Ala-Asp/His) box polypeptide 3
2.01	0.50	0.01	LIV-1 protein, estrogen regulated
2.01	0.50	0.01	discs, large (Drosophila) homolog 1

Figure 25 – Microarray of IGF-1 positive and negative breast tumours

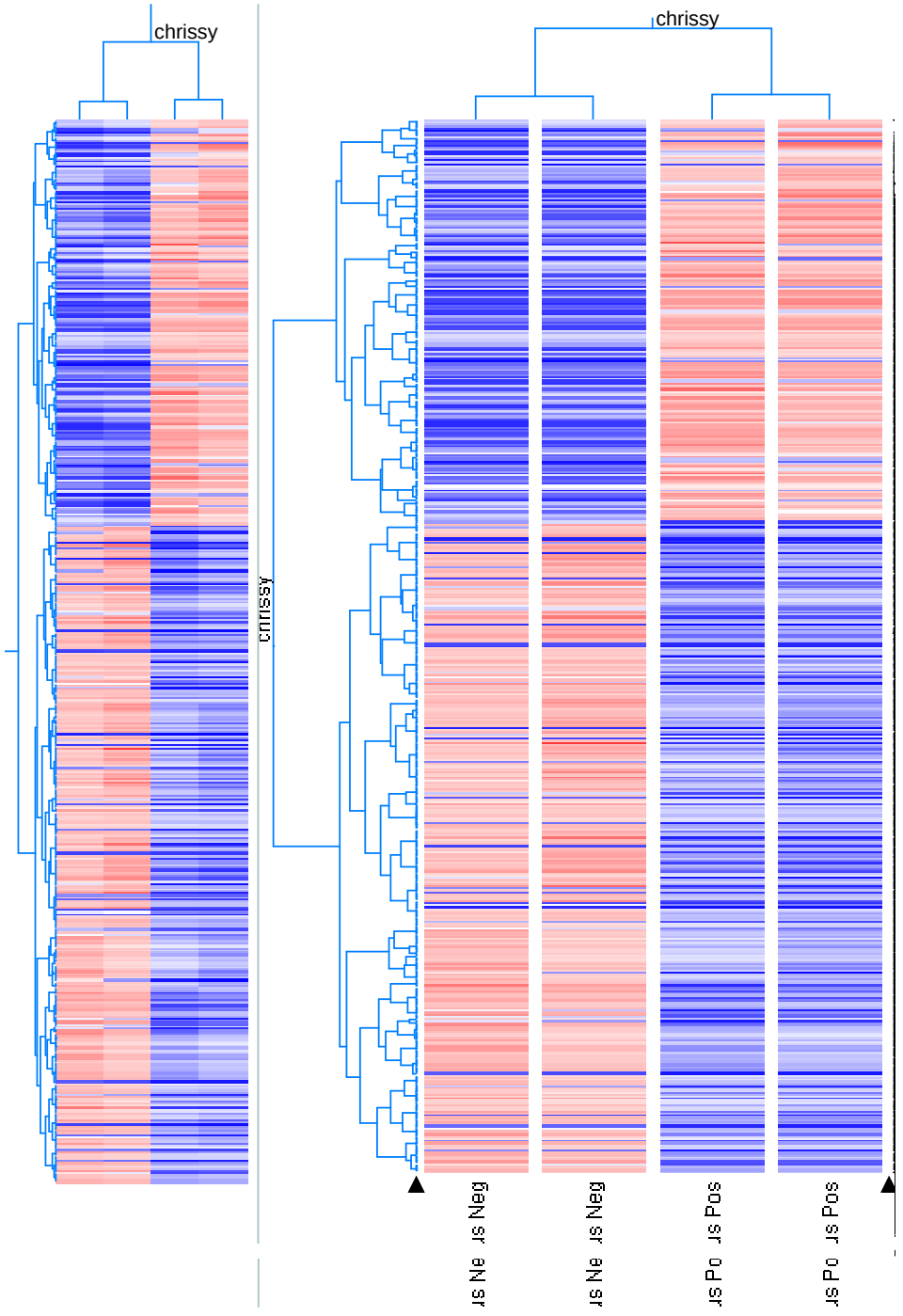

7. Discussion

IGF-1 expression in breast tissue

This study confirmed the expression of IGF-1 and its receptor in human breast tissue. We found using ribogreen that breast tumours produced 3-4 times more IGF-1 RNA than normal breast tissue. Interestingly using RT-PCR, IGF-1 appeared to be down regulated in breast tumours compared to normal tissue ($p<0.0001$). In addition we found 10 tumours and 4 normal samples did not express IGF-1 at all. Previously Peyrat et al did not detect IGF-1 mRNA in 4 breast cancers[123]. This possibly indicates a sub group of breast tumours which do not express IGF-1. We found over expression of Somatostatin in IGF-1 negative breast tumours compared to IGF-1 positive tumours. However no other gene was overexpressed in IGF-1 negative tumours. The implication is that IGF-1 negative tumours may be more aggressive than IGF-1 positive tumours however more research into the clinical details of IGF-1 negative tumours must be performed. Another study has similarly shown expression of IGF-1 mRNA in breast cancer tissue samples, and in situ hybridization studies have shown that the message originates from the stromal cells adjacent to normal lobules. IGF-1 mRNA however was not found in human breast cancer cell lines[33].Yee et al also found no IGF-1 mRNA in breast cancer cell lines, but RNA extracted from breast tissue had easily detectable IGF-1 mRNA. Again in situ hybridization showed the IGF-1 mRNA was expressed in the stromal cells, and not by normal or malignant epithelial cells[32]. This could explain how in our study we found IGF-1 to be down

regulated in breast tumours compared to normal breast tissue. Similarly Chong et al discovered that IGF-1 expression was lower in cancerous tissue compared to adjacent non-neoplastic breast tissue, thus supporting a paracrine relationship between cancerous tissue and benign breast tissue[124]. A further paper has also shown IGF-1 expression to be lower in tumour tissue than normal breast tissue [40]. Interestingly they also discovered increased IGF-1 mRNA expression in normal breast tissue from women with positive family history of breast cancer, indicating that IGF-1 may play a role as a breast cancer risk factor. In conclusion, looking at my results, I feel that IGF-1 expression was increased in breast tumours compared to normal breast tissue. The RT-PCR results show the opposite findings due to IGF-1 mRNA being expressed in stromal cells and not by malignant breast cells.

Limitations of RT-PCR

Real-time RT-PCR is now widely used for characterising or confirming gene expression patterns and comparing mRNA levels in different sample populations. Recent improvements in internal standards, references for normalising data and new mathematical models to analyse data have improved its use as a possible diagnostic tool. However there remain some concerns about how quantitative and informative real-time RT-PCR is. A wide variety of protocols exist amongst research laboratories, and there is no universally accepted validation of normalising data thereby leading to difficulties in reproducing data. Improvements have led to the

development of standard templates[125] which allows comparison between experiments and use of internal standards to reduce variation in template starting amounts and operator loading error.

One of the major difficulties with this study was the *in vivo* RNA extraction from whole tissue samples. The heterogeneity of cell types within the sample leads to an averaging out of the expression in different cell types and perhaps the expression profile of a specific cell type may be masked or even lost. Previous studies have shown significant differences in gene expressing profiles of microdissected and bulk tissue samples. This may be particularly problematic when comparing normal and malignant breast tissue. Normal tissue directly adjacent to a tumour may be phenotypically normal but it may display an altered gene expression due to its proximity to the tumour. In order to overcome this problem, we obtained normal breast tissue an average of 10cm away from the main tumour site, which was then confirmed as normal tissue by the pathology department.

Breast tissue comprises of many different cell types including glandular epithelial cells, myoepithelial cells, stromal fibroblasts, adipocytes, vascular endothelial cells and others. This will therefore cause a large difference in gene expression in normal and malignant breast tissue and will confound changes due to malignant tissue only. This issue could be addressed by using laser capture microdissection to extract only breast tumour cells to look purely at their gene expression only.

Laser capture micodissection is a novel technique that allows the extraction of a pure subpopulation of cells from heterogenous *in vivo* tissue samples. A brief laser pulse is directed at cells within a tissue

section on a glass slide and individual cells may be selected and gene expression then determined at an RNA and protein level. The main drawback of this technique is that a very small sample is obtained making RNA isolation difficult and good quality RNA is essential for successful RT-PCR. This technique is also classically performed using archival formalin-fixed paraffin-embedded tissue specimens and the RNA yielded from these cells may have undergone extensive degradation and also the use of fixatives may well alter the results. New commercial kits have been developed in order to overcome these problems and so the future use of this technology may improve the validity of our results.

IGF-1R expression and tumour associated genes

We observed that IGF-1R expression was increased in breast tumours and previous studies have shown that IGF-1R expressing in primary breast tumours is very common[24;126;127]. Indeed Law et al showed that IGF-1R was universally expressed in all breast cancer subtypes (luminal, triple-negative and HER2+)[128]. In addition the presence of phosphorylated IGF-1R could be a predictor for IGF-1 targeted therapy such as monoclonal antibodies to IGF-1R[129]. Currently more than 70 clinical trials involving a variety of drugs are underway, with the IGF-1R becoming one of the most intensively investigated targets in oncology[130]. CP-751,871 is a fully human IgG_2 monoclonal antibody antagonist of IGF-1R which has been used in a phase 1 clinical study on patients with refractory solid tumours[131].

PCNA is a proliferation marker and is thought to be closely related to cell proliferation. Immunostaining for PCNA is a useful prognostic factor and can be used as an indication of the degree of malignancy in breast cancer[132]. It is no surprise that we found PCNA to be increased in tumours compared to normal tissue, indicating that more proliferation occurs in tumours than normal breast tissue. There was no significant difference in PCNA expression in IGF-1 positive or negative tumors.

VEGF is known to be up regulated in several cancers, particularly colon[133]. It plays an important role in tumour angiogenesis[134] and *in vitro* studies have shown that IGF-1 regulates VEGF transcription[135]. We found VEGF-165 expression to be significantly upregulated in breast tumours compared to normal breast tissue (p=0.01). Interestingly VEGF-189 expression was not increased. A previous paper has shown that VEGF-165 but not VEGF-189 stimulates vasculogenesis and bone marrow cell migration into Ewing's sarcoma tumours *in vivo*[136]. Kirkpatrick et al similarly found VEGF-165 to be significantly over expressed in tumour tissue compared to adjacent normal breast tissue{Kirkpatrick, 2004 125 /id. However VEGF-189 expression in tumour tissue was not significantly different to the expression in adjacent non-cancerous tissue. This tends to indicate that VEGF-165 is more important in breast tumourigenisis than VEGF-189.

Vitamin D is known to inhibit proliferation of breast cancer *in vitro* and *in vivo*[137] and has been shown to block the mitogenic effects of IGF-1[138-140]. The mechanism by which this occurs is unclear. It may be due to its regulation of IGF-1R[139] or upregulation of inhibitory IGFBPs or perhaps a modulation of the downstream effects of IGF-1 signalling. We found Vitamin D receptor was over expressed in breast tumours related to

normal breast tissue. This has previously been reported in other studies[141;142]. No change was seen in 1 alpha hydroxylase expression in malignant and normal breast tissue suggesting that paracrine vitamin D is not important in breast proliferation.

We observed that hTERT expression was markedly upregulated in breast tumours. hTERT has previously been found to be expressed in the majority of breast cancers[143] with levels being significantly higher in breast cancer than in adjacent non-cancerous tissue or fibroadenomas[144]. It has a sensitivity of 50% and a specificity of 90% in the ability to detect malignancy in breast tissue. A further study found hTERT mRNA expression to be associated with that of the VEGF189 and VEGF 165 isoforms, suggesting a possible pathway through which high expression of hTERT might be linked to worsened disease prognosis[145]. As VEGF is known to increase the likelihood of tumour metastasis it would be expected that high levels of hTERT might also be correlated with increased lymph node positivity.

GHR was found to be over expressed in normal breast tissue. There is expression of GH and GHR in the majority of normal and malignant breast cells[146]. Previous papers have found GHR expression in epithelial cells of normal, proliferative and neoplastic lesions of the breast[147]. There has also been demonstrated the stromal expression of GHR genes in normal breast tissue. Thus the putative role of Growth hormone in the progression of proliferative mammary disorders is not due to grossly altered levels of receptor expression[147]. As GHR has been found in malignant and normal cells it is diffcult to explain why GHR was over expressed in normal tissue in our study. There was no difference in GHR or GH expression in IGF-1 positive or negative breast tumours.

Somatostatin was found to be increased in IGF-1 negative tumours in our study. Expression of Somatostatin receptors in human primary breast cancer is widespread. Previous papers have shown Somatostatin receptor subtype 2 expression being significantly higher in breast cancers than in normal breast tissue[148]. Interestingly we found no significant difference in Somatostatin receptor 5 expression levels between tumour and benign breast tissue.

Furthermore we found no significant difference in expression of IGFBP-3, GH, Ghrelin, Ghrelin 1B receptor, cmyc, or Cox-2 in tumour or benign breast tissue. There were high levels of IGFBP-3, cmyc and Cox-2 expressed in both malignant and benign breast tissue. There were medium levels of GH, ghrelin and ghrelin 1B receptor expression in malignant and benign breast tissue.

Immunohistochemistry

Using immunohistochemical DAB staining we demonstrated IGF-1 expression in liver and normal and malignant breast samples. We showed lots of IGF-1 highlighting when IGF-1 positive samples were stained with fluorescence dye, but little staining in IGF-1 negative samples. This shows a correlation between the RT-PCR IGF-1 positive or negative status of breast tumours and the immunohistochemical staining.

GH staining was seen in all 10 IGF-1 positive samples with a wide area of staining visible, and staining was not present in the 13 IGF-1 negative samples.

Ghrelin immunohistochemical staining was done using fluorescent staining and samples showed extent staining throughout the tissue. Again this correlates with the RT-PCR expression of ghrelin in all normal and malignant breast tissue, showing that ghrein was present in all samples of breast tissue.

Serum IGF-1 and IGFBP-3

IGF-1 levels were significantly lower in patients taking Tamoxifen, however no effect was seen on serum IGFBP-3 levels. The IGF-1: BP-3 ratio was also found to be significantly higher in women with breast cancer prior to surgery, thereby agreeing with previous epidemiological studies. Tamoxifen has been shown to significantly reduce serum levels of IGF-1[31;149-151] but to have no effect on IGFBP-3[152]. Circulating levels of IGF-1 and IGFBP-3 are however strongly affected by nutritional status[153;154] and catabolic stress that accompanies surgery[155;156]. This may therefore be one of the reasons for a fall in IGF-1 following surgery. However in this study no fall in IGF-1 was observed in the group not taking Tamoxifen post-operatively. This indicated that the fall in IGF-1 is mainly due to Tamoxifen.

The mechanism by which Tamoxifen alters the IGF-1 axis has not been fully elucidated. It is thought that Tamoxifen blocks the oestrogen receptor, interfering with the production of growth hormone from the pituitary, and so reducing the amount of IGF-1 produced by the liver and released into the circulation. One study has also suggested that Tamoxifen may work via a pituitary-independent action of reducing IGF-1 in the peripheral tissue[47]. Tamoxifen also has direct anti-oestrogen effects on breast cancer cells and may well reduce the amount of IGF-1 and IGFBP-3 produced by the cells themselves[149;157]

Primary breast explants culture

We wanted to clarify the expression of IGF-1 in normal and malignant breast tissue over 24-48 hours and observe effects that ghrelin would have on IGF-1 expression. In order to do this we developed a novel, physiologically relevant explant system to provide us with more clinically relevant information than cell line work can provide. The main difference in methodology involved the use of breast tissue rather than using cancer cell lines which have previously undergone many mutations and may not be physiologically relevant. There were however a few potential areas for error in our experimental technique. One variable factor was the time taken to transfer breast tissue from the patient into the experimental culture media. In order to standardise this and mimic *in vivo* conditions, all samples were collected immediately after surgical excision and placed in media warmed to 37^{o}C. Another variable factor in comparing the samples was a difference in weight and composition of breast tissue, which may influence supply of oxygen and experimental substance. Normal breast tissue in particular consists of a varying amount of fat and fibrous tissue which may influence the weight. To minimise this factor, all samples were cut into sizes weighing approximately 10-20mg. Every effort was made with normal breast tissue to excise all visible fatty tissue away so that only glandular tissue was used in experiments.
The LDH and MTS assays and standardization of absorbance allowed us to validate our novel culture technique. The MTS assay is a rapid method of assessing cell viability and is used to measure changes in cell viability or proliferation. In actively metabolising cells, an increase in MTS conversion is spectrophotometrically quantified. Comparison of this value to an untreated control provides an increase in cellular metabolic activity.

Conversely, in cells that are undergoing apoptosis or necrosis, MTS reduction decreases, reflecting the loss of cell viability.

For the assessment of cell death we used the LDH assay. Cell death or cytotoxicity is classically evaluated by the quantification of plasma membrane damage. Lactate dehydrogenase (LDH) is a stable enzyme present in all cell types, and rapidly released into cell culture medium upon damage of the plasma membrane. LDH therefore is the most widely used marker in cytotoxicicity study.

The MTS assays demonstrated that normal and malignant breast tissue can be kept alive for 96 hours in culture conditions. This was also supported by the LDH assay technique using triton as a positive control. Again malignant and normal breast tissues were found to be alive at 96 hours, although there was an increase in the LDH levels at 96 hours in both the normal and malignant breast tissue. In our study we only performed MTS assays on 9 normal and 9 breast tumour samples. In order to expand this study, more samples of breast tissue should be used in primary breast explant culture to study the effects of IGF-1 and GH on gene expressions of IGF-1R, PCNA, VEGF, Vitamin D, hTERT, GHR, Somatostatin, cox-2 gherlin and IGFBP-3. There are advantages to using samples of normal and malignant breast tissue that have been kept alive for 96 hours. It gives much more detail on how real breast tissue would react to the effects of IGF-1 or GH, compared to using cell lines, which have previously undergone mutations and may not be physiologically relevant.

Normal and malignant breast tissue was then cultured in media only or ghrelin. The IGF-1 mRNA expression was markedly reduced when breast tissue was cultured with ghrelin compared to media only. This is difficult to explain and may be due to the paracrine or autocrine effects of ghrelin on breast tissue directly rather than via the associated release of GH from

the pituitary gland. It has been shown in a previous paper that ghrelin causes a significant inhibition of cell proliferation in three different human breast cancer cell lines (MCF7, T47D and MDA-MB231) by binding to GH secretagogue receptors[14]. This would tie in with the marked reduction in IGF-1 that we found.

Microarray

Gene expression profiling by microarray analysis has identified breast cancer signatures that are important for prognosis and treatment. Microarray data has been widely used to discover biomarkers predictive of response to endocrine therapy in oestrogen receptor-positive breast cancer[158]. Indeed microarray is convenient and feasible for the analysis of IGF-1 expression in breast cancer, however a study has shown no significant correlation of the IGF-1 expression with the overall survival rate of patients[159]. We performed microarray on one IGF-1 positive and one IGF-1 negative breast cancer specimen. Figure 25 shows the image acquisition and data analysis which is the final step of microarray experiments. The aim is to produce an image of the surface of the hybridized array. The slide is dried and placed into a laser scanner to determine how much labeled cDNA (probe) is bound to each target spot. Laser excitation of the incorporated targets yields an emission with characteristic spectra, which is measured using a confocal laser microscope. The microarray software has used blue lines on the microarray to represent genes upregulated in the experimental sample, red to represent genes that are downregulated in the experimental sample, and white to represent those genes of equal abundance in both IGF-1 positive and IGF-1 negative samples.

There were 39 genes which seemed to be over expressed in IGF-1 positive breast cancer. These include tubulin alpha 3, which has been previously found to be overexpressed in malignant breast tumours immunohistochemically[160] Transforming growth factor beta 1, a multifunctional peptide that controls proliferation and differentiation, was also upregulated 2.15 fold in the IGF-1 positive tumours[161]. In addition it has been shown to promote the formation of lung metastases in animal models of breast cancer[161]. We also found an over expression of carcinoembryonic antigen-related cell adhesion molecule 1 (CEACAM 1) in the IGF-1 positive breast tumour which was upregulated 3.35 fold. CEACAM is known to be an intracellular adhesion molecule that is known to be over expressed in a variety of human cancers including colon, breast and lung. It exhibits marked angiogenic properties *in vitro* and *in vivo* and it is associated with tumourigensis, tumour cell adhesion invasion and metastasis[162]. One the genes down regulated (<2fold) in the IGF-1 positive tumours was suppression of tumourigenicity 13. This is an abundant highly conserved protein that binds heat shock protein and has previously been shown to be down regulated in breast, colorectal and ovarian carcinoma[163]. Further classification of the genes up regulated in IGF-1 positive breast cancers will help to elucidate the mechanisms by which IGF-1 influences the pathogenesis of breast cancer.

We only performed microarray on 2 breast tumour samples. This was due to the expense of the microarray chips and the limitations of microarray, with it being non-quantitive and semi-accurate. The advantage of microarray is that it shows information regarding many genes affected. In order to expand this study I would perform microarray on a greater number of IGF-1 positive and negative breast tumour samples and look at the clinical relevance regarding IGF-1 status and the difference in gene expression between IGF-1 positive and negative tumours.

Clinical potential

The major role played by the GH/IGF-1 axis in the development and behaviour of breast cancer and its interaction with estrogens may have important clinical implications. As serum IGF-1 appears to be a major determinant of subsequent breast cancer development, measurements of its levels may be of predictive value in assessing future breast cancer risk. It may also lead to chemopreventation through serum IGF-1 reduction. Targeting the GH/IGF-1 axis might also be of value in the development of novel treatments for breast cancer. Several strategies are currently being employed to inhibit IGF signalling: monoclonal antibodies against the IGF-1 receptor inhibit breast cancer cell proliferation *in vitro* and block the mitogenic effects of exogenous IGF-1[129]. This blockade also inhibits the *in vivo* growth of estrogen-independent breast cancer cells[129]. Dominant negative mutants of the IGF-I receptor suppress adhesion and invasion of breast cancer cell lines[164]. Selective inhibitors of the IGF-1 receptor also inhibit proliferation and enhance apoptosis by increasing the response of tumour cells to ionising radiation[165] The IGF-1 receptor can also be targeted by small molecular inhibitors of the IGF-1R tyrosine kinase, and molecular agents such as antisense and small interfering RNAs[127;166]. Dalotuzumab is a recombinant humanized monoclonal antibody targeted against IGF-1 receptor which has been used for the potential intravenous treatment of cancer[167]. It acts by inhibiting IGF-1 and IGF-2 mediated tumour cell proliferation, IGFR-1 autophosphorylation and Akt phosphorylation. In multiple cancer cell lines and in mouse xenograft models, dalotuzumab displays significant

antitumour activity, in particular against breast cancer. In addition coadministration of Dalotuzumab with other anti cancer agents, such as Taxanes enhanced the *in vivo* and *in vitro* antitumour activity of dalotuzumab. At the moment several clinical trials are undergoing to evaluate Dalotuzumab use alone and in combination with other anticancer agents to treat several solid tumours[167].An alternative, but less practical method for reducing IGF-1 action is to limit its bioavailabilty by transfection of IGFBPs[168;169].

Somatostatin analogues exert antiproliferative effects both *in vivo* and *in vitro*, in part by inhibiting GH release and therefore reducing IGF-I levels, eg octreotide reduces breast cancer growth by 50% in mice[3]. However, the results in humans have been disappointing, and no study has reported either an objective tumour response or a significant difference in overall or disease-free survival[170-172]. It is possible that combination therapy with tamoxifen, octreotide and a prolactin antagonist might be more beneficial[173].

To date the most potent therapy for reducing serum IGF-1 levels is Pegvisomant, the novel GH-receptor antagonist[174]. It is intriguing that in nude mice xenografted with human colorectal cancer cell lines, Pegvisomant treatment caused a 39% reduction in tumour volume and a 44% reduction in tumour weight[175]. Pegvisomant also demonstrates inhibitory effects against breast cancer cell lines implanted into athymic mice[176]. Whether this can be translated to human breast cancer *in vivo* remains to be seen.

A major cause of recurrence and treatment failure in breast cancer is the development of resistance to oestrogen manipulation. The significant cross talk between IGF-1 and oestrogen-mediated signalling has been proposed as an important mechanism for the development of this resistance[177]. Therefore targeting the IGF-1 pathway may be a novel

approach to overcoming this resistance. A study has shown the inhibition of the IGF-1R pathway and aromatase to be synergistic in two independent oestrogen-dependant *in vitro* models of breast cancer[178]. More over synergism of a selective IGF-1R inhibitor (NVP-AEW541) and letrozole correlated with induction of apoptosis. Therefore combination of IGF-1R inhibitors and letrozole may hold promise for the treatment of patients with oestrogen-dependent breast cancer.

Similarly, it has been suggested that the IGF-1 signalling pathway also interferes with the antiproliferative actions of trastuzumab[179]. Trastuzumab (Herceptin) is a humanized monoclonal antibody directed against the extracellular domain of the tyrosine kinase receptor ERBB2. ErbB2 is a member of the epidermal growth factor receptor family and has been implicated in cellular proliferation, apoptosis and angiogenesis. It is overexpressed in 25-30% of breast cancers and is associated with an aggressive phenotype and poor prognosis. Trastuzumab is an effective inhibitor of the growth of breast cancers overexpressing ErbB2, although not all respond and most become resistant within 12 months. This is associated with increased signalling through the IGF-I receptor[179]. In addition, IGF-I and ErbB2 receptors are known to heterodimerise. The resultant activated receptor cannot bind trastuzumab and consequently deregulated signalling from this heterodimer occurs[180]. Confirmation of an association between IGF-I receptor activation and resistance to trastuzumab would support a future role for combination treatment with anti-IGF-I receptor and anti-ErbB2 therapies[181].

Overexpression of IGF-1R has been shown to reduce trastuzumab-mediated growth arrest of HER2-overexpressing breast cancer cells[179]. In addition it has been shown that IGF-1R induces phosphorylation of HER2 specifically in trastuzumab-refractory breast cancer cells[180]. IGF-1R blockade using a specific kinase inhibitor, antibody, or IGF-1 binding

protein restored trastuzumab response to resistant cells[179;180]. This supports the importance of the IGF-1 signalling pathway in trastuzumab resistance.

Further study has shown that the phenolic compound nordihydroguaiaretic acid (NDGA) promoted cell death of tratuzumab-naive and trastuzumab-refractory HER2-overexpressing breast cancer cell lines[182]. NDGA has been shown to induce DNA fragmentation, cleavage of poly (ADP-ribose) polymerase and caspase-3, and inhibition of colony formation. Combination treatment with NDGA and trastuzumab suppresses proliferation and survival of trastuzumab-refractory cells to a greater degree than either agent alone. This suggests that NDGA increases the sensitivity of refractory cells to trastuzumab. Derivatives of NDGA are currently in clinical trial for other solid tumours. The data strongly suggests the further study of NDGA as a potential therapeutic against breast cancers that have progressed on trastuzumab[182].

Ultimately the GH/IGF-1 axis has been shown to play an important role in both normal mammary development and carcinogenesis. It is possible that measuring serum IGF-1 and IGFBP-3 levels may prove to be useful in women at increased risk of developing breast cancer, and may provide useful information should breast cancer subsequently develop. However further clinical trials are required, with larger numbers of patients, to determine the detailed effects of IGF-1R antagonists, GH antagonists and somatostatin agonists in the treatment of breast cancer.

8. Conclusion

We have shown the expression of IGF-1 in normal and malignant breast tissue, with the Ribogreen method showing that breast tumours produce 3-4 times more IGF-1 RNA than normal breast tissue. Interestingly, looking at our RT-PCR results, it showed that IGF-1 mRNA was significantly down regulated in breast tumours compared to normal breast tissue. This may be accounted for by the large number of cells present in breast tissue, which may affect the results. This may indicate a place for laser capture microdissection so that mRNA from only breast tumour cells can be examined. My research has shown expression of IGF-1R, PCNA, VEGF-165, Vitamin D receptor and HTERT all to be over expressed in breast tumour tissue compared to normal breast tissue. The up regulation of these genes fits in with the cell proliferation, angiogenesis and reduced apoptosis that occurs in malignant tissue. It also explains the importance of developing selective inhibitors to the IGF-1R, such as Dalotuzumab, which is currently undergoing several clinical trials into the treatment of breast cancer.

In summary, using a viable system for keeping normal and malignant breast tissue alive for up to 96 hours, using immunohistochemical staining of IGF-1, looking at serum levels of IGF-1 in women with breast cancer, and using microarray, we have established a role for the GH-IG-1 axis in the development and progression of breast cancer. This indicates the role for a novel treatment for breast cancer using antagonists to the GH-IGF-1 axis.

Tissue storage consent form '02

CONSENT FORM

TO BE USED WHERE AN OPERATION OR INVESTIGATION WILL INVOLVE REMOVAL AND STORAGE OF TISSUE, ORANS OR BODY PARTS FROM THE PATIENT

Four copies of this form should be obtained.
One should be given to the patient, one filed in the hospital notes, one retained by the researcher and one given to pathology with the specimen.

Patient's details:

Name.....

Hospital number.....

D.O.B.....

Patient's condition requiring treatment

.....

Intended operation / investigation

.....

Tissue, organs or body parts involved

.....

Tissue samples will be taken during your procedure, and sent to the hospital laboratories. This is routine practice essential for diagnosis and for planning further treatment. However in some cases more tissue will be removed than is needed for these tests. The aim of this form is to ask whether we may keep the remainder of the breast tissue that has been removed, to use in our research.

In our department we carry out research on breast disease. In your particular case, examples of the type of research we might plan include testing DNA and RNA (gene testing), growing cells from the sample in an incubator, analyzing the chemicals made by the cells in the sample, and finding out why the cells behave abnormally. Such research improves our understanding of these diseases.

By signing this form you will only be giving us permission to store your tissue for future research of this type. Any use that we want to make of it in the future will have first to be approved by our local Research Ethics Committee, which is an independent panel of experts who assess all research projects for safety, ethical acceptability and who protect patients' interests. Most of the work that we envisage will have no direct implications for your personal health. This may be because the tissue cannot be identified as yours, or it may simple be because of the type of research involved.

However in some circumstances we may wish to use your tissue which we can link back to you and your clinical record. Such research may have direct consequences for you or for your family. If it does, we would first ask the Research Ethics Committee and having obtained their approval for the research; we would always come back to you to explain the implications, and would then ask your consent to proceed. You would of course have the opportunity to refuse permission at that stage. If we do not believe our research will have implications for you or your relatives, and the Research Ethics Committee approves the research without your further consent, then we will not ask your permission.

Further details of the type of research we do are on the other side of this page, and will be explained to you by the doctor signing the form.

The information obtained from our research could be published in scientific journals and discussed at scientific and medical conferences. It would b completely anonymous. If we decided that it would be helpful to publish or discuss information about your case alone, it would still be anonymous but we would not go ahead without obtaining your consent again.

There is always a possibility that tissue, which cannot be linked back to you, may be used in the commercial development of medical technology. We would only ask for your consent to such development in relation to your tissue if for any reason it could be linked to you.

You do not have to agree to the storage of your tissue. You are free to decide not to participate.

I confirm that I have explained the nature of the tissue, organs or body parts that it is intended to remove. I have explained that they may be stored for use at a later date, in research as well as for diagnosis. I have explained this in terms which, in my judgment are suited to the understanding of the patient and/or guardian if the patient is a child.

Signature.....
Date.....

Name of practitioner seeking consent
(PRINT).....

FURTHER DETAILS OF THE PLANNED RESEARCH

Breast tumours are growths arising from the glands f the breast, and in the first instance the best treatment is to remove them surgically. You will shortly be undergoing an operation to remove your tumour, and this will be taken to the Pathology Department who will cut the tumour into very thin sections so that it can be examined under the microscope. This is an important part of your investigation as it will give your doctors detailed information about which will help them to provide you with the best treatment. However, a lot of the tissue is then left over, and we store this in the Pathology Department. We are very interested as to how these tumours start in the first place. We believe it is probably due to a change in the DNA, the information molecule at the center of every cell. Our research studies examine the cells of breast tumours to see how they are different from normal cells, and what makes them act as tumours. To this end, we may look at different types of chemical within the tumour, including DNA, RNA and protein molecules, which we can compare with normal tissue. We may also look at the way that these tumours make hormones when they are in test tubes, and see what controls their hormone production and also what makes the cells divide. No information relating to you personally will be used, but we may look at details such as your sex, age, the size of the tumour, and the particular abnormal cells. If we find any changes within the tumour, we my need to re-contact you for a blood sample or we may take one now if blood samples are taken as part of your current treatment. This would merely be to compare the results in the tumour to your blood to see whether the changes within the tumour were significant, and this would have no relation to your particular disease.

TO BE COMPLETED BY THE PATIENT / PARENT / GUARDIAN

Please read this form carefully. You will be given a copy.

If there is anything that you do not understand about the explanation and information you have been given, or if you want more information, you should ask the doctor before you sign the form.

If you understand the explanation and agree to the proposed plan, please print your name and sign in the space indicated below. Please note that you will also be asked to sign a separate consent form for the operation or investigation itself.

1. I understand that I am consenting for my tissue to be stored for research of a particular kind.

2. I understand that any further use of my tissue in the future for research of this kind will be approved by the local Research Ethics Committee.

3. I understand that if our research is thought likely to have any implications for me or my family, you will explain them to me, and ask my specific consent before proceeding with it.

4. I understand that if it is believed that our research will have no such implications, and if the Research Ethics Committee has approved the research, I will not be asked for further permission.

5. I understand that I will e asked to give consent for the commercial use of any tissue that can be linked back to me.

Signature.....Date.....

Name (please PRINT).....Relationship: Patient/Parent/Guardian/Other*
**(please delete as necessary)*

This form should be witnessed by another person independent from the doctors looking after the patient. This could for example be a relative or member of the nursing staff.

Witness signature.....Date.....

Name (please PRINT).....Relationship.....

Where relevant, a translator should sign below to confirm they have interpreted the information on this completed form for the above patient in terms which they believe he or she can understand.

Translator signature.....Date.....

Name (please PRINT).....Language used.....

Name and address of the Principal Investigator responsible for storing the patient's material (please PRINT):

.....

.....

Telephone number: .....

Appendix B. Patient tumour characteristics

Sample No.	Specimen	Patient age	Prev op	Previous Histol	Histol	Size	Grade	LN	Vasc inv	Associated DCIS	ER	PR
100N	Right Prophylactic mastectomy	49	yes	R WLE+AC. 2.8cm G3 0/10 LN ER+PR+	no cancer	n/a	n/a	none	none	none	no	no
101N/T	Left mast and AC	68	no	none	IDC	16mm	3	1/10 micomet	yes	HGDCIS	0	0
102N/T	Left WLE and AC	45	no	none	IDC	25mm	2	1/15 LN	yes	HGDCIS	8	7
103N/T	Right mast and AC	94	yes	R WLE+AS. IDC G2 0/3LN. Recurrence axillary tail	IDC	7mm	2	4/12 LN	yes	none	7	8
104N/T	Left mast and AC	61	no	none	DCIS	14mm	n/a	0/12 LN	no	DCIS	8	8
105N/T	Right WLE and AC	54	no	none	IDC	23mm	2	2/14 LN	no	HGDCIS	8	8
106N/T	Left WLE and AC	50	no	none	Tub+lob	13mm	1	0/11 LN	no	DCIS	7	5
107N/T	Left WLE and AC	65	no	none	IDC	14mm	2	0/13 LN	no	none	8	4
108N/T	Left WLE and AC	67	no	none	IDC	9mm	2	0/12 LN	no	DCIS	8	7
109N/T	Left mast and AC	83	no	none	IDC	21mm	2	0/15 LN	no	none	7	8

110N/T	Right WLE and AC	31	no	none	IDC	17mm	2	1/14 LN	no	no	8	5
111N/T	Right WLE and AS	78	yes	Left breast - fibroadenosis	IDC	13mm	2	0/4 LN	no	no	0	0
112N	Bilat proph mastectomy	72	no	none	hyperplasia	n/a	n/a	none	no	no	no	no
113N/T	Right WLE and AS	77	no	none	IDC	15mm	2	1/17 LN	no	DCIS	7	6
114N/T	Right WLE and AS	56	no	none	IDC	8mm	1	0/19 LN	no	DCIS	7	8
115N/T	Left mast and AC	88	no	none	IDC	15mm	1	0/9 LN	no	no	8	7
116N/T	Right WLE and AC	77	no	none	Tubular	18mm	1	0/15 LN	no	DCIS	8	8
117N/T	Right WLE and AC	91	no	none	IDC	23mm	1	0/6 LN	no	no	8	8
118N/T	Left mast and LD recon	58	no	none	Ductal+lob	53mm	2	none	yes	no	6	3
119N	Right WLE	60	no	none	radial scar	21mm	n/a	none	no	no	no	no
120N/T	Left WLE and AS	66	no	none	IDC	8mm	1	0/5 LN	no	HGDCIS	8	8
121N/T	Right WLE and AS	61	no	none	IDC	14mm	3	1/6 LN	no	DCIS	6	7
122N/T	Left mast and AC	71	no	none	lobular	55mm	2	16/18	yes	no	8	6
123N/T	Right WLE and AC	73	no	none	IDC	12mm	2	0/23 LN	no	HGDCIS	8	6
124N/T	Right mast and AC	49	no	none	IDC	40mm	3	4/15 LN	yes	HGDCIS	5	8
125N/T	Right WLE and AC	40	no	none	IDC	18mm	2	8/20 LN	yes	DCIS	8	8
126N/T	Right WLE and As	60	no	none	Tubular	11mm	1	0/4 LN	no	no	7	8
127N/T	Right mast and AC	77	no	none	IDC	16mm	3	19/19 LN	yes	HGDCIS	0	0

128N/T	Right WLE and AC	45	no	none	AMC	22mm	3	0/14 LN	yes	no	0	3
129N/T	Right WLE and AC	87	no	none	IDC	23mm	3	0/15 LN	no	no	8	4
130N/T	Right mastectomy	45	yes	G3 IDC 0/12 LN	IDC	29mm	2	none	no	DCIS	7	7
131N/T	Left WLE and AC	76	no	none	mucinous	15mm	1	0/28 LN	no	no	7	7
132N/T	Right WLE	76	no	none	IDC	16mm	3	none	yes	HGDCIS	8	8
133N/T	Right WLE and AC	64	no	none	IDC	21mm	2	15/18 LN	yes	HGDCIS	0	0
134N/T	Left WLE and AS	82	no	none	mucinous	11mm	2	0/3 LN	no	no	8	6
135N/T	Right mast and AC	71	no	none	Ductal+lob	10mm	2	1/10 LN	yes	DCIS	7	7
136N/T	Left WLE and AC	86	no	none	IDC	20mm	3	0/14 LN	no	DCIS	8	7
137N/T	Left mast and AC	78	no	none	IDC	20mm	3	2/11 LN	no	DCIS	7	4
138N/T	Right WLE and AC	84	no	none	DCIS	16mm	n/a	0/9 LN	no	DCIS	7	6
139N	Right compl mast	65	yes	11mm G3 IDC	none	n/a	n/a	none	no	no	no	no
140N/T	Left WLE and AC	85	no	none	IDC	24mm	2	1/18 LN	on	DCIS	7	4
141N/T	Left WLE and AS	65	no	none	IDC	10mm	3	1/11 LN	no	HGDCIS	0	0
142 N/T	Right WLE and AC	80	no	none	IDC	11mm	3	1/15 LN	yes	HGDCIS	8	0

143N/T	Right mast and AC	67	no	none	IDC	70mm	3	2/12 LN	yes	HGDCIS	7	6
144N/T	Left mast and AC	49	no	none	IDC	50mm	2	5/14 LN	yes	HGDCIS	6	5
145N/T	Left WLE and AC	64	no	none	Tubular	22mm	1	1/11 LN	no	no	8	8
146N/T	Left compl mast	79	yes	12mmG2 IDC	Ductal+lob	19mm	3	0/2 LN	yes	no	7	5
147N/T	Left mast and AC	48	no	none	IDC	10mm	1	0/30 LN	no	DCIS	8	5
148N/T	Right WLE and AS	61	no	none	Tubular	16mm	1	0/4 LN	no	no	6	4
149N	Right WLE and AS	60	no	none	IDC	9mm	2	0/5 LN	yes	DCIS	8	8
150N/T	Right mast and AC	50	no	none	IDC	24mm	2	2/22 LN	no	DCIS	7	6
151N	Right compl mast	53	yes	23mmG2 IDC	DCIS	2mm	n/a	none	no	DCIS	8	8
152N/T	Left mast and AS	58	no	none	HGDCIS	9mm	n/a	0/1 LN	no	HGDCIS	6	4
153N/T	Left mast and AS	58	no	none	HGDCIS	5mm	n/a	0/4 LN	no	HGDCIS	7	8
154N	Left WLE and AS	71	no	none	IDC	7mm	1	0/7 LN	no	DCIS	8	8
155N/T	Right mast and AC	77	no	none	IDC	60mm	3	0/18 LN	no	no	0	0
156N/T	Right mast and AC	67	yes	G2 0/2LN	IDC	42mm	3	19/19 LN	yes	no	4	0

157N/T	Left mastand AC	87	no	non	IDC	25mm	3	0/10LN	no	no	0	0
158N	Right WLE and SLNB	67	no	none	IDC	7mm	3	0/4 LN	no	DCIS	7	7
159N	Right mast and AC	71	yes	G3 IDC	Fibrotic	n/a	n/a	0/10 LN	no	no	no	no
160N/T	Left mast and AC	40	no	none	Ductal+lob	18mm	1	0/15 LN	no	DCIS	7	8
161N/T	Right WLE and AC	91	no	none	IDC	20mm	2	0/9 LN	no	no	8	8
162N/T	Left WLE and AS	71	no	none	IDC	17mm	3	3/8 LN	no	HGDCIS	7	6
163N	Right WLE and AS	61	no	none	IDC	5mm	3	4/5 LN	no	HGDCIS	6	4
164N/T	Left compl mast	72	yes	G3 21mm IDC 0/9 LN	IDC	45mm	3	none	yes	DCIS	0	0
165N	Right WLE	71	yes	DCIS	DCIS	15mm	n/a	none	no	DCIS	7	6
166N/T	Right WLE and AS	76	no	none	IDC	16mm	2	1/5 LN	no	DCIS	0	0
167N/T	Right mast and AC	48	yes	DCIS	IDC	28mm	3	1/9 LN	yes	no	5	8
168N	Left breast reduction	54	yes	9mm G1 IDC 0/6 LN	Fibrocystic	n/a	n/a	none	no	no	no	no
169N	Left WLE	68	yes	G2 IDC 4/8 LN	HGDCIS	2mm	n/a	none	no	HGDCIS	6	4

170N	Right WLE and AS	66	yes	radial scar	IDC	8mm	2	0/4 LN	no	HGDCIS	7	7
171N	Proph bilat mast	62	no	none	Fibrocystic	n/a	n/a	0/14 LN	no	no	no	no
172N/T	Left WLE and AC	56	no	none	Squamous	19mm	3	2/24 LN	no	HGDCIS	4	4
173N/T	Right mast	66	yes	8mm IDC	Ductal+lob	8mm	2	none	no	DCIS	7	8
174N/T	Left mast and AS	76	yes	G2 IDC 1/11LN	HGDCIS	22mm	n/a	1/4 LN	yes	HGDCIS	0	2
175N/T	Right mast and AC	86	yes	left mast	ILC	35mm	2	0/7 LN	no	no	8	5
176N/T	Right WLE and AC	74	no	none	HGDCIS	19mm	3	0/15 LN	yes	HGDCIS	0	3
177N	Left breast reduction	65	yes	G3 IDC	Hyperplasia	n/a	n/a	none	no	no	no	no
178N/T	Left WLE and AS	48	no	none	IDC	15mm	2	1/4 LN	no	DCIS	7	4
179N	Right mast and AS	63	no	none	IDC	21mm	1	0/8 LN	no	DCIS	8	8
180N	Left WLE	77	no	none	HGDCIS	35mm	n/a	none	no	HGDCIS	0	0
181N/T	Right WLE and AC	81	no	none	IDC	13mm	1	0/10 LN	no	no	7	7
182N/T	Right mast and AC	71	no	none	IDC	50mm	3	12/20 LN	no	no	7	8
183N/T	Right mast and AC	51	no	none	Ductal+lob	22mm	3	2/10 LN	yes	DCIS	7	8
184N/T	Left mast and AS	57	no	none	IDC	9mm	2	0/4 LN	no	DCIS	7	8
185N/T	Left mast	87	no	none	ILC	75mm	2	4/14	no	DCIS	7	2

	and AC							LN				
186N/T	Right mastectomy	72	yes	21mm G2 IDC	Ductal+lob	15mm	2	none	no	no	7	4
187N/T	Left mast and AS	60	no	none	IDC	8mm	3	0/6 LN	yes	HGDCIS	4	7
188N/T	Left mastectomy	84	no	none	IDC	11mm	3	0/7 LN	no	DCIS	8	7
189N/T	Left WLE and AS	64	no	none	Ductal+lob	14mm	1	0/5 LN	no	no	7	7
190N/T	Left mast and AC	39	no	none	IDC	32mm	3	2/12 LN	no	HGDCIS	6	8
191N/T	Right mast and AC	79	no	none	Ductal+lob	18mm	2	2/11 LN	no	HGDCIS	7	4
192N/T	Right mast and AC	54	no	none	ILC	28mm	1	0/12 LN	no	DCIS	7	4
193N/T	Left mastectomy	69	yes	fibrocystic	maligant phyllodes	60mm	n/a	none	no	no	no	no
194N/T	Left mast and AS	65	no	none	ILC	8mm	2	0/2 LN	no	LCIS	7	6
195N/T	Left WLE and AS	67	no	none	IDC	22mm	2	0/6 LN	no	no	7	7
196N/T	Right mast and AC	63	no	none	IDC	19mm	3	1/9 LN	yes	HGDCIS	5	7
197N/T	Left WLE and AC	70	no	none	IDC	35mm	2	0/18 LN	no	DCIS	6	5
198N	Exc right breast lump	33	no	none	Fibroadenoma	n/a	n/a	none	no	no	no	no
199N	Exc right	38	no	none	Hamartoma	n/a	n/a	none	no	no	no	no

	breast lump											
200N	Exc right breast lump	41	no	none	Fibroadenoma	n/a	n/a	none	no	no	no	no
201N	Left reduction mastectomy	63	yes	right WLE and AC	Fibrocystic change	n/a	n/a	none	no	no	no	no
202N/T	Left mast and AC	79	no	none	IDC	80mm	3	0/12 LN	no	no	0	0
203N/T	Right mast and AC	48	no	none	IDC	20mm	3	4/9 LN	yes	DCIS	0	2
204N/T	Right WLE and AC	83	no	none	IDC	24mm	3	1/10 LN	no	DCIS	7	5
205N/T	Right mast and AC	61	yes	benign lump	IDC	15mm	1	1/10 LN	no	no	8	8
206N/T	Right mast and AC	60	no	none	IDC	19mm	3	0/12 LN	no	no	5	6
207N	Exc right breast lump	38	no	none	Hamartoma	n/a	n/a	none	no	no	no	no
208N	Exc right breast lump	26	no	none	Fibroadenoma	n/a	n/a	none	no	no	no	no
209N/T	Right WLE and AC	81	no	none	IDC	30mm	2	6/6 LN	no	no	8	0
210N/T	Left WLE and AC	50	no	none	IDC	27mm	3	0/13 LN	no	no	0	0
211N	Proph left mast	78	yes	12mm DCIS	fibrosis	n/a	n/a	none	no	no	no	no
212N/T	Right mast and AC	87	no	none	IDC	40mm	3	10/16 LN	yes	HGDCIS	0	0

213N/T	Right mastectomy	75	yes	R WLE and AC	IDC	12mm	3	none	no	no	0	3
214N	Exc right breast lump	42	no	none	fibrosis	n/a	n/a	none	no	no	no	no
215N	Exc left breast lump	38	no	none	Hamartoma	n/a	n/a	none	no	no	no	no
216N	Exc right breast lump	28	no	none	Hamartoma	n/a	n/a	none	no	no	no	no
217N/T	Left WLE and AC	82	no	none	IDC	16mm	2	2/19 LN	no	HGDCIS	8	6
218N/T	Left WLE and AC	61	no	none	Muscinous	40mm	2	0/9 LN	no	DCIS	8	8
219N/T	Right WLE and AC	43	no	none	IDC	3mm	3	0/9 LN	no	HGDCIS	0	0
220N/T	Left mast and AC	59	no	none	IDC	45mm	3	1/12 LN	yes	DCIS	8	6
221N	Exc of right breast lump	26	no	none	Fibroadenoma	n/a	n/a	none	no	no	no	no
222N/T	Left mast and AC	66	no	none	IDC	14mm	2	0/17 LN	no	DCIS	6	6
223*N/T*	Left WLE and AC	57	no	none	IDC	26mm	3	0/13 LN	no	DCIS	7	8
224N	Exc left breast lump	40	no	none	Fibroadenoma	n/a	n/a	none	no	no	no	no
225N/T	Left mast and AC	41	no	none	IDC	50mm	2	0/16 LN	no	HGDCIS	8	4
226N/T	Left mast and AC	60	no	none	IDC	22mm	2	14/14 LN	yes	HGDCIS	0	0
227N	Exc right	38	no	none	Fibroadenoma	n/a	n/a	none	no	no	no	no

	breast lump											
228N	Proph right mastectomy	60	yes	Left mast and AC	Normal	n/a	n/a	none	no	no	no	no
229N	Exc of left breast lump	39	no	none	radial scar	n/a	n/a	none	no	no	no	no
230N	Exc of right breast lump	25	no	none	Fibroadenoma	n/a	n/a	none	no	no	no	no
231N	Exc of left breast lump	75	no	none	Fibrofatty	n/a	n/a	none	no	no	no	no
232N/T	Right mast and AS	66	no	none	IDC	12mm	2	0/4 LN	no	no	8	7
233N	Exc left breast lump	52	no	none	Hamartoma	n/a	n/a	none	no	no	no	no
234N/T	Left mast and AC	78	no	none	Mucinous	50mm	2	4/6 LN	no	no	8	7
235N/T	Right mast and AC	76	no	none	ILC	16mm	2	0/15 LN	no	DCIS	8	3
236N/T	Right WLE and AC	95	no	none	Papillary	4mm	2	0/9 LN	no	DCIS	8	8
237N/T	Left WLE and AC	71	no	none	IDC	19mm	3	16/18 LN	no	no	0	0
238N/T	Right mast and AC	86	no	none	IDC	26mm	3	0/15 LN	no	no	0	4
239N/T	Left WLE and AC	51	no	none	IDC	17mm	2	2/16 LN	no	HGDCIS	3	8
240N/T	Left mast and SLNB	64	yes	duct excision	IDC	30mm	1	1/10 LN	no	DCIS	8	7
241N/T	Right mast and AC	68	yes	G3 IDC	IDC	11mm	3	0/6 LN	no	DCIS	7	4

242N/T	Left mast and AC	70	no	none	IDC	35mm	3	9/10 LN	yes	no	8	0
243N/T	Left mast and AC	69	no	none	Ductal+lob	12mm	3	0/10 LN	no	HGDCIS	8	7
244N/T	L mast and AC	60	no	none	IDC	17mm	2	0/11 LN	no	HGDCIS	6	7
245N/T	Left WLE and AC	67	no	none	IDC	27mm	3	0/11 LN	no	LCIS	0	0
246N/T	Right mast and AC	58	no	none	IDC	45mm	3	1/13 LN	yes	HGDCIS	7	3
247N	Exc right breast lump	45	no	none	Hamartoma	n/a	n/a	none	no	no	no	no
248N/T	Left mast and AC	70	no	none	IDC	60mm	3	2/15 LN	yes	DCIS	8	8
249N/T	Left mast and AC	69	yes	mastect	IDC	14mm	3	0/7 LN	no	HGDCIS	0	0
250N	Right mast and AC	72	no	none	IDC	40mm	3	5/15 LN	no	DCIS	4	2
251N	Exc right breast lump	39	no	none	Hamartoma	n/a	n/a	none	no	no	no	no
252N	Exc left breast lump	25	no	none	Fibroadenoma	n/a	n/a	none	no	no	no	no
253N/T	Right mast and AC	58	no	none	IDC	12mm	3	0/15 LN	no	HGDCIS	0	0
254N	Left breast reduction	38	no	none	Normal	n/a	n/a	none	no	no	no	no
255N	Exc left breast lump	69	no	none	Normal	n/a	n/a	none	no	no	no	no
256N	Exc left	37	no	none	Fibroadenoma	n/a	n/a	none	no	no	no	no

	breast lump											
257N	Exc left breast lump	40	no	none	Normal	n/a	n/a	none	no	no	no	no
258N/T	Left mast and AC	59	no	none	IDC	70mm	3	14/16 LN	yes	HGDCIS	0	0
259N/T	Left mast and AC	66	yes	Right mast+AC	Papillary	35mm	2	0/10 LN	no	no	0	0
260N	Bilat breast reduction	44	no	none	Normal	n/a	n/a	none	no	no	no	no
261N	Exc right breast lump	36	no	none	Fibroadenoma	n/a	n/a	none	no	no	no	no
262N	Exc right breast lump	51	no	none	Fibroadenoma	n/a	n/a	none	no	no	no	no
263N	Exc left breast lump	46	no	none	Fibrosis	n/a	n/a	none	no	no	no	no
264N/T	Right mast and SLNB	60	no	none	IDC	12mm	1	0/5 LN	no	no	7	2
265N	Exc left breast lump	28	no	none	Fibroadenoma	n/a	n/a	none	no	no	no	no
266T	Exc left breast lump	62	yes	Left mast	IDC	10mm	2	none	no	no	6	7
267N/T	Left WLE	78	yes	Left mast	ILC	12mm	2	none	no	no	0	0
268N	Exc left breast lump	68	no	none	Lipoma	n/a	n/a	none	no	no	no	no
269N/T	Left mast and AS	64	no	none	IDC	13mm	2	0/4 LN	no	DCIS	5	5
270N	Right WLE	28	no	none	Hamartoma	n/a	n/a	none	no	no	no	no
271N/T	Exc right breast lump	48	no	none	IDC	8mm	1	none	no	no	0	0

272N	Exc left breast lump	59	no	none	Inflamed cyst	n/a	n/a	none	no	no	no	no
273N/T	Left mast and AC	85	no	none	IDC	19mm	3	0/7 LN	no	HGDCIS	8	5
274N/T	Right WLE and AC	74	no	none	IDC	33mm	3	10/19 LN	yes	DCIS	8	8
275N/T	Left WLE and AC	50	no	none	IDC	17mm	3	0/15LN	no	no	0	0
276N/T	Left mast and AC	80	no	none	IDC	66mm	3	1/14 LN	no	DCIS	8	5
277N/T	Right mast and AC	53	no	none	IDC	18mm	2	5/5 LN	no	no	7	4
278N/T	Right mast and AS	60	yes	R WLE	IDC	22mm	3	2/11 LN	no	no	7	6
279N/T	Left compl mast	60	yes	18mm G3 IDC	IDC	13mm	3	none	no	HGDCIS	7	6
280N/T	Right mast and AC	57	no	none	IDC	22mm	3	1/19 LN	no	no	0	0
281N/T	Left mast and AS	59	no	none	IDC	18mm	2	0/4 LN	no	DCIS	7	8
282N	Exc left breast lump	29	no	none	Fibroadenoma	n/a	n/a	none	no	no	no	no
283N	Exc right breast lump	28	no	none	Fibroadenoma	n/a	n/a	none	no	no	no	no
284N	Exc right breast lump	34	no	none	Hamartoma	n/a	n/a	none	no	no	no	no
285N/T	Left mast and AC	70	no	none	IDC	16mm	2	0/15 LN	no	DCIS	6	7

Reference List

(1) Le Roith D, Bondy C, Yakar S, Liu JL, Butler A. The Somatomedin Hypothesis: 2001. *Endocr Rev* 2001; 22(1):53-74.

(2) Kojima M, Hosoda H, Date Y, Nakazato M, Matsuo H, Kangawa K. Ghrelin is a growth-hormone-releasing acylated peptide from stomach. *Nature* 1999; 402(6762):656-660.

(3) Dolan JT, Miltenburg DM, Granchi TS, Miller CC, Brunicardi FC. Treatment of metastatic breast cancer with somatostatin analogues--a meta-analysis. *Ann Surg Oncol* 2001; 8(3):227-233.

(4) Date Y, Kojima M, Hosoda H, Sawaguchi A, Mondal MS, Suganuma T et al. Ghrelin, a Novel Growth Hormone-Releasing Acylated Peptide, Is Synthesized in a Distinct Endocrine Cell Type in the Gastrointestinal Tracts of Rats and Humans. *Endocrinology* 2000; 141(11):4255-4261.

(5) Sakata I, Nakamura K, Yamazaki M, Matsubara M, Hayashi Y, Kangawa K et al. Ghrelin-producing cells exist as two types of cells, closed- and opened-type cells, in the rat gastrointestinal tract. *Peptides* 2002; 23(3):531-536.

(6) Hosoda H, Kojima M, Matsuo H, Kangawa K. Ghrelin and des-acyl ghrelin: two major forms of rat ghrelin peptide in gastrointestinal tissue. *Biochem Biophys Res Commun* 2000; 279(3):909-913.

(7) Arvat E, Di Vito L, Broglio F, Papotti M, Muccioli G, Dieguez C et al. Preliminary evidence that Ghrelin, the natural GH secretagogue (GHS)-receptor ligand, strongly stimulates GH secretion in humans. *J Endocrinol Invest* 2000; 23(8):493-495.

(8) Sun Y, Ahmed S, Smith RG. Deletion of ghrelin impairs neither growth nor appetite. *Mol Cell Biol* 2003; 23(22):7973-7981.

(9) Tschop M, Smiley DL, Heiman ML. Ghrelin induces adiposity in rodents. *Nature* 2000; 407(6806):908-913.

(10) Cummings DE, Purnell JQ, Frayo RS, Schmidova K, Wisse BE, Weigle DS. A Preprandial Rise in Plasma Ghrelin Levels Suggests a Role in Meal Initiation in Humans. *Diabetes* 2001; 50(8):1714-1719.

(11) Ukkola O, Ravussin E, Jacobson P, Snyder EE, Chagnon M, Sjostrom L et al. Rapid Communications: Mutations in the Preproghrelin/Ghrelin Gene Associated with Obesity in Humans. *J Clin Endocrinol Metab* 2001; 86(8):3996-3999.

(12) Gnanapavan S, Kola B, Bustin SA, Morris DG, McGee P, Fairclough P et al. The tissue distribution of the mRNA of ghrelin and subtypes of its receptor, GHS-R, in humans. *J Clin Endocrinol Metab* 2002; 87(6):2988.

(13) Jeffery PL, Murray RE, Yeh AH, McNamara JF, Duncan RP, Francis GD et al. Expression and function of the ghrelin axis, including a novel preproghrelin isoform, in human breast cancer tissues and cell lines. *Endocr Relat Cancer* 2005; 12(4):839-850.

(14) Cassoni P, Papotti M, Ghe C, Catapano F, Sapino A, Graziani A et al. Identification, Characterization, and Biological Activity of Specific Receptors for Natural (Ghrelin) and Synthetic Growth Hormone Secretagogues and Analogs in Human Breast Carcinomas and Cell Lines. *J Clin Endocrinol Metab* 2001; 86(4):1738-1745.

(15) Furlanetto RW, DiCarlo JN. Somatomedin-C Receptors and Growth Effects in Human Breast Cells Maintained in Long-Term Tissue Culture. *Cancer Res* 1984; 44(5):2122-2128.

(16) Humbel RE. Insulin-like growth factors I and II. *Eur J Biochem* 1990; 190(3):445-462.

(17) Zapf J, Schmid C, Froesch ER. Biological and immunological properties of insulin-like growth factors (IGF) I and II. *Clin Endocrinol Metab* 1984; 13(1):3-30.

(18) Chen JC, Shao ZM, Sheikh MS, Hussain A, LeRoith D, Roberts CT et al. Insulin-like growth factor-binding protein enhancement of insulin-like growth factor-I (IGF-I)-mediated DNA synthesis and IGF-I binding in a human breast carcinoma cell line. *J Cell Physiol* 1994; 158(1):69-78.

(19) Zapf J, Froesch ER. Insulin-like growth factors/somatomedins: structure, secretion, biological actions and physiological role. *Horm Res* 1986; 24(2-3):121-130.

(20) Jones JI, Clemmons DR. Insulin-Like Growth Factors and Their Binding Proteins: Biological Actions. *Endocr Rev* 1995; 16(1):3-34.

(21) Jones JI, Gockerman A, Busby WH, Jr., Wright G, Clemmons DR. Insulin-Like Growth Factor Binding Protein 1 Stimulates Cell Migration and Binds to the {alpha}5{beta}1 Integrin by Means of its Arg-Gly-Asp Sequence. *PNAS* 1993; 90(22):10553-10557.

(22) Mohan S, Baylink DJ. IGF-binding proteins are multifunctional and act via IGF-dependent and -independent mechanisms. *J Endocrinol* 2002; 175(1):19-31.

(23) Mohan S, Baylink DJ, Pettis JL. Insulin-like growth factor (IGF)-binding proteins in serum--do they have additional roles besides modulating the endocrine IGF actions? *J Clin Endocrinol Metab* 1996; 81(11):3817-3820.

(24) Papa V, Gliozzo B, Clark GM, McGuire WL, Moore D, Fujita-Yamaguchi Y et al. Insulin-like Growth Factor-I Receptors Are Overexpressed and Predict a Low Risk in Human Breast Cancer. *Cancer Res* 1993; 53(16):3736-3740.

(25) Jackson JG, White MF, Yee D. Insulin receptor substrate-1 is the predominant signaling molecule activated by insulin-like growth factor-I, insulin, and interleukin-4 in estrogen receptor-positive human breast cancer cells. *J Biol Chem* 1998; 273(16):9994-10003.

(26) Surmacz E. Function of the IGF-I receptor in breast cancer. *J Mammary Gland Biol Neoplasia* 2000; 5(1):95-105.

(27) Baserga R. The insulin-like growth factor I receptor: a key to tumor growth? *Cancer Res* 1995; 55(2):249-252.

(28) Ullrich A, Gray A, Tam AW, Yang-Feng T, Tsubokawa M, Collins C et al. Insulin-like growth factor I receptor primary structure: comparison with insulin receptor suggests structural determinants that define functional specificity. *EMBO J* 1986; 5(10):2503-2512.

(29) Xu S, Cwyfan-Hughes SC, van der Stappen JW, Sansom J, Burton JL, Donnelly M et al. Insulin-like growth factors (IGFs) and IGF-binding proteins in human skin interstitial fluid. *J Clin Endocrinol Metab* 1995; 80(10):2940-2945.

(30) Campbell PG, Novak JF, Yanosick TB, McMaster JH. Involvement of the plasmin system in dissociation of the insulin-like growth factor-binding protein complex. *Endocrinology* 1992; 130(3):1401-1412.

(31) Helle SI, Holly JM, Tally M, Hall K, Vander SJ, Lonning PE. Influence of treatment with tamoxifen and change in tumor burden on the IGF-system in breast cancer patients. *Int J Cancer* 1996; 69(4):335-339.

(32) Yee D, Paik S, Lebovic GS, Marcus RR, Favoni RE, Cullen KJ et al. Analysis of insulin-like growth factor I gene expression in malignancy: evidence for a paracrine role in human breast cancer. *Mol Endocrinol* 1989; 3(3):509-517.

(33) Cullen KJ, Allison A, Martire I, Ellis M, Singer C. Insulin-like growth factor expression in breast cancer epithelium and stroma. *Breast Cancer Res Treat* 1992; 22(1):21-29.

(34) Rajaram S, Baylink DJ, Mohan S. Insulin-Like Growth Factor-Binding Proteins in Serum and Other Biological Fluids: Regulation and Functions. *Endocr Rev* 1997; 18(6):801-831.

(35) Jernstrom H, Deal C, Wilkin F, Chu W, Tao Y, Majeed N et al. Genetic and Nongenetic Factors Associated with Variation of Plasma Levels of Insulin-like Growth Factor-I and Insulin-like Growth Factor-binding Protein-3 in Healthy Premenopausal Women. *Cancer Epidemiol Biomarkers Prev* 2001; 10(4):377-384.

(36) Lyons WR. Hormonal Synergism in Mammary Growth. *Proc R Soc B* 1958; 149(936):303-325.

(37) Ng ST, Zhou J, Adesanya OO, Wang J, LeRoith D, Bondy CA. Growth hormone treatment induces mammary gland hyperplasia in aging primates. *Nat Med* 1997; 3(10):1141-1144.

(38) Ruan W, Kleinberg DL. Insulin-like growth factor I is essential for terminal end bud formation and ductal morphogenesis during mammary development. *Endocrinology* 1999; 140(11):5075-5081.

(39) Gebauer G, Jager W, Lang N. mRNA expression of components of the insulin-like growth factor system in breast cancer cell lines, tissues, and metastatic breast cancer cells. *Anticancer Res* 1998; 18(2A):1191-1195.

(40) Voskuil DW, Bosma A, Vrieling A, Rookus MA, van 't Veer LJ. Insulin-like growth factor (IGF)-system mRNA quantities in normal and tumor breast tissue of women with sporadic and familial breast cancer risk. *Breast Cancer Res Treat* 2004; 84(3):225-233.

(41) Yee D, Lee AV. Crosstalk between the insulin-like growth factors and estrogens in breast cancer. *J Mammary Gland Biol Neoplasia* 2000; 5(1):107-115.

(42) Laban C, Bustin SA, Jenkins PJ. The GH-IGF-I axis and breast cancer. *Trends Endocrinol Metab* 2003; 14(1):28-34.

(43) Guvakova MA, Surmacz E. Tamoxifen interferes with the insulin-like growth factor I receptor (IGF-IR) signaling pathway in breast cancer cells. *Cancer Res* 1997; 57(13):2606-2610.

(44) Lonning PE, Hall K, Aakvaag A, Lien EA. Influence of Tamoxifen on Plasma Levels of Insulin-like Growth Factor I and Insulin-like Growth Factor Binding Protein I in Breast Cancer Patients. *Cancer Res* 1992; 52(17):4719-4723.

(45) Bonanni B, Johansson H, Gandini S, Guerrieri-Gonzaga A, Torrisi R, Sandri MT et al. Effect of low dose tamoxifen on the insulin-like growth factor system in healthy women. *Breast Cancer Res Treat* 2001; 69(1):21-27.

(46) Tannenbaum GS, Gurd W, Lapointe M, Pollak M. Tamoxifen attenuates pulsatile growth hormone secretion: mediation in part by somatostatin. *Endocrinology* 1992; 130(6):3395-3401.

(47) Huynh HT, Tetenes E, Wallace L, Pollak M. In vivo inhibition of insulin-like growth factor I gene expression by tamoxifen. *Cancer Res* 1993; 53(8):1727-1730.

(48) Huynh H, Pollak M. Enhancement of tamoxifen-induced suppression of insulin-like growth factor I gene expression and serum level by a somatostatin analogue. *Biochem Biophys Res Commun* 1994; 203(1):253-259.

(49) Stewart AJ, Johnson MD, May FE, Westley BR. Role of insulin-like growth factors and the type I insulin-like growth factor receptor in the estrogen-stimulated proliferation of human breast cancer cells. *J Biol Chem* 1990; 265(34):21172-21178.

(50) Stewart AJ, Westley BR, May FE. Modulation of the proliferative response of breast cancer cells to growth factors by oestrogen. *Br J Cancer* 1992; 66(4):640-648.

(51) Lee AV, Jackson JG, Gooch JL, Hilsenbeck SG, Coronado-Heinsohn E, Osborne CK et al. Enhancement of insulin-like growth factor signaling in human breast cancer: estrogen regulation of insulin receptor substrate-1 expression in vitro and in vivo. *Mol Endocrinol* 1999; 13(5):787-796.

(52) Holly JM, Gunnell DJ, Davey Smith G. Growth hormone, IGF-I and cancer. Less intervention to avoid cancer? More intervention to prevent cancer? *J Endocrinol* 1999; 162(3):321-330.

(53) BAILEY FW. Hypophysectomy or adrenalectomy; their use in management of advanced malignant disease as observed in clinics in Europe. *Calif Med* 1956; 85(6):413-415.

(54) VanGilder JC. The place of hypophysectomy in the management of metastatic breast cancer. *Conn Med* 1975; 39(1):3-4.

(55) Stoll BA. Growth hormone and breast cancer. *Clin Oncol (R Coll Radiol)* 1992; 4(1):4-5.

(56) Michels KB, Trichopoulos D, Robins JM, Rosner BA, Manson JE, Hunter DJ et al. Birthweight as a risk factor for breast cancer. *Lancet* 1996; 348(9041):1542-1546.

(57) THISSEN JP, KETELSLEGERS JM, UNDERWOOD LE. Nutritional Regulation of the Insulin-Like Growth Factors. *Endocr Rev* 1994; 15(1):80-101.

(58) Frankel S, Gunnell DJ, Peters TJ, Maynard M, Smith GD. Childhood energy intake and adult mortality from cancer: the boyd orr cohort study. *BMJ* 1998; 316(7130):499-504.

(59) Emerman JT, Leahy M, Gout PW, Bruchovsky N. Elevated growth hormone levels in sera from breast cancer patients. *Horm Metab Res* 1985; 17(8):421-424.

(60) Love RR, Rose DP. Elevated bioactive prolactin in women at risk for familial breast cancer. *Eur J Cancer Clin Oncol* 1985; 21(12):1553-1554.

(61) Peyrat JP, Bonneterre J, Hecquet B, Vennin P, Louchez MM, Fournier C et al. Plasma insulin-like growth factor-1 (IGF-1) concentrations in human breast cancer. *Eur J Cancer* 1993; 29A(4):492-497.

(62) Hankinson SE, Willett WC, Colditz GA, Hunter DJ, Michaud DS, Deroo B et al. Circulating concentrations of insulin-like growth factor-I and risk of breast cancer. *Lancet* 1998; 351(9113):1393-1396.

(63) Byrne C, Colditz GA, Willett WC, Speizer FE, Pollak M, Hankinson SE. Plasma insulin-like growth factor (IGF) I, IGF-binding protein 3, and mammographic density. *Cancer Res* 2000; 60(14):3744-3748.

(64) Walker K, Fletcher O, Johnson N, Coupland B, McCormack VA, Folkerd E et al. Premenopausal mammographic density in relation to cyclic variations in endogenous sex hormone levels, prolactin, and insulin-like growth factors. *Cancer Res* 2009; 69(16):6490-6499.

(65) Moschos SJ, Mantzoros CS. The role of the IGF system in cancer: from basic to clinical studies and clinical applications. *Oncology* 2002; 63(4):317-332.

(66) Orme SM, McNally RJQ, Cartwright RA, Belchetz PE. Mortality and Cancer Incidence in Acromegaly: A Retrospective Cohort Study. *J Clin Endocrinol Metab* 1998; 83(8):2730-2734.

(67) Wright AD, Hill DM, Lowy CLAR, Fraser TR. Mortality in Acromegaly. *QJM* 1970; 39(1):1-a.

(68) Allen NE, Roddam AW, Allen DS, Fentiman IS, Dos Santos Silva I, Peto J et al. A prospective study of serum insulin-like growth factor-I (IGF-I), IGF-II, IGF-binding protein-3 and breast cancer risk. *Br J Cancer* 2005; 92(7):1283-1287.

(69) Key TJ, Appleby PN, Reeves GK, Roddam AW. Insulin-like growth factor 1 (IGF1), IGF binding protein 3 (IGFBP3), and breast cancer risk: pooled individual data analysis of 17 prospective studies. *Lancet Oncol* 2010; 11(6):530-542.

(70) Gooch JL, Van Den Berg CL, Yee D. Insulin-like growth factor (IGF)-I rescues breast cancer cells from chemotherapy-induced cell death--proliferative and anti-apoptotic effects. *Breast Cancer Res Treat* 1999; 56(1):1-10.

(71) Sinha YN, Vlahakis G, Vanderlaan WP. Serum, pituitary and urine concentrations of prolactin and growth hormone in eight strains of mice with varying incidence of mammary tumors. *Int J Cancer* 1979; 24(4):430-437.

(72) Hadsell DL, Greenberg NM, Fligger JM, Baumrucker CR, Rosen JM. Targeted expression of des(1-3) human insulin-like growth factor I in transgenic mice influences mammary gland development and IGF-binding protein expression. *Endocrinology* 1996; 137(1):321-330.

(73) Tornell J, Carlsson B, Pohjanen P, Wennbo H, Rymo L, Isaksson O. High frequency of mammary adenocarcinomas in metallothionein promoter-human growth hormone transgenic mice created from two different strains of mice. *J Steroid Biochem Mol Biol* 1992; 43(1-3):237-242.

(74) Kleinberg DL, Wood TL, Furth PA, Lee AV. Growth Hormone and Insulin-Like Growth Factor-I in the Transition from Normal Mammary Development to Preneoplastic Mammary Lesions. *Endocr Rev* 2009; 30(1):51-74.

(75) Arteaga CL, Kitten LJ, Coronado EB, Jacobs S, Kull FC, Allred DC et al. Blockade of the type I somatomedin receptor inhibits growth of human breast cancer cells in athymic mice. *J Clin Invest* 1989; 84(5):1418-1423.

(76) Wu Y, Cui K, Miyoshi K, Hennighausen L, Green JE, Setser J et al. Reduced circulating insulin-like growth factor I levels delay the onset of chemically and genetically induced mammary tumors. *Cancer Res* 2003; 63(15):4384-4388.

(77) Glondu M, Liaudet-Coopman E, Derocq D, Platet N, Rochefort H, Garcia M. Down-regulation of cathepsin-D expression by antisense gene transfer inhibits tumor growth and experimental lung metastasis of human breast cancer cells. *Oncogene* 2002; 21(33):5127-5134.

(78) Friend KE. Cancer and the potential place for growth hormone receptor antagonist therapy. *Growth Horm IGF Res* 2001; 11 Suppl A:S121-S123.

(79) Fink L, Seeger W, Ermert L, Hanze J, Stahl U, Grimminger F et al. Real-time quantitative RT-PCR after laser-assisted cell picking. *Nat Med* 1998; 4(11):1329-1333.

(80) Sheils OM, Sweeney EC. TSH receptor status of thyroid neoplasms--TaqMan RT-PCR analysis of archival material. *J Pathol* 1999; 188(1):87-92.

(81) Kaplan JC, Kahn A, Chelly J. Illegitimate transcription: its use in the study of inherited disease. *Hum Mutat* 1992; 1(5):357-360.

(82) Bieche I, Onody P, Laurendeau I, Olivi M, Vidaud D, Lidereau R et al. Real-time reverse transcription-PCR assay for future management of ERBB2-based clinical applications. *Clin Chem* 1999; 45(8 Pt 1):1148-1156.

(83) Chien A, Edgar DB, Trela JM. Deoxyribonucleic acid polymerase from the extreme thermophile Thermus aquaticus. *J Bacteriol* 1976; 127(3):1550-1557.

(84) Saiki RK, Scharf S, Faloona F, Mullis KB, Horn GT, Erlich HA et al. Enzymatic amplification of beta-globin genomic sequences and restriction site analysis for diagnosis of sickle cell anemia. *Science* 1985; 230(4732):1350-1354.

(85) Saiki RK, Gelfand DH, Stoffel S, Scharf SJ, Higuchi R, Horn GT et al. Primer-directed enzymatic amplification of DNA with a thermostable DNA polymerase. *Science* 1988; 239(4839):487-491.

(86) Buell GN, Wickens MP, Payvar F, Schimke RT. Synthesis of full length cDNAs from four partially purified oviduct mRNAs. *J Biol Chem* 1978; 253(7):2471-2482.

(87) Gerard GF, Fox DK, Nathan M, D'Alessio JM. Reverse transcriptase. The use of cloned Moloney murine leukemia virus reverse transcriptase to synthesize DNA from RNA. *Mol Biotechnol* 1997; 8(1):61-77.

(88) DeStefano JJ, Buiser RG, Mallaber LM, Myers TW, Bambara RA, Fay PJ. Polymerization and RNase H activities of the reverse transcriptases from avian myeloblastosis, human immunodeficiency, and Moloney murine leukemia viruses are functionally uncoupled. *J Biol Chem* 1991; 266(12):7423-7431.

(89) Zhang J, Byrne CD. Differential priming of RNA templates during cDNA synthesis markedly affects both accuracy and reproducibility of quantitative competitive reverse-transcriptase PCR. *Biochem J* 1999; 337 (Pt 2):231-241.

(90) Adams MW, Kelly RM. Thermostability and thermoactivity of enzymes from hyperthermophilic Archaea. *Bioorg Med Chem* 1994; 2(7):659-667.

(91) Perler FB, Kumar S, Kong H. Thermostable DNA polymerases. *Adv Protein Chem* 1996; 48:377-435.

(92) Myers TW, Gelfand DH. Reverse transcription and DNA amplification by a Thermus thermophilus DNA polymerase. *Biochemistry* 1991; 30(31):7661-7666.

(93) Poddar SK, Sawyer MH, Connor JD. Effect of inhibitors in clinical specimens on Taq and Tth DNA polymerase-based PCR amplification of influenza A virus. *J Med Microbiol* 1998; 47(12):1131-1135.

(94) Cusi MG, Valassina M, Valensin PE. Comparison of M-MLV reverse transcriptase and Tth polymerase activity in RT-PCR of samples with low virus burden. *Biotechniques* 1994; 17(6):1034-1036.

(95) Leutenegger CM, Mislin CN, Sigrist B, Ehrengruber MU, Hofmann-Lehmann R, Lutz H. Quantitative real-time PCR for the measurement of feline cytokine mRNA. *Vet Immunol Immunopathol* 1999; 71(3-4):291-305.

(96) Beckman RA, Mildvan AS, Loeb LA. On the fidelity of DNA replication: manganese mutagenesis in vitro. *Biochemistry* 1985; 24(21):5810-5817.

(97) Ferre F. Quantitative or semi-quantitative PCR: reality versus myth. *PCR Methods Appl* 1992; 2(1):1-9.

(98) Montgomery RA, Dallman MJ. Semi-quantitative polymerase chain reaction analysis of cytokine and cytokine receptor gene expression during thymic ontogeny. *Cytokine* 1997; 9(10):717-726.

(99) Wang AM, Doyle MV, Mark DF. Quantitation of mRNA by the polymerase chain reaction. *Proc Natl Acad Sci U S A* 1989; 86(24):9717-9721.

(100) Vanden Heuvel JP, Tyson FL, Bell DA. Construction of recombinant RNA templates for use as internal standards in quantitative RT-PCR. *Biotechniques* 1993; 14(3):395-398.

(101) Reischl U, Kochanowski B. Quantitative PCR. A survey of the present technology. *Mol Biotechnol* 1995; 3(1):55-71.

(102) Gilliland G, Perrin S, Blanchard K, Bunn HF. Analysis of cytokine mRNA and DNA: detection and quantitation by competitive polymerase chain reaction. *Proc Natl Acad Sci U S A* 1990; 87(7):2725-2729.

(103) Scheuermann RH, Bauer SR. Polymerase chain reaction-based mRNA quantification using an internal standard: analysis of oncogene expression. *Methods Enzymol* 1993; 218:446-473.

(104) Raeymaekers L. Quantitative PCR: theoretical considerations with practical implications. *Anal Biochem* 1993; 214(2):582-585.

(105) Karge WH, III, Schaefer EJ, Ordovas JM. Quantification of mRNA by polymerase chain reaction (PCR) using an internal standard and a nonradioactive detection method. *Methods Mol Biol* 1998; 110:43-61.

(106) Bustin SA. Absolute quantification of mRNA using real-time reverse transcription polymerase chain reaction assays. *J Mol Endocrinol* 2000; 25(2):169-193.

(107) Edwards DR, Denhardt DT. A study of mitochondrial and nuclear transcription with cloned cDNA probes. Changes in the relative abundance of mitochondrial transcripts after stimulation of quiescent mouse fibroblasts. *Exp Cell Res* 1985; 157(1):127-143.

(108) Winer J, Jung CK, Shackel I, Williams PM. Development and validation of real-time quantitative reverse transcriptase-polymerase chain reaction for monitoring gene expression in cardiac myocytes in vitro. *Anal Biochem* 1999; 270(1):41-49.

(109) Bustin SA, Gyselman VG, Williams NS, Dorudi S. Detection of cytokeratins 19/20 and guanylyl cyclase C in peripheral blood of colorectal cancer patients. *Br J Cancer* 1999; 79(11-12):1813-1820.

(110) Cale JM, Millican DS, Itoh H, Magness RR, Bird IM. Pregnancy induces an increase in the expression of glyceraldehyde-3-phosphate dehydrogenase in uterine artery endothelial cells. *J Soc Gynecol Investig* 1997; 4(6):284-292.

(111) Calvo EL, Boucher C, Coulombe Z, Morisset J. Pancreatic GAPDH gene expression during ontogeny and acute pancreatitis induced by caerulein. *Biochem Biophys Res Commun* 1997; 235(3):636-640.

(112) Puissant C, Bayat-Sarmadi M, Devinoy E, Houdebine LM. Variation of transferrin mRNA concentration in the rabbit mammary gland during the pregnancy-lactation-weaning cycle and in cultured mammary cells. A comparison with the other major milk protein mRNAs. *Eur J Endocrinol* 1994; 130(5):522-529.

(113) Mansur NR, Meyer-Siegler K, Wurzer JC, Sirover MA. Cell cycle regulation of the glyceraldehyde-3-phosphate dehydrogenase/uracil DNA glycosylase gene in normal human cells. *Nucleic Acids Res* 1993; 21(4):993-998.

(114) Spanakis E. Problems related to the interpretation of autoradiographic data on gene expression using common constitutive transcripts as controls. *Nucleic Acids Res* 1993; 21(16):3809-3819.

(115) Paule MR, White RJ. Survey and summary: transcription by RNA polymerases I and III. *Nucleic Acids Res* 2000; 28(6):1283-1298.

(116) Barbu V, Dautry F. Northern blot normalization with a 28S rRNA oligonucleotide probe. *Nucleic Acids Res* 1989; 17(17):7115.

(117) Bustin SA. Quantification of mRNA using real-time reverse transcription PCR (RT-PCR): trends and problems. *J Mol Endocrinol* 2002; 29(1):23-39.

(118) Hsu SM, Raine L, Fanger H. A comparative study of the peroxidase-antiperoxidase method and an avidin-biotin complex method for studying polypeptide hormones with radioimmunoassay antibodies. *Am J Clin Pathol* 1981; 75(5):734-738.

(119) Hsu SM, Raine L, Fanger H. Use of avidin-biotin-peroxidase complex (ABC) in immunoperoxidase techniques: a comparison between ABC and unlabeled antibody (PAP) procedures. *J Histochem Cytochem* 1981; 29(4):577-580.

(120) Morrell DJ, Dadi H, More J, Taylor AM, Dabestani A, Buchanan CR et al. A monoclonal antibody to human insulin-like growth factor-I: characterization, use in radioimmunoassay and effect on the biological activities of the growth factor. *J Mol Endocrinol* 1989; 2(3):201-206.

(121) Decker T, Lohmann-Matthes ML. A quick and simple method for the quantitation of lactate dehydrogenase release in measurements of cellular cytotoxicity and tumor necrosis factor (TNF) activity. *J Immunol Methods* 1988; 115(1):61-69.

(122) Higuchi R, Fockler C, Dollinger G, Watson R. Kinetic PCR analysis: real-time monitoring of DNA amplification reactions. *Biotechnology (N Y)* 1993; 11(9):1026-1030.

(123) Peyrat JP, Bonneterre J, Vennin PH, Jammes H, Beuscart R, Hecquet B et al. Insulin-like growth factor 1 receptors (IGF1-R) and IGF1 in human breast tumors. *J Steroid Biochem Mol Biol* 1990; 37(6):823-827.

(124) Chong YM, Williams SL, Elkak A, Sharma AK, Mokbel K. Insulin-like growth factor 1 (IGF-1) and its receptor mRNA levels in breast cancer and adjacent non-neoplastic tissue. *Anticancer Res* 2006; 26(1A):167-173.

(125) Willey JC, Crawford EL, Jackson CM, Weaver DA, Hoban JC, Khuder SA et al. Expression measurement of many genes simultaneously by quantitative RT-PCR using standardized mixtures of competitive templates. *Am J Respir Cell Mol Biol* 1998; 19(1):6-17.

(126) Ellis MJ, Jenkins S, Hanfelt J, Redington ME, Taylor M, Leek R et al. Insulin-like growth factors in human breast cancer. *Breast Cancer Res Treat* 1998; 52(1-3):175-184.

(127) Riedemann J, Macaulay VM. IGF1R signalling and its inhibition. *Endocr Relat Cancer* 2006; 13 Suppl 1:S33-S43.

(128) Law JH, Habibi G, Hu K, Masoudi H, Wang MY, Stratford AL et al. Phosphorylated insulin-like growth factor-i/insulin receptor is present in all breast cancer subtypes and is related to poor survival. *Cancer Res* 2008; 68(24):10238-10246.

(129) Sachdev D, Li SL, Hartell JS, Fujita-Yamaguchi Y, Miller JS, Yee D. A chimeric humanized single-chain antibody against the type I insulin-like growth factor (IGF) receptor renders breast cancer cells refractory to the mitogenic effects of IGF-I. *Cancer Res* 2003; 63(3):627-635.

(130) Gualberto A, Pollak M. Emerging role of insulin-like growth factor receptor inhibitors in oncology: early clinical trial results and future directions. *Oncogene* 2009; 28(34):3009-3021.

(131) Haluska P, Shaw HM, Batzel GN, Yin D, Molina JR, Molife LR et al. Phase I dose escalation study of the anti insulin-like growth factor-I receptor monoclonal antibody CP-751,871 in patients with refractory solid tumors. *Clin Cancer Res* 2007; 13(19):5834-5840.

(132) Narita T, Funahashi H, Satoh Y, Takagi H. Proliferating cell nuclear antigen immunostaining in breast cancer and its relation to prognosis. *Jpn J Clin Oncol* 1993; 23(1):20-25.

(133) Wong MP, Cheung N, Yuen ST, Leung SY, Chung LP. Vascular endothelial growth factor is up-regulated in the early pre-malignant stage of colorectal tumour progression. *Int J Cancer* 1999; 81(6):845-850.

(134) Tanigawa N, Amaya H, Matsumura M, Lu C, Kitaoka A, Matsuyama K et al. Tumor angiogenesis and mode of metastasis in patients with colorectal cancer. *Cancer Res* 1997; 57(6):1043-1046.

(135) Akagi Y, Liu W, Zebrowski B, Xie K, Ellis LM. Regulation of vascular endothelial growth factor expression in human colon cancer by insulin-like growth factor-I. *Cancer Res* 1998; 58(17):4008-4014.

(136) Zhou Z, Reddy K, Guan H, Kleinerman ES. VEGF(165), but not VEGF(189), stimulates vasculogenesis and bone marrow cell migration into Ewing's sarcoma tumors in vivo. *Mol Cancer Res* 2007; 5(11):1125-1132.

(137) James SY, Mackay AG, Colston KW. Effects of 1,25 dihydroxyvitamin D3 and its analogues on induction of apoptosis in breast cancer cells. *J Steroid Biochem Mol Biol* 1996; 58(4):395-401.

(138) Vink-van WT, Pols HA, Buurman CJ, Birkenhager JC, van Leeuwen JP. Inhibition of insulin- and insulin-like growth factor-I-stimulated growth of human breast cancer cells by 1,25-dihydroxyvitamin D3 and the vitamin D3 analogue EB1089. *Eur J Cancer* 1996; 32A(5):842-848.

(139) Xie SP, James SY, Colston KW. Vitamin D derivatives inhibit the mitogenic effects of IGF-I on MCF-7 human breast cancer cells. *J Endocrinol* 1997; 154(3):495-504.

(140) Pirianov G, Colston KW. Interaction of vitamin D analogs with signaling pathways leading to active cell death in breast cancer cells. *Steroids* 2001; 66(3-5):309-318.

(141) Berger U, Wilson P, McClelland RA, Colston K, Haussler MR, Pike JW et al. Immunocytochemical detection of 1,25-dihydroxyvitamin D3 receptor in breast cancer. *Cancer Res* 1987; 47(24 Pt 1):6793-6799.

(142) Freake HC, Abeyasekera G, Iwasaki J, Marcocci C, MacIntyre I, McClelland RA et al. Measurement of 1,25-dihydroxyvitamin D3 receptors in breast cancer and their relationship to biochemical and clinical indices. *Cancer Res* 1984; 44(4):1677-1681.

(143) Kirkpatrick KL, Mokbel K. The significance of human telomerase reverse transcriptase (hTERT) in cancer. *Eur J Surg Oncol* 2001; 27(8):754-760.

(144) Kirkpatrick KL, Ogunkolade W, Elkak AE, Bustin S, Jenkins P, Ghilchick M et al. hTERT expression in human breast cancer and non-cancerous breast tissue: correlation with tumour stage and c-Myc expression. *Breast Cancer Res Treat* 2003; 77(3):277-284.

(145) Kirkpatrick KL, Newbold RF, Mokbel K. The mRNA expression of hTERT in human breast carcinomas correlates with VEGF expression. *J Carcinog* 2004; 3(1):1.

(146) Gebre-Medhin M, Kindblom LG, Wennbo H, Tornell J, Meis-Kindblom JM. Growth hormone receptor is expressed in human breast cancer. *Am J Pathol* 2001; 158(4):1217-1222.

(147) Mertani HC, Garcia-Caballero T, Lambert A, Gerard F, Palayer C, Boutin JM et al. Cellular expression of growth hormone and prolactin receptors in human breast disorders. *Int J Cancer* 1998; 79(2):202-211.

(148) Orlando C, Raggi CC, Bianchi S, Distante V, Simi L, Vezzosi V et al. Measurement of somatostatin receptor subtype 2 mRNA in breast cancer and corresponding normal tissue. *Endocr Relat Cancer* 2004; 11(2):323-332.

(149) Pollak M, Costantino J, Polychronakos C, Blauer SA, Guyda H, Redmond C et al. Effect of tamoxifen on serum insulinlike growth factor I levels in stage I breast cancer patients. *J Natl Cancer Inst* 1990; 82(21):1693-1697.

(150) Pollak MN, Huynh HT, Lefebvre SP. Tamoxifen reduces serum insulin-like growth factor I (IGF-I). *Breast Cancer Res Treat* 1992; 22(1):91-100.

(151) Lahti EI, Knip M, Laatikainen TJ. Plasma insulin-like growth factor I and its binding proteins 1 and 3 in postmenopausal patients with breast cancer receiving long term tamoxifen. *Cancer* 1994; 74(2):618-624.

(152) Vadgama JV, Wu Y, Datta G, Khan H, Chillar R. Plasma insulin-like growth factor-I and serum IGF-binding protein 3 can be associated with the progression of breast cancer, and predict the risk of recurrence and the probability of survival in African-American and Hispanic women. *Oncology* 1999; 57(4):330-340.

(153) Clemmons DR, Thissen JP, Maes M, Ketelslegers JM, Underwood LE. Insulin-like growth factor-I (IGF-I) infusion into hypophysectomized or protein-deprived rats induces specific IGF-binding proteins in serum. *Endocrinology* 1989; 125(6):2967-2972.

(154) Bang P, Brismar K, Rosenfeld RG, Hall K. Fasting affects serum insulin-like growth factors (IGFs) and IGF-binding proteins differently in patients with noninsulin-dependent diabetes mellitus versus healthy nonobese and obese subjects. *J Clin Endocrinol Metab* 1994; 78(4):960-967.

(155) Davies SC, Wass JA, Ross RJ, Cotterill AM, Buchanan CR, Coulson VJ et al. The induction of a specific protease for insulin-like growth factor binding protein-3 in the circulation during severe illness. *J Endocrinol* 1991; 130(3):469-473.

(156) Ross R, Miell J, Freeman E, Jones J, Matthews D, Preece M et al. Critically ill patients have high basal growth hormone levels with attenuated oscillatory activity associated with low levels of insulin-like growth factor-I. *Clin Endocrinol (Oxf)* 1991; 35(1):47-54.

(157) Winston R, Kao PC, Kiang DT. Regulation of insulin-like growth factors by antiestrogen. *Breast Cancer Res Treat* 1994; 31(1):107-115.

(158) Luo J, Ellis MJ. Microarray data analysis in neoadjuvant biomarker studies in estrogen receptor-positive breast cancer. *Breast Cancer Res* 2010; 12(4):112.

(159) Sheen-Chen SM, Chou FF, Hsu W, Huang CC, Eng HL, Tang RP. Lack of prognostic value of insulin-like growth factor-1 in patients with breast cancer: analysis with tissue microarray. *Anticancer Res* 2007; 27(5B):3541-3544.

(160) Kuroda H, Saito K, Kuroda M, Suzuki Y. Differential expression of glu-tubulin in relation to mammary gland disease. *Virchows Arch* 2010; 457(4):477-482.

(161) Tobin SW, Douville K, Benbow U, Brinckerhoff CE, Memoli VA, Arrick BA. Consequences of altered TGF-beta expression and responsiveness in breast cancer: evidence for autocrine and paracrine effects. *Oncogene* 2002; 21(1):108-118.

(162) Lewis-Wambi JS, Cunliffe HE, Kim HR, Willis AL, Jordan VC. Overexpression of CEACAM6 promotes migration and invasion of oestrogen-deprived breast cancer cells. *Eur J Cancer* 2008; 44(12):1770-1779.

(163) Shi ZZ, Zhang JW, Zheng S. What we know about ST13, a co-factor of heat shock protein, or a tumor suppressor? *J Zhejiang Univ Sci B* 2007; 8(3):170-176.

(164) Surmacz E. Growth factor receptors as therapeutic targets: strategies to inhibit the insulin-like growth factor I receptor. *Oncogene* 2003; 22(42):6589-6597.

(165) Wen B, Deutsch E, Marangoni E, Frascona V, Maggiorella L, Abdulkarim B et al. Tyrphostin AG 1024 modulates radiosensitivity in human breast cancer cells. *Br J Cancer* 2001; 85(12):2017-2021.

(166) Bohula EA, Playford MP, Macaulay VM. Targeting the type 1 insulin-like growth factor receptor as anti-cancer treatment. *Anticancer Drugs* 2003; 14(9):669-682.

(167) Scartozzi M, Bianconi M, Maccaroni E, Giampieri R, Berardi R, Cascinu S. Dalotuzumab, a recombinant humanized mAb targeted against IGFR1 for the treatment of cancer. *Curr Opin Mol Ther* 2010; 12(3):361-371.

(168) Oh Y, Gucev Z, Ng L, Muller HL, Rosenfeld RG. Antiproliferative actions of insulin-like growth factor binding protein (IGFBP)-3 in human breast cancer cells. *Prog Growth Factor Res* 1995; 6(2-4):503-512.

(169) Nickerson T, Huynh H, Pollak M. Insulin-like growth factor binding protein-3 induces apoptosis in MCF7 breast cancer cells. *Biochem Biophys Res Commun* 1997; 237(3):690-693.

(170) Di LA, Ferrari L, Bajetta E, Bartoli C, Vicario G, Moglia D et al. Biological and clinical evaluation of lanreotide (BIM 23014), a somatostatin analogue, in the treatment of advanced breast cancer. A pilot study by the I.T.M.O. Group. Italian Trials in Medical Oncology. *Breast Cancer Res Treat* 1995; 34(3):237-244.

(171) Hejna M, Schmidinger M, Raderer M. The clinical role of somatostatin analogues as antineoplastic agents: much ado about nothing? *Ann Oncol* 2002; 13(5):653-668.

(172) Pollak M. The potential role of somatostatin analogues in breast cancer treatment. *Yale J Biol Med* 1997; 70(5-6):535-539.

(173) Bontenbal M, Foekens JA, Lamberts SW, de Jong FH, van Putten WL, Braun HJ et al. Feasibility, endocrine and anti-tumour effects of a triple endocrine therapy with tamoxifen, a somatostatin analogue and an antiprolactin in post-menopausal metastatic breast cancer: a randomized study with long-term follow-up. *Br J Cancer* 1998; 77(1):115-122.

(174) Yin D, Vreeland F, Schaaf LJ, Millham R, Duncan BA, Sharma A. Clinical pharmacodynamic effects of the growth hormone receptor antagonist pegvisomant: implications for cancer therapy. *Clin Cancer Res* 2007; 13(3):1000-1009.

(175) Dagnaes-Hansen F, Duan H, Rasmussen LM, Friend KE, Flyvbjerg A. Growth hormone receptor antagonist administration inhibits growth of human colorectal carcinoma in nude mice. *Anticancer Res* 2004; 24(6):3735-3742.

(176) Divisova J, Kuiatse I, Lazard Z, Weiss H, Vreeland F, Hadsell DL et al. The growth hormone receptor antagonist pegvisomant blocks both mammary gland development and MCF-7 breast cancer xenograft growth. *Breast Cancer Res Treat* 2006; 98(3):315-327.

(177) Lee AV, Cui X, Oesterreich S. Cross-talk among estrogen receptor, epidermal growth factor, and insulin-like growth factor signaling in breast cancer. *Clin Cancer Res* 2001; 7(12 Suppl):4429s-4435s.

(178) Lisztwan J, Pornon A, Chen B, Chen S, Evans DB. The aromatase inhibitor letrozole and inhibitors of insulin-like growth factor I receptor synergistically induce apoptosis in in vitro models of estrogen-dependent breast cancer. *Breast Cancer Res* 2008; 10(4):R56.

(179) Lu Y, Zi X, Zhao Y, Mascarenhas D, Pollak M. Insulin-like growth factor-I receptor signaling and resistance to trastuzumab (Herceptin). *J Natl Cancer Inst* 2001; 93(24):1852-1857.

(180) Nahta R, Yuan LX, Zhang B, Kobayashi R, Esteva FJ. Insulin-like growth factor-I receptor/human epidermal growth factor receptor 2 heterodimerization contributes to trastuzumab resistance of breast cancer cells. *Cancer Res* 2005; 65(23):11118-11128.

(181) Camirand A, Lu Y, Pollak M. Co-targeting HER2/ErbB2 and insulin-like growth factor-1 receptors causes synergistic inhibition of growth in HER2-overexpressing breast cancer cells. *Med Sci Monit* 2002; 8(12):BR521-BR526.

(182) Rowe DL, Ozbay T, Bender LM, Nahta R. Nordihydroguaiaretic acid, a cytotoxic insulin-like growth factor-I receptor/HER2 inhibitor in trastuzumab-resistant breast cancer. *Mol Cancer Ther* 2008; 7(7):1900-1908.